

Genotoxicity of Synthetic Nanomaterials

Zur Erlangung des akademischen Grades eines

DOKTORS DER NATURWISSENSCHAFTEN

(Dr. rer. nat.)

der Fakultät für Chemie und Biowissenschaften der
Universität Karlsruhe (TH)
vorgelegte

DISSERTATION

von

Kathrin Barbara Fischer

aus Würzburg

2009

Dekan: Prof. Dr. S. Bräse

Referent: Prof. Dr. H. F. Krug

Koreferent: Prof. Dr. M. Metzler

Tag der mündlichen Prüfung: 08.07.2009

Summary

More and more products containing nano-sized components are available. However, exposure to nanomaterials is growing faster than the knowledge about possible adverse health effects. Studies with airborne ultrafine particulate matter showed that inhalation of nanoparticles induced inflammatory reactions in the lung, which were stronger than for inhalation of micron-sized particles. Moreover, the cancer incidence is elevated after inhalation of ultrafine particulate matter as a consequence of oxidative stress and oxidative DNA damage. Thus, there is concern that the inhalative exposure to novel, synthetically produced nanomaterials may lead to carcinogenesis, mainly via increased generation of reactive oxygen species by the nanomaterials.

The objective of this work was hence to evaluate the genotoxic potential of synthetically produced nanomaterials in a human epithelial lung cell line (A549) as a model of exposure via inhalation. A set of vanadium oxide compounds of different chemical compositions (V_2O_3 and V_2O_5) and of different sizes (bulk and nanosized) was used to be able to compare the effects of closely related substances. After characterization of the materials, biological testing revealed solubility-dependent cellular uptake, cytotoxicity and stimulation of proliferation. Moreover, the generation of reactive oxygen species was found for all soluble vanadium oxides. A genotoxic potential including the oxidation of DNA bases (8-oxo-guanine), DNA strand breaks (comet assay) and G2/M cell cycle arrest was found for two substances of intermediate solubility, nano V_2O_3 and bulk V_2O_5 , and to a lesser extent, for soluble vanadate ions. No induction of micronuclei was observed in the micronucleus test, but a possible disturbance of mitosis and an alteration of nuclear morphology by soluble vanadium oxides. Genotoxicity is apparently not directly correlated to solubility but caused by other mechanisms that still have to be unraveled.

The genotoxicity testing of several nanomaterials produced at large-scale (TiO_2 , ZnO, carbon black) showed no genotoxic potential for TiO_2 and ZnO in the comet assay and the micronucleus test. Carbon black was weakly genotoxic, inducing micronuclei at high concentrations, but no DNA strand breaks in the comet assay.

The main conclusions were that 1. The biological effects of bulk and nanomaterial are clearly different. Due to higher solubility, the vanadium oxide nanomaterials caused higher cytotoxicity than the corresponding bulk materials. This underlines the

importance of a thorough characterization including the analysis of solubility. This may help to estimate the toxicological behavior of novel nanomaterials and to derive correlations which enable the prediction of the toxicity of materials with similar physico-chemical characteristics. 2. Some of the nanomaterials tested in this work were genotoxic (nano V_2O_3 , carbon black) but no parameter correlated to genotoxicity could be found. Thus, genotoxicity testing for novel nanomaterials, using preferentially standardized conditions, is still required to assess the genotoxic potential of nanomaterials and to prevent adverse health effects.

Zusammenfassung

Es sind immer mehr Produkte erhältlich, die Bestandteile in Nanogröße enthalten. Die Exposition gegenüber Nanomaterialien wächst jedoch schneller als das Wissen über mögliche negative Auswirkungen auf die Gesundheit. Studien mit Feinstaub zeigten, dass die Inhalation von Nanopartikeln Entzündungsreaktionen in der Lunge auslöste, die stärker waren als bei der Inhalation von Partikeln in Mikrometergröße. Außerdem erhöhte sich die Häufigkeit von Krebs nach der Inhalation von ultrafeinen Partikeln auf Grund von oxidativem Stress und oxidativen DNA Schäden. Es besteht also die Sorge, dass die inhalative Exposition gegenüber neuartigen, synthetischen Nanomaterialien zur Krebsentstehung führen könnte; vor allem durch die erhöhte Produktion von reaktiven Sauerstoffspezies durch Nanomaterialien.

Das Ziel dieser Arbeit war folglich, das genotoxische Potential synthetisch produzierter Nanomaterialien in einer humanen Lungenepithelzelllinie (A549), als Model für die Exposition durch Inhalation, zu analysieren. Verschiedene Vanadiumoxide unterschiedlicher chemischer Zusammensetzung (V_2O_3 and V_2O_5) und Größe ("bulk" und "nano") wurden verwendet, um die Effekte ähnlicher Substanzen vergleichen zu können. Nach der Charakterisierung der Materialien wurden in biologischen Experimenten eine Löslichkeits-abhängige Aufnahme in die Zellen, Zytotoxizität und Stimulation der Proliferation festgestellt. Weiterhin wurde für alle löslichen Vanadiumoxide die Produktion von reaktiven Sauerstoffspezies gefunden. Ein genotoxisches Potential, das die Oxidation von DNA-Basen (8-oxo-Guanin), DNA-Strangbrüche (*Comet Assay*) und einen Zellzyklusarrest in der G2/M-Phase umfasste, zeigten zwei Substanzen von mittlerer Löslichkeit, nano V_2O_3 und bulk V_2O_5 , und in einem geringeren Ausmaß, Vanadationen. Im Mikrokerntest wurde keine Induktion von Mikrokernen beobachtet, jedoch eine mögliche Beeinträchtigung der Mitose und eine Veränderung der Kernmorphologie durch lösliche Vanadiumoxide. Die Genotoxizität ist offenbar nicht direkt mit der Löslichkeit korreliert, sondern durch andere Mechanismen verursacht, die noch erforscht werden müssen.

Genotoxizitäts-Tests einiger Nanomaterialien, die in großem Maßstab produziert werden (TiO_2 , ZnO, *Carbon Black*, d.h. Industrieruß), zeigten im *Comet Assay* und im Mikrokerntest kein genotoxisches Potential für TiO_2 und ZnO. *Carbon black* war

schwach genotoxisch durch die Induktion von Mikrokernen in hohen Konzentrationen, verursachte aber keine DNA-Strangbrüche im *Comet Assay*.

Die wichtigsten Schlussfolgerungen waren: 1. Die biologischen Effekte von Bulk- und Nanomaterialien unterscheiden sich deutlich. Auf Grund einer höheren Löslichkeit war die Zytotoxizität von Vanadiumoxid-Nanomaterialien höher als die der entsprechenden Bulkmaterialien. Dies unterstreicht die Wichtigkeit einer gründlichen Charakterisierung einschließlich der Untersuchung der Löslichkeit. Das kann helfen, das toxikologische Verhalten neuartiger Nanomaterialien abzuschätzen und Korrelationen zu finden, die die Vorhersage der Toxizität von Materialien mit ähnlichen physiko-chemischen Eigenschaften ermöglichen. 2. Einige der getesteten Nanomaterialien waren genotoxisch (nano V_2O_3 , *Carbon Black*), es konnte aber kein Parameter gefunden werden, der mit der Genotoxizität korreliert. Aus diesem Grund ist die Untersuchung der Genotoxizität neuartiger Nanomaterialien, vorzugsweise unter standardisierten Bedingungen, weiterhin erforderlich, um das genotoxische Potential von Nanomaterialien zu beurteilen und negative Auswirkungen auf die Gesundheit zu verhindern.

Table of Contents

Summary	I
Zusammenfassung	III
Abbreviations	IX
1 Introduction	1
1.1 <i>Nanotechnology</i>	1
1.2 <i>Inhalation toxicology and nanotoxicology</i>	2
1.3 <i>Reactive oxygen / nitrogen species and oxidative stress</i>	4
1.3.1 Reactive oxygen species and reactive nitrogen species	4
1.3.2 Oxidative stress	5
1.3.3 Oxidative stress in carcinogenesis	6
1.4 <i>Genotoxicity</i>	6
1.4.1 Direct genotoxicity	7
1.4.1.1 DNA adducts	7
1.4.1.2 Chemical modification of DNA	7
1.4.2 Indirect genotoxicity	9
1.4.2.1 Enzyme inhibition	9
1.4.2.2 Interference with cell division	10
1.4.3 Consequences of genotoxicity and cellular responses	11
1.4.3.1 Base modifications	11
1.4.3.2 DNA strand breaks	12
1.4.3.3 Micronuclei	12
1.4.3.4 Fate of cells with persisting DNA damage	14
1.4.4 Increased genotoxicity for nanoparticles?	17
1.5 <i>Vanadium oxides</i>	18
1.5.1 Occurrence and applications	18
1.5.2 Exposure	19
1.5.3 Generation of ROS by vanadium oxides	20
1.5.4 Biological effects and toxicity	20
1.5.5 Genotoxicity of vanadium oxides	21
1.6 <i>Objective of this work</i>	22
2 Materials and Methods	24
2.1 <i>Material</i>	24

2.1.1	Technical equipment	24
2.1.2	Software	24
2.1.3	Consumables	25
2.1.4	Chemicals	25
2.1.5	Kits	26
2.1.6	Bulk and nanomaterials.....	27
2.1.7	Cell culture: cell lines, medium and supplements.....	27
2.2	<i>Methods</i>	28
2.2.1	Cell culture	28
2.2.1.1	Culture of A549 cells	28
2.2.1.2	Cryoconservation of cells.....	29
2.2.2	Preparation of test substances.....	29
2.2.2.1	Preparation of particles.....	29
2.2.2.2	Preparation of vanadium oxides	29
2.2.2.3	Preparation of vanadate solution	30
2.2.3	Characterization of test materials.....	30
2.2.3.1	Preparation of nanomaterials for characterization by transmission electron microscopy.....	30
2.2.3.2	Determination of the solubility of vanadium oxides.....	30
2.2.4	Analysis of vanadium oxide uptake into cells	31
2.2.5	Determination of the protein concentration (BCA assay)	32
2.2.6	Cell viability assays	33
2.2.6.1	Proliferation assay I (cell number)	33
2.2.6.2	Proliferation assay II (AlamarBlue™ assay)	33
2.2.6.3	Proliferation assay III (BrdU assay)	34
2.2.6.4	Toxicity assay I (MTT assay)	34
2.2.6.5	Toxicity assay II (XTT assay).....	35
2.2.6.6	Toxicity assay III (Lactate dehydrogenase assay).....	36
2.2.7	Detection of reactive oxygen / nitrogen species (ROS / RNS)	38
2.2.7.1	2',7'-dichlorofluorescein (DCF) assay	38
2.2.7.2	Dihydrorhodamine (DHR) assay.....	38
2.2.8	Genotoxicity assays	40
2.2.8.1	Comet assay (single cell gel electrophoresis).....	40
2.2.8.2	Micronucleus test.....	42

2.2.8.3	Biotrin OxyDNA test.....	44
2.2.9	Cell cycle analysis.....	45
3	Results	47
3.1	<i>Characterization of vanadium oxides</i>	<i>48</i>
3.1.1	<i>Metric characterization</i>	<i>48</i>
3.1.2	<i>Solubility of vanadium oxides.....</i>	<i>49</i>
3.2	<i>Vanadium oxides are taken up into cells.....</i>	<i>51</i>
3.3	<i>Vanadium uptake is correlated to solubility.....</i>	<i>52</i>
3.4	<i>Low vanadium oxide concentrations stimulate proliferation</i>	<i>52</i>
3.5	<i>Acute toxicity of vanadium oxides</i>	<i>54</i>
3.6	<i>(Soluble) vanadium oxides generate reactive oxygen species.....</i>	<i>56</i>
3.7	<i>Nano vanadium trioxide, bulk vanadium pentoxide and vanadate induce oxidation of DNA bases.....</i>	<i>59</i>
3.8	<i>Nano vanadium trioxide and bulk vanadium pentoxide induce DNA strand breaks</i>	<i>62</i>
3.9	<i>No induction of micronuclei by vanadium oxides.....</i>	<i>63</i>
3.10	<i>Soluble vanadium oxides change nuclear morphology and mitosis</i>	<i>67</i>
3.11	<i>Nano vanadium trioxide, bulk vanadium pentoxide and vanadate induce cell cycle arrest.....</i>	<i>69</i>
3.12	<i>No induction of DNA strand breaks by TiO₂, CB and ZnO nanoparticles ...</i>	<i>71</i>
3.13	<i>No induction of micronuclei by TiO₂</i>	<i>73</i>
3.14	<i>Carbon black nanoparticles induce micronuclei at high concentrations</i>	<i>74</i>
3.15	<i>No induction of micronuclei by ZnO nanoparticles</i>	<i>75</i>
4	Discussion	77
4.1	<i>Solubility for different vanadium oxides differs: higher solubility for nanomaterials</i>	<i>79</i>
4.2	<i>Uptake of vanadium into A549 cells is correlated to solubility.....</i>	<i>81</i>
4.3	<i>Two-sided effect of vanadium oxides: Low concentrations stimulate proliferation, high concentrations induce cytotoxicity</i>	<i>83</i>
4.4	<i>ROS generation by soluble vanadium oxides.....</i>	<i>86</i>
4.5	<i>Genotoxicity of nano V₂O₃ and bulk V₂O₅: DNA oxidation, strand breaks and cell cycle arrest</i>	<i>89</i>
4.6	<i>No increase in micronucleated cells – but morphological changes in cell nuclei</i>	<i>93</i>

4.7	<i>Genotoxic potential of TiO₂, CB and ZnO</i>	96
4.8	<i>Conclusions</i>	100
4.8.1	Biological effects and genotoxicity differ for bulk and nano vanadium oxides	100
4.8.2	Mechanisms of bulk versus nanotoxicity of vanadium oxides	101
4.8.3	Genotoxicity of different nanomaterials is different.....	102
4.8.4	Are standard genotoxicity tests suitable for the testing of nanomaterials?	104
4.8.5	Nanomaterials – is there a cancer risk?	105
5	List of Tables and Figures	107
6	References	109
	Publications	130
	Curriculum Vitae	131
	Acknowledgements / Danksagungen	133

Abbreviations

8-oxo-G	8-oxo-guanine
BCA	Bicinchoninic acid
BET	Brunauer-Emmet-Teller
BrdU	5-bromo-2'-deoxy-uridine
BSA	Bovine serum albumin
bV ₂ O ₃	Bulk vanadium trioxide
bV ₂ O ₅	Bulk vanadium pentoxide
CB	Carbon black
CDK	Cyclin-dependent kinase
Chk	Checkpoint kinase
DAPI	4'-6-diamidino-2-phenylindole
DCF	2',7'-dichlorofluorescein
DEG	Diethylene glycol
DHR	Dihydrorhodamine
DMEM	Dulbecco's modified Eagle's medium
DMSO	Dimethyl sulfoxide
DNA-PKcs	DNA dependent protein kinase catalytic subunit
EDTA	Ethylenediaminetetraacetic acid
FCS	Fetal calf serum
FITC	Fluorescein isothiocyanate
GTP	Guanosine triphosphate
H ₂ DCF-DA	2',7'-dichlorodihydrofluorescein-diacetate
HBSS	Hank's Balanced Salt Solution
HO-1	Heme oxygenase 1
ICP-OES	Inductively coupled plasma optical emission spectrometry
IL	Interleukin
INT	2-[4-iodophenyl]-3-[4-nitrophenyl]-5-phenyltetrazoliumchloride
LDH	Lactate dehydrogenase
MAP	Microtubule associated proteins
MAPK	Mitogen-activated protein kinase
MMS	Methyl-methane sulfonate
MNNG	N-methyl-N'-nitro-N-nitroso-guanidin

MT	Microtubules
MTT	3-(4,5-dimethylthiazol-2-yl)-2,5-diphenyltetrazolium bromide
NAD ⁺	Nicotine-adenine dinucleotide
NDI	Nuclear division index
nV ₂ O ₃	Nano vanadium trioxide
nV ₂ O ₅	Nano vanadium pentoxide
OGG	Oxoguanine glycosylase
PAH	Polycyclic aromatic hydrocarbons
PBS	Phosphate buffered saline
PFA	Paraformaldehyde
PMSF	Phenylmethylsulfonyl fluoride
PP	Protein phosphatase
RNS	Reactive nitrogen species
ROS	Reactive oxygen species
RT	Room temperature
SDS	Sodium dodecyl sulfate
SiO ₂	Silicon dioxide
TEM	Transmission electron microscopy
TiO ₂	Titanium dioxide
TNF α	Tumor necrosis factor alpha
UV	Ultraviolet (light)
V(III/IV/V)	Vanadium (oxidation state)
XTT	2,3-bis[2-methoxy-4-nitro-5-sulfopheny]-2H-tetrazolium-5-carboxyanilide inner salt
ZnO	Zinc oxide

1 Introduction

1.1 Nanotechnology

Nanotechnology has entered our every-day life. More and more products are launched and sold that contain nanosized components. These nanostructures display numerous novel features, as reduction to the nanometer level brings about important changes in the physico-chemical behavior of a substance. Quantum effects and the fact that the ratio of surface atoms to atoms on the inside is much higher for nano than for bulk structures are responsible for the particular characteristics of nanosized materials. Electrical conductivity, mechanical strength, surface reactivity and optical properties of nanomaterials are often altered significantly compared to bulk material (Nel *et al.* 2006).

Examples for the use of nanomaterials range from antimicrobial agents, bioimaging, catalysis, cosmetics, drug delivery, diagnostic purposes, production of semiconductors and nanowires, surface coatings, composite materials (“nanoceramics”), functional fibers for clothing and sports equipment to novel approaches in cancer therapy (Borm *et al.* 2004; Chen *et al.* 2004; Hunt 2004; Oberdorster 2004; Oberdorster *et al.* 2005; Hardman 2006; Horton *et al.* 2006; Jordan *et al.* 2006; Chen *et al.* 2007; Reddy *et al.* 2007).

Materials that are able to accomplish such diverse tasks are certainly very different one from another. Nevertheless, nanomaterials that share certain features can be put into groups such as fibrous nanomaterials (e.g. carbon nanotubes), metal oxide nanoparticles (e.g. silica, titaniumdioxide) or quantum dots (fluorescent particles consisting of a metalloid crystalline core and a shell). Anyway, the common feature of all nanomaterials is, by definition, their size. To be classified as “nano”, a material has to measure below 100 nm in at least one dimension (Kurath *et al.* 2006).

“Nano” is greek and means “dwarf”. As we know from fairy tales, there are different kinds of dwarfs: friendly, useful dwarfs (as the “Heinzelmännchen”, who do the work for you at night), dwarfs who can perform real miracles, but lateron become awkward (Rumpelstiltskin, spinning straw to gold but demanding the child of the queen) and the ugly, mean dwarfs (as in Snow White and Rose Red; a dwarf turning a prince into a bear). This trias of good, good under certain conditions and bad is most likely the same for nanomaterials.

1.2 Inhalation toxicology and nanotoxicology

Nanosized structures have been around during almost the entire life of our planet: Volcanic eruptions and combustion processes such as forest fires have been producing nanoparticles long before mankind acquired the ability to generate nanoparticles. But since then, the number of nanoparticles that we are exposed to is continuously growing. On the one hand, nanoparticles occur incidentally: Traffic leads to abrasion of tires and emission of diesel soot; combustion processes, heating, cooking and smoking increase the particle load in the air. On the other hand, the growing industrial production of nanoparticles for various applications increases the possibility to come into contact with nanosized structures both for humans and the environment.

Nowadays, the average concentration of particulate matter ranges between 20 to 50 $\mu\text{g}/\text{m}^3$ in cities of industrialized countries (Kreyling *et al.* 2006). Even though only 10% of the mass of the particulate matter are ultra-fine particles, their number concentration comprises more than 90% of the particles (Wichmann *et al.* 2000). Once inhaled, the fate of the particles depends largely on their size. Very large (micron-sized) and very small particles (1 nm) are deposited preferentially in the nasopharyngeal compartment (90%). Particles of a size of 5 nm are distributed quite equally to the nose, the tracheobronchial and the alveolar region (each ~30%). Deposition in the alveolar region is predominant for 20-nm particles (~50%) (Oberdorster *et al.* 2005). Therefore, most nanomaterials will be able to penetrate deep into the lung and reach the sensitive area of gas exchange.

Upon deposition on the lung epithelium, the particles may be phagocytosed by alveolar macrophages and thus cleared from the lung. This is also a size-dependent process which works best for particles >100 nm. For smaller sizes, a clearance of only 20% has been observed (Oberdorster *et al.* 2005). Particles that escape clearance can be taken up by epithelial cells and have been found intracellularly in different cellular compartments, but mostly outside the nucleus (Savic *et al.* 2003; Limbach *et al.* 2005; Chithrani *et al.* 2007; Gojova *et al.* 2007; Limbach *et al.* 2007; Suzuki *et al.* 2007; Barnes *et al.* 2008). Another possibility for particles is to translocate into the interstitium and consequently gain access to all body compartments via lymph or blood vessels. An important secondary target organ where nanoparticles have been retrieved, is the liver (Takenaka *et al.* 2001; Nemmar

et al. 2002; Oberdorster *et al.* 2002; Borm *et al.* 2004). To summarize, inhalation of nanoparticles has to be taken into consideration as an important route of exposure.

To assess the consequences of an exposure to nanosized structures, the field of nanotoxicology evolved. Its objectives are, according to Oberdörster, the “safety evaluation of engineered nanostructures and nanodevices” (Oberdorster *et al.* 2005). Nanotoxicology can make use of the previous studies that have examined the health effects of airborne ultrafine particulate matter. Besides carbon, particulate matter contains also numerous metals (including Fe, Ni, Ti, S, Cd, Pb, V, Zn) and metal oxides (Knaapen *et al.* 2002; Fritsch *et al.* 2006) which are nowadays frequently the constituents of intentionally produced synthetic nanosized metal oxide particles. For particulate matter, it has been shown that the exposure to elevated levels can be responsible for respiratory and cardio-vascular diseases (Peters *et al.* 1997a; Peters *et al.* 1997b; Ghio *et al.* 2000; Gold *et al.* 2000; Peters *et al.* 2000; Prescott *et al.* 2000; Donaldson *et al.* 2001; Ghio *et al.* 2001; Peters *et al.* 2001a; Peters *et al.* 2001b; Borm *et al.* 2004; Duggen 2004).

On the cellular level, various nanomaterials (Ag, carbon black, single-walled carbon nano tubes, SiO₂, TiO₂, ZnO, CdSe quantum dots) lead to a decrease in cell viability in different cell types (alveolar macrophages, primary mouse fibroblasts, primary hepatocytes, human lymphoblastoid cells) (Derfus *et al.* 2004; Kisin *et al.* 2007; Wang *et al.* 2007a; Wang *et al.* 2007b; Ahamed *et al.* 2008; Yang *et al.* 2009). Moreover, a release of inflammatory mediators (IL-6, IL-8, TNF α , arachidonic acid) has been observed after exposure to nanosized material (Hashimoto *et al.* 2000; Diabate *et al.* 2002; Schaumann *et al.* 2004; Wottrich *et al.* 2004; Monteiller *et al.* 2007). The generation of reactive oxygen species (ROS) and oxidative stress was observed after exposure of cells to metal oxide nanomaterials (Limbach *et al.* 2007; Karlsson *et al.* 2008; Yang *et al.* 2009). Furthermore, for some types of particles (Ag, Al₂O₃, cobalt, TiO₂, carbon black, carbon nanotubes, CuO, ZnO), DNA damage was found after exposure (Kisin *et al.* 2007; Mroz *et al.* 2007; Papageorgiou *et al.* 2007; Wang *et al.* 2007a; Ahamed *et al.* 2008; Colognato *et al.* 2008; Karlsson *et al.* 2008; Mroz *et al.* 2008; Balasubramanyam *et al.* 2009; Yang *et al.* 2009).

Thus, there is concern that nanomaterials may have negative consequences for human health. However, for many of the novel, synthetically produced nanomaterials, the biological effects and the underlying mechanisms are largely unknown. For this reason, I examined the cellular effects of synthetic metal oxide nanomaterials. In

particular, I was focusing on their influence on genomic DNA, i.e. their genotoxic potential, for which oxidative stress is supposed to be an important mechanism.

1.3 Reactive oxygen / nitrogen species and oxidative stress

1.3.1 Reactive oxygen species and reactive nitrogen species

Reactive oxygen species (ROS) and reactive nitrogen species (RNS) are one of the major threats to cellular integrity. The term ROS/RNS includes e.g. superoxide anions ($\cdot\text{O}_2^-$), hydroxyl radicals ($\cdot\text{OH}$), and nitrogen monoxide ($\cdot\text{NO}$). These molecules contain unpaired electrons (i.e. they are radicals) and consequently exhibit a high reactivity. ROS also designates non-radicals like hydrogen peroxide (H_2O_2) or hypochlorous acid (HOCl), which also possess a high reactivity.

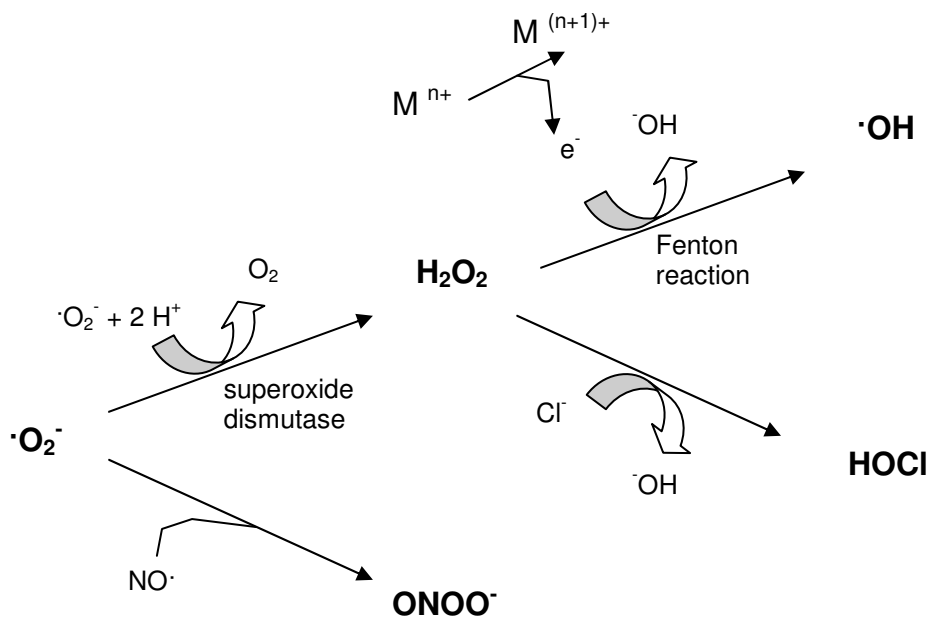


Fig. 1 Generation and conversion of reactive oxygen/nitrogen species.

Superoxide anion ($\cdot\text{O}_2^-$) can either react with $\text{NO}\cdot$ to form peroxynitrite (ONOO^-) or is converted by the enzyme superoxide dismutase to hydrogen peroxide (H_2O_2). H_2O_2 either generates hypochlorous acid (HOCl) or is converted to hydroxyl radical ($\cdot\text{OH}$) in the presence of electrons derived from transition metals (M) (Fenton reaction). Modified after Valko, 2006.

ROS are generated endogenously by the cellular metabolism itself. For example, during electron transport in the mitochondrial electron transport chain, electron “leakage” can occur (Genova *et al.* 2004) leading to the generation of superoxide anions (Loschen *et al.* 1971). Moreover, ROS are generated deliberately by immune

cells (macrophages, neutrophils, eosinophils) during inflammation as a defense against microorganisms (“oxidative burst”) (Valko *et al.* 2006).

Furthermore, numerous toxic substances (e.g. metal ions) or irradiation lead to the exogenous generation of ROS (Lloyd *et al.* 1997; Klotz *et al.* 2001; Riemschneider *et al.* 2002; Barthel *et al.* 2007). As Fig. 1 shows, ROS can be converted into other forms of ROS, yielding species with lower (H_2O_2) or higher reactivity ($\cdot\text{OH}$) (Sies 1993).

Because of their high reactivity, ROS oxidize components of the cell, e.g. membrane lipids, proteins or the DNA. The stability of different ROS varies significantly. The highly reactive hydroxyl radical with a half-life of 10^{-9} s will most likely react at or very close to the place of its generation, whereas the much more “stable” hydrogen peroxide is able to translocate to other cellular compartments before performing oxidation (Shacter *et al.* 1988; Sies 1993).

Cells acquired diverse mechanisms to eliminate ROS, e.g. anti-oxidative substances like glutathione, carotenes (Valko *et al.* 2004), vitamin C (Wayner *et al.* 1986) or E (Dean *et al.* 1987), or enzymes that convert highly reactive ROS into less reactive products. For example, superoxide dismutase catalyzes the conversion of superoxide anion to hydrogen peroxide, which in turn can be converted to water by the enzyme catalase (Gruber *et al.* 1990; Sies 1993; Michiels *et al.* 1994).

1.3.2 Oxidative stress

If the cellular anti-oxidative defense is no longer able to cope with ROS, “oxidative stress” occurs (Sies 1991). Excessive ROS generation can be the result of additional production of oxygen radicals by toxic substances or irradiation, or a decreased amount of antioxidants or impaired anti-oxidative enzymes (Sies 1993).

The consequences of the oxidation of cellular structures and molecules can be fatal: Protein oxidation may result in inhibition of enzymes. Major targets are for example phosphatases, where an oxidation of the sulphhydryl residues of cysteins results in the formation of disulfide bonds and subsequently in changes of the protein conformation (Valko *et al.* 2006). Oxidative modification of DNA bases can lead to mutations and strand breaks; e.g. oxidation of guanine may induce G:C to A:T transversions or

strand breaks if the oxidized base is excised. Peroxidation of phospholipids that constitute membrane bilayers results in membrane damage. Degradation of the oxidatively damaged structures and cellular malfunction are possible consequences. Finally, the induction of apoptosis or necrosis may lead to cell death.

1.3.3 Oxidative stress in carcinogenesis

Numerous studies confirm the importance of oxidative stress as a mechanism of genotoxicity and in the pathogenesis of several diseases, for example in carcinogenesis (reviewed in Mates *et al.* 2008; Toyokuni 2008; Valko *et al.* 2006). Tumor formation occurs mainly by two mechanisms: Firstly, the direct interaction of ROS with DNA leads to mutations and DNA damage (e.g. strand breaks). In many cancers, an elevated level of 8-oxo-guanine (8-oxo-G), a major product of DNA oxidation, has been observed (Mates *et al.* 2008). Moreover, the products of the oxidation of cellular molecules can also damage the DNA. For example, lipid peroxidation generates malondialdehyde and 4-hydroxy-2-nonenal. Both are potent mutagens (Marquez *et al.* 2007). Secondly, ROS have been found to interfere with intracellular signalling pathways regulating cell proliferation. These include signal transduction pathways using the transcription factors activating protein-1 (AP-1) and nuclear factor kappa B (NFκB), p53, HIF-1 and nuclear factor of activated T-cells (NFAT) (Valko *et al.* 2006), as well as Ras-coupled mitogen-activated protein kinase (MAPK) cascades (Sugden *et al.* 2006). The activation of these signalling pathways finally leads to the transcription of genes involved in cell growth regulation resulting in elevated cell proliferation.

Nevertheless, high levels of ROS can also exert the opposite effect, namely the induction of apoptosis (Valko *et al.* 2006; Mates *et al.* 2008).

1.4 Genotoxicity

The term “genotoxic” has been used for the first time in 1973 by Hermann Druckrey during a conference on “Evaluation of genetic risks of environmental chemicals” in Sweden. He stated: “In order to describe the components of chemical interaction with genetic material, the term genotoxic is proposed as a general expression to cover toxic, lethal and heritable effects to karyotic and extrakaryotic genetic material in germinal and somatic cells.” (Weisburger *et al.* 2000).

Since then, genotoxicity has become an important field of toxicological research, and genotoxicity testing is nowadays an integral part of the toxicity assessment of chemical substances, as the integrity of the DNA is essential for cells, whole organisms and their offspring.

A genotoxic action can be due to a number of different mechanisms, which I will describe in the following chapter. In general, there are two ways for substances to affect the DNA: either via direct interaction and alteration of the DNA or indirect mechanisms which cause DNA damage or genome alterations via intermediate steps or compounds.

1.4.1 Direct genotoxicity

Direct genotoxicity includes the formation of DNA-adducts and the modification of DNA components such as DNA bases and the phospho-deoxyribose-backbone.

1.4.1.1 DNA adducts

In case a substance gets into direct contact with the DNA (either it enters the nucleus or attacks the DNA during mitosis), DNA adducts can be formed. This has been extensively studied for polycyclic aromatic hydrocarbons (PAH), such as benzo[a]pyrene. The addition of such bulky molecules to the DNA bases leads to increased lability of the glycosidic bond and consequently a higher rate of depurination and the occurrence of abasic sites. Moreover, bulky modifications hinder DNA replication (Baird *et al.* 2005).

Recently, the possibility of DNA adduct formation has been suggested for fullerenes (Balbus *et al.* 2007). Furthermore, adduct formation may also be of some relevance in particle genotoxicity as airborne particles often contain PAH (Li *et al.* 2003).

1.4.1.2 Chemical modification of DNA

The most important chemical modifications of the DNA are alkylation and oxidation.

Alkylating substances transfer methyl- or ethyl-groups to nucleotides, yielding mainly 7-alkylguanine and 3-alkyladenine. Alkylation products are either often directly mutagenic (e.g. O⁶-methylguanine pairs with thymine instead of cytosine) or cause DNA strand breaks during the repair of alkylation damage (Sedgwick 2004; Wyatt *et al.* 2006). Examples for alkylating chemicals are methyl-methane sulfonate (MMS) or

N-methyl-N'-nitro-N-nitroso-guanidin (MNNG). In this work, MMS was used as a positive control for DNA damage and DNA strand breaks.

Of great importance for this study is the oxidative modification of DNA bases, as cells are likely exposed to oxidative stress after treatment with nanomaterials. Specific DNA modifications have been described for different ROS, e.g. the deamination or nitration of bases for peroxynitrite or the formation of 5-chlorouracil for HOCl (Whiteman *et al.* 1997; Burney *et al.* 1999; Whiteman *et al.* 1999; Tuo *et al.* 2000). However, the hydroxyl radical is supposed to be the most relevant ROS in the oxidation of the DNA (Pryor 1988). Due to their short half-life, hydroxyl radicals affecting the DNA are mostly produced from the more stable H_2O_2 via Fenton reactions in proximity of the DNA. Hundreds of different kinds of oxidized bases have been identified, e.g. 8-oxo-7,8-dihydroguanine, 5-hydroxymethyluracil, 5-hydroxyuracil, 5-hydroxyadenine, 8-hydroxyadenine and 2,6-diamino-4-hydroxy-5-formamidopyrimidine (Wiseman *et al.* 1996) of which 8-oxo-7,8-dihydroguanine (8-oxo-G, see Fig. 2) is by far the most important and the best studied oxidation product. Guanine is oxidized preferentially due to its low oxidation potential (Neeley *et al.* 2006).

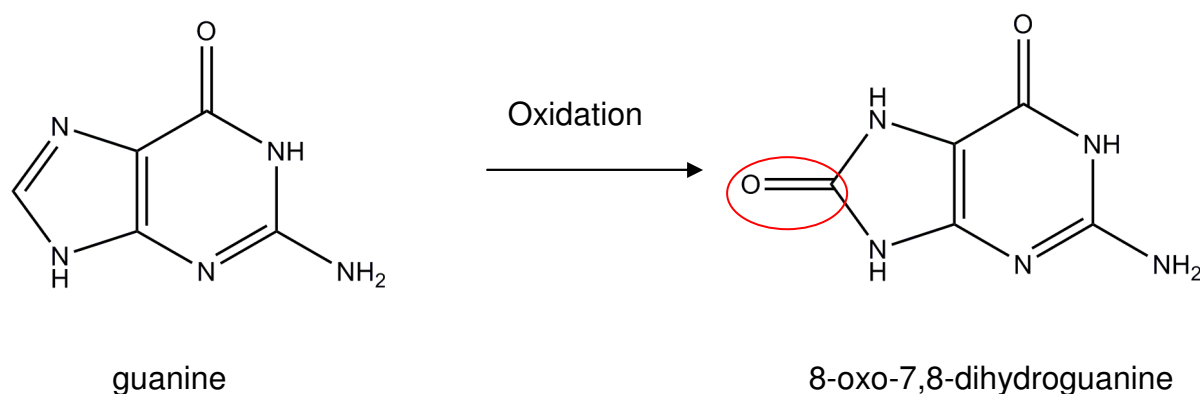


Fig. 2 Oxidation of guanine to 8-oxo-7,8-dihydroguanine.

In the presence of ROS, guanine becomes oxidized at the C8-position (red circle) to yield 8-oxo-7,8-dihydroguanine.

8-oxo-G can end up in the DNA by two ways: Either guanine in the DNA is directly oxidized, or guanine contained in the guanosine triphosphate (GTP) pool of the cell is oxidized and subsequently inserted into the DNA during DNA synthesis. In the first case, 8-oxo-G can, in addition to the usual pairing with cytosine, combine with adenine (Fig. 3). If this mispairing is not removed before DNA replication, a thymine

will be inserted opposite to the “wrong” adenine, hence, a G:C to T:A transversion results (Akasaka *et al.* 1994). In the second case, the 8-oxo-GTP-nucleotide is preferentially inserted opposite to an adenine, leading to an A:T to C:G transversion (Grollman *et al.* 1993; Demple *et al.* 1994). In any case, these are mutagenic lesions, which, if they affect important genes (e.g. tumor-suppressor genes, oncogenes) can have fatal consequences for the cell.

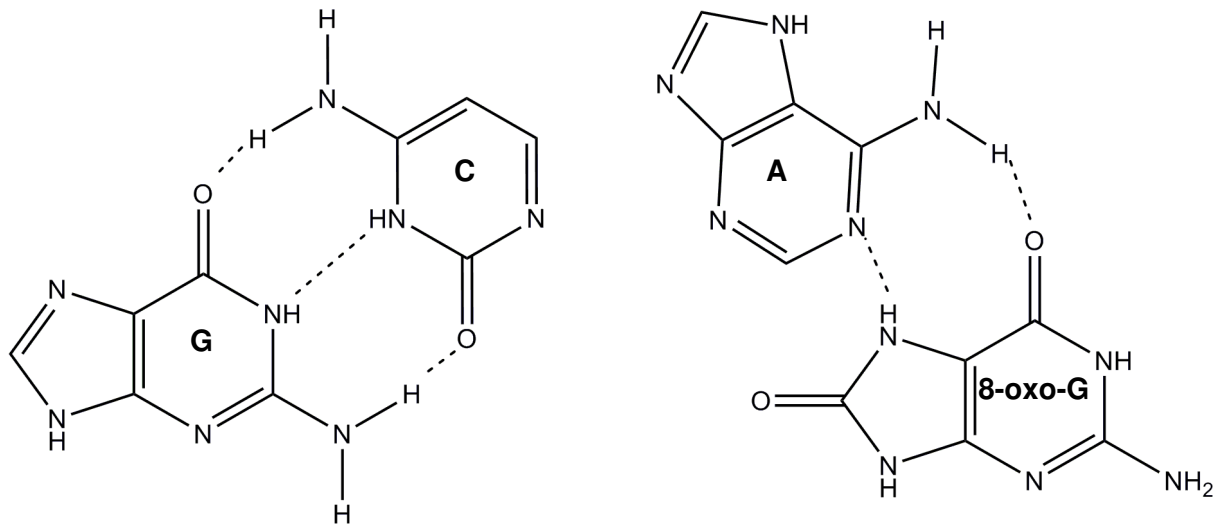


Fig. 3 Base pairing of guanine and 8-oxo-guanine in the DNA.

Left: Guanine (G) usually pairs via three hydrogen bonds (dashed lines) with cytosine (C). Right: In addition to pairing with cytosine, 8-oxo-guanine (8-oxo-G) is able to pair with adenine (A) via two hydrogen bonds.

Besides oxidation of DNA bases, the sugar-phosphate-backbone of the DNA can as well be a target of ROS. Abstraction of hydrogen atoms generates sugar radicals which result in DNA strand breaks, base free sites or intramolecular cyclization (Eastman *et al.* 1992; Dizdaroglu *et al.* 2002).

1.4.2 Indirect genotoxicity

Indirect genotoxicity means that the DNA is not affected directly by a chemical substance, but indirectly via inhibition or disturbance of enzymes (e.g. replicative or repair enzymes) or processes (mitosis) that are important for the integrity and the maintenance of the DNA.

1.4.2.1 Enzyme inhibition

One major way to indirect genotoxicity is the inhibition of enzymes involved in DNA synthesis and maintenance. These enzymes may be affected by the direct binding of

a chemical substance (leading to competitive or non-competitive inhibition, depending on the nature of the binding) or by oxidation. Oxidation of catalytically important amino acid residues (the SH-group of cysteine or the OH-groups of serine, tyrosine or threonine) in the catalytic centre of the enzyme can lead to catalytical disfunction of the enzyme whereas modification of residues outside of the catalytical centre may induce conformational changes which hinder substrate binding.

Enzymes that have been described to be involved in indirect genotoxicity include DNA repair proteins (e.g. MLH2, MSH, OGG1, XPD, PARP) (Kirsch-Volders *et al.* 2003; Mateuca *et al.* 2006), topoisomerases (TOPO II) (Ferguson *et al.* 1994), DNA-methylases (MGMT) (Das *et al.* 2004), histone deacetylases (Eot-Houllier *et al.* 2009) and many others.

1.4.2.2 Interference with cell division

Cell division is a cellular process which is especially vulnerable towards genotoxins. The replication of the DNA has to be accomplished successfully and without errors. Moreover, the spindle apparatus has to be set up correctly, and the right number of chromosomes has to be drawn towards the poles. Disturbance of the mitotic spindle and chromosome segregation therefore represents another mechanism of indirect genotoxicity.

Mitosis involves a plethora of proteins and structures, but I will present only a few examples which are relevant to the experiments presented in this work.

Essential mitotic processes which, if impaired, lead to genotoxicity, include the assembly of the mitotic spindle, the attachment of the spindle fibers to the chromosomes and the separation of the chromosomes during anaphase.

The mitotic spindle consists of microtubules (MT). The attachment of the microtubules to the chromosomes is dependent on proper kinetochore structure and function and several proteins that correct misattachments, e.g. the microtubule depolymerase MCAK and the protein kinase Aurora B (Lan *et al.* 2004; Ohi *et al.* 2004; Cimini *et al.* 2005). If chromosomes are not attached to MTs, lagging chromosomes result that will not be drawn to the poles. If wrong attachment occurs, e.g. syntelic attachment (both chromatids are connected to MTs from only one pole), daughter cells result of which one disposes of one excess chromosome, and one which lacks a chromosome.

Polymerization and depolymerization of microtubules, which is essential for spindle formation and chromosome segregation, are regulated by numerous factors, e.g.

protein phosphatases (protein phosphatase 1, PP1, and protein phosphatase 2A, PP2A, Cdc25 and Cdc14), and the phosphoprotein stathmin. Phosphorylation of stathmin induces tubulin polymerization and hence the formation of the mitotic spindle; dephosphorylation of stathmin leads to depolymerization and is thus important for chromosome separation (Le Hegarat *et al.* 2003).

Cdc25 phosphatases control the activity of cyclin-dependent kinase 1 (CDK1) which is responsible for mitotic entry. CDK1 phosphorylates tubulin, which leads to MT polymerization. Inhibition of Cdc25 induces delayed mitotic spindle assembly, chromosome capture and metaphase plate formation (Cazales *et al.* 2007).

Cdc14 phosphatases are key regulators of mitotic exit by deactivating CDKs. They coordinate chromosome segregation with mitotic spindle disassembly and cytokinesis. Furthermore, the human Cdc14B is responsible for microtubule bundling and stabilization (Cho *et al.* 2005; Trinkle-Mulcahy *et al.* 2006). If Cdc14 phosphatases are impaired, the consequences include defects in mitotic progression, multipolar spindles, inhibition of cytokinesis and incomplete chromosome segregation (Nalepa *et al.* 2004).

1.4.3 Consequences of genotoxicity and cellular responses

Various phenomena can be observed in cells exposed to genotoxic agents. Among them are mutations, DNA strand breaks and micronuclei. Cells can respond to DNA damage by DNA repair, cell cycle arrest or apoptosis.

1.4.3.1 Base modifications

The mutagenic potential of DNA alkylation and oxidation was described in chapter 1.4.1.2. The modification of bases entails the possibility of mispairing and hence base transversions or transitions. This kind of DNA damage is corrected by the base-excision repair (Abalea *et al.* 1998). A glycosylase enzyme (e.g. hMYH or the oxoguanine glycosylase OGG1 in humans) excises the modified base by breaking the N-glycosidic bond. An abasic site occurs that is recognized by an AP endonuclease (which can also be an integral part of bifunctional glycosylases as OGG1). This enzyme nicks the DNA at the 5'-end and creates a free 3'-OH group. DNA polymerase beta replaces the abasic nucleotide using its exonuclease activity. The repaired DNA is finally ligated by a DNA ligase (LigIII)/XRCC1 (Ide *et al.* 2004; Fortini *et al.* 2007).

1.4.3.2 DNA strand breaks

DNA breakage can result from a direct attack on the DNA molecule, e.g. by hydroxyl radicals which abstract hydrogen atoms from the phosphate-sugar backbone. The consequences are single- and double strand breaks. Moreover, DNA strand breaks occur also during repair of oxidation or alkylation damage.

The measurement of DNA strand breaks has become an important feature of genotoxicity testing and is mostly done by the comet assay. The neutral comet assay detects only double strand breaks, whereas the more widely used alkaline comet assay detects both single and double strand breaks as well as abasic sites.

DNA single strand breaks can be repaired using the complementary strand. Double strand breaks are repaired either via homologous recombination or via non-homologous end-joining. Homologous recombination requires at first the resection of the 5' end of the damaged chromosome. In the following strand invasion an overhanging 3' end of the damaged chromosome "invades" the undamaged homologous chromosome leading to formation of a Holliday junction. DNA strands are then completed and resolved to end up with the repaired DNA (Sung *et al.* 2006). Non-homologous end-joining requires recognition of the break by the Ku heterodimer (Ku70 and Ku80) and the kinase DNA-PKcs (DNA dependent protein kinase catalytic subunit). XRCC4 and ligase IV then perform ligation and DNA polymerases finally close the gaps (Pastwa *et al.* 2003).

1.4.3.3 Micronuclei

Micronuclei are small cellular structures that resemble the main nucleus, but with only 1/16 to 1/3 of the diameter of the main nucleus. Micronuclei result either from whole chromosomes or chromosome fragments that were not distributed properly during mitosis and are consequently surrounded by their own nuclear membrane (Fig. 4).

Substances which induce micronuclei that contain a whole chromosome are called "aneugens". The underlying mechanisms which cause lagging chromosomes are for example defects in the chromosome segregation machinery, deficiencies in the cell cycle controlling genes, failure of the mitotic spindle, misattachment of tubulin fibers at the kinetochore, premature tubulin depolymerization, defects in centromeric DNA (e.g. hypomethylation) in kinetochore proteins or kinetochore structure.

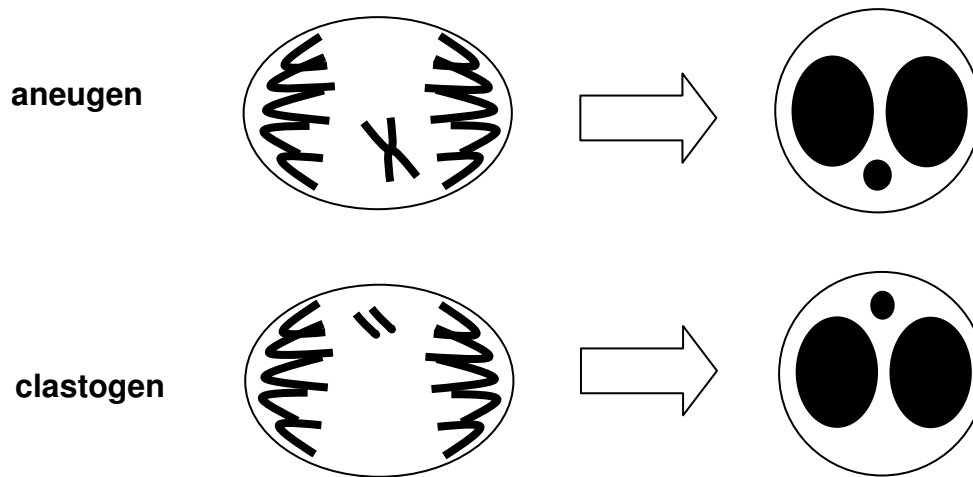


Fig. 4 Formation of micronuclei.

Micronuclei arise either from whole chromosomes (upper panel, aneugen) or from chromosome fragments (lower panel, clastogen) that cannot be distributed properly during mitosis. Modified after Bonassi *et al.* 2007.

Substances which are responsible for micronuclei containing only chromosome fragments are called “clastogens” Such micronuclei can result from DNA double-strand breaks, conversion of single strand breaks into double strand breaks after cell replication, or an inhibition of DNA synthesis. Moreover, defective repair of chromosome breaks may result in an asymmetrical chromosome rearrangement producing a dicentric chromosome (containing two centromeres) and an acentric fragment (without centromere). The acentric fragment cannot be attached to the mitotic spindle and hence lags behind to form a micronucleus. (The dicentric chromosome may give rise to a nucleoplasmatic bridge: MTs from both poles may be attached at the two centromeres. The chromosome is thus drawn to opposite poles of the cells resulting in the formation of a nucleoplasmatic bridge between the two daughter nuclei). Another mechanism of micronuclei formation is gene amplification. Amplified DNA is localized to specific sites at the periphery of the nucleus. Nuclear buds are formed to eliminate the amplified DNA. Consequently, breakage-fusion-bridge cycles of the nuclear buds lead to the formation of micronuclei (Cimini *et al.* 2005; Mateuca *et al.* 2006; Fenech 2007).

Bonassi *et al.* showed that an increase in the number of micronuclei is correlated with an increased cancer incidence (Bonassi *et al.* 2007). Thus, the micronucleus assay is an important test to evaluate the genotoxicity of chemical compounds. Besides the genotoxic potential, numerous other parameters can be scored in this assay in parallel, giving a comprehensive view of the toxicological behavior of a substance.

The micronucleus test is therefore often called “cytome assay”. Examples for additional parameters are the nuclear division index (NDI, indicative for cytostatic properties), the number of apoptotic cells, the number of mitotic cells, the number of nucleoplasmatic brigdes (indicative for chromosome rearrangements) and the number of nuclear buds (indicative for gene amplification) (Fenech 2007).

Micronuclei are rarely remediated, e.g. by reincorporation of whole chromosomes into the nucleus (Mateuca *et al.* 2006). However, the elimination of micronucleated cells by induction of apoptosis may occur (Decordier *et al.* 2002).

1.4.3.4 Fate of cells with persisting DNA damage

As described above, a cell has various possibilities to repair DNA damage. However, if the DNA damage is irreparable, other mechanisms protect the organism against the threat a cell with defective DNA constitutes, namely cell cycle arrest and apoptosis.

Fig. 5 shows a simplified overview of the pathways which lead to cell cycle arrest or apoptosis after DNA damage. The recognition of DNA damage leads to an activation of kinases (ATM, DNA-PK) which cause an accumulation of p53, either directly or via checkpoint kinases (Chk1/2). p53 can then induce cell cycle arrest through activation of p21^{Cip1} and the subsequent inhibition of cyclin-dependent kinases (CDKs). Cell cycle arrest can also be mediated via inhibition of Cdc25 phosphatase by Chk1/2, which results in inactivation of CDKs. Cell cycle arrest provides the cell with time to accomplish successful DNA repair. If the DNA damage is irreparable, apoptosis can be triggered by p53 via Bax (Zhou *et al.* 2000).

If these mechanisms fail, e.g. because one of the components is dysfunctional due to a mutation or inhibited as a consequence of protein oxidation, cells might accumulate even more DNA damage and finally become tumor cells.

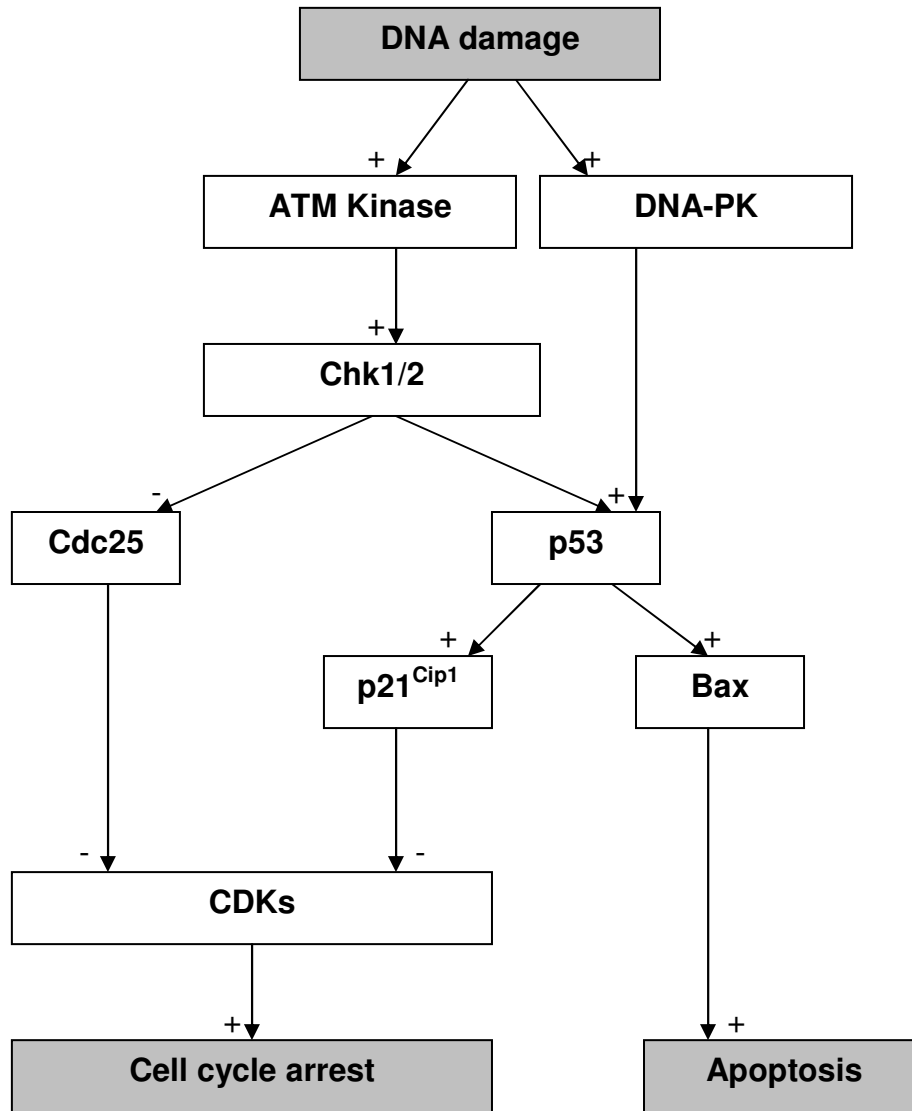


Fig. 5 Cellular responses to DNA damage.

Cells unable to repair DNA damage undergo cell cycle arrest or apoptosis. A schematic, simplified pathway of the induction of both events is shown: DNA damage leads to the activation of ATM kinase or DNA-protein kinase (DNA-PK). ATM Kinase activates checkpoint kinases (Chk1/2) which either negatively regulate Cdc25 phosphatase which inhibits cyclin-dependent kinases (CDKs) and induces cell cycle arrest or positively regulate p53. p53 can also be activated by DNA-PK directly. Accumulation of p53 then leads on the one hand to activation of p21^{Cip1} which inhibits cyclin-dependent kinases (CDKs). This results in cell cycle arrest. On the other hand, p53 can also induce apoptosis via the pro-apoptotic Bax protein. (+) activation; (-) inactivation. Modified after Zhou, 2000.

Fig. 6 summarizes possible mechanisms exerted by a genotoxic substance including primary and secondary genotoxicity, the direct or indirect affection of the DNA, the possible lesions and consequences and the progress to carcinogenesis via an elevated cell proliferation.

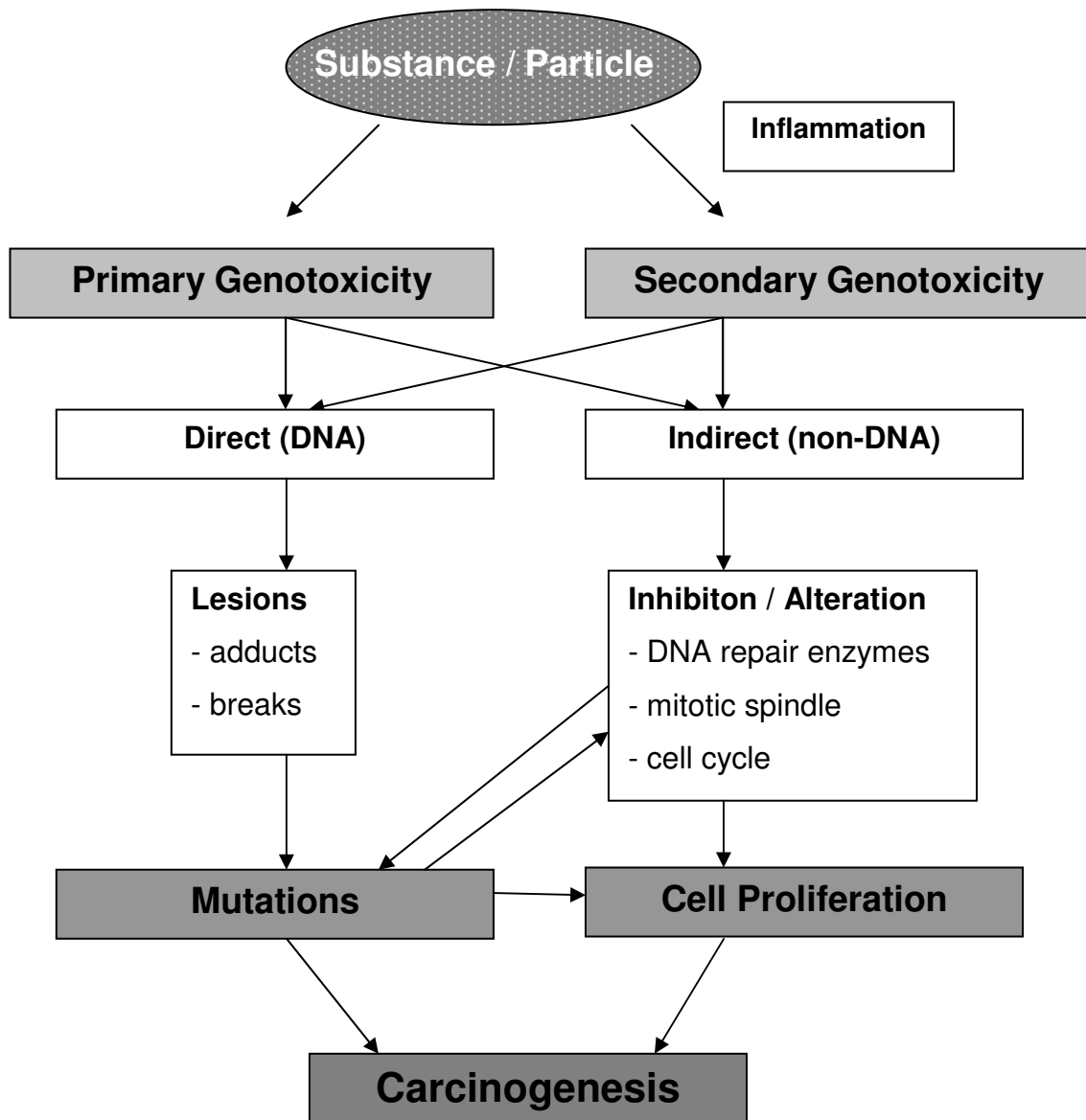


Fig. 6 Overview over mechanisms of genotoxicity elicited by a genotoxic substance/particle.

A genotoxic substance can either directly induce genotoxic actions (primary genotoxicity) or induce inflammation which results in oxidative stress leading to DNA damage (secondary genotoxicity). The target can either be the DNA itself (direct genotoxicity) or processes involved in the maintenance and the integrity of the DNA (indirect genotoxicity). The consequences for both ways are mutations and enhanced cell proliferation which finally may result in carcinogenesis. Modified after Kirsch-Volders, 2002.

1.4.4 Increased genotoxicity for nanoparticles?

Most of the nanoparticles that are produced to date are composed of chemical substances that have been used for several decades as bulk substances (e.g. TiO₂ or SiO₂). The toxicity of these bulk materials has consequently been tested and evaluated extensively. Why is there concern that nanomaterials are more harmful to cells and the DNA than the corresponding bulk material?

As mentioned above, reduction to the nanometer scale brings about novel characteristics. Thus, nanomaterials display other properties than their corresponding bulk substances. One of the most important advantages of nanomaterials is their high specific surface, which is moreover much more reactive than the surface of bulk materials. This is due to the fact that nanoobjects frequently have structural defects in crystal planes which disrupt the well-structured electronic configuration of the material. The consequences are reactive sites that allow the transfer of electrons to e.g. molecular oxygen which generates superoxide anion (Nel *et al.* 2006). Such electron transfer processes lead to elevated levels of ROS and subsequently to oxidative stress which in turn induces oxidative DNA damage.

Moreover, there is no need for direct ROS generation via the nanomaterial itself to induce oxidative DNA damage. Exposure to high concentrations of particles often results in inflammatory reactions which are characterized by a release of ROS from inflammatory cells (macrophages, neutrophils, eosinophils). This so-called oxidative burst is a protective mechanism against invading microorganisms, but these reactive oxygen species can as well induce DNA damage. This phenomenon is called secondary genotoxicity (Schins 2002). It has been shown that inflammatory reactions are more pronounced upon inhalation of nanomaterials than after inhalation of larger sized materials (Borm *et al.* 1996; Monteiller *et al.* 2007).

Another possibility of how ROS can induce DNA damage is via the oxidative toxification of inhaled substances which are precursors of DNA-damaging compounds. For example, the ROS released by neutrophils are able to transform aromatic compounds such as benzene into more carcinogenic metabolites (Tuo *et al.* 1998).

Furthermore, there is concern that nanoparticles (e.g. fullerenes (Balbus *et al.* 2007)), could directly bind to the DNA (if they were able to enter the nucleus). This would lead to the formation of adducts that hinder DNA replication. Binding of nanoparticles to proteins involved in the synthesis, maintenance and DNA repair may be another

mechanism leading to DNA damage (Borm *et al.* 2004; Donaldson *et al.* 2004; Kreyling *et al.* 2004).

The high specific surface of nanomaterials also brings about an increased solubility in comparison to bulk material (Borm *et al.* 2006; Pickrell *et al.* 2006; Franklin *et al.* 2007). Leaching of ions, especially of genotoxic metal ions, is hence another mechanism which is more relevant for nanomaterials than for bulk material.

At last, it is also possible that particles act like “Trojan horses”. Airborne particles may “collect” volatile chemical substances which otherwise would not have been able to enter the alveolar region and to deposit in the lung. Thus, exposure to nanomaterials may provide new ways of exposure to environmental and possibly genotoxic chemicals (Schins 2002; Balbus *et al.* 2007).

To conclude, the genotoxicity of nanomaterials may be increased in comparison to their corresponding bulk materials because of 1. The elevated production of ROS (both direct and indirect) 2. The binding to DNA and proteins leading to hindrance of DNA-related processes 3. The enhanced solubility leading to release of genotoxic metal ions and 4. The introduction of toxic chemicals into the lung or the toxification of pre-carcinogens.

Most of these mechanisms are hypothetical and poorly studied. However, knowledge about the genotoxic potential of nanomaterials is highly important. Thus, I focused in this work on examining the genotoxicity of synthetically produced nanomaterials, in particular vanadium oxide nanomaterials.

1.5 Vanadium oxides

1.5.1 Occurrence and applications

Vanadium (V) is a transition metal which occurs naturally in the earth crust in various chemical compounds. As many transition metals, it exists in various oxidation states. The most common are V(III), V(IV) and V(V). Vanadium finds application mainly in ferrous alloys increasing the strength of steel used as tools or implants. Moreover, vanadium is found in mineral oil and in almost all coals, in concentrations ranging from extremely low to 10 g/kg for coal and up to 1.4 g/kg in Venezuelan crude oils. Combustion of these sources of energy leads to the release of particulate matter containing vanadium oxides (Aragon *et al.* 2005).

In this work, two different vanadium oxides were used: vanadium trioxide (V_2O_3) and vanadium pentoxide (V_2O_5). Vanadium oxides, in particular vanadium pentoxide (V_2O_5), are important catalysts for the synthesis of e.g. sulphuric acid. Further applications include their use as corrosion inhibitor, as coating for welding electrodes, as photographic developer, and in colloidal solution for anti-static layers on photographic material. Moreover, the colorful vanadium oxides are also used as blue and yellow pigments for ceramics and as ultraviolet light (UV) absorbers in glass. The total world production of V_2O_5 in 1996 was 59.500 tons (Ivancsits *et al.* 2002; IARC 2006).

Nanosized vanadium oxides are novel substances which may find application mainly as catalysts (Feldmann 2003). TiO_2 nanoparticles coated with vanadium pentoxide are used industrially to remove nitrous oxide from exhaust gases of combustion power plants and in biomaterials to increase the strength of implants (Bhattacharya *et al.* 2008).

1.5.2 Exposure

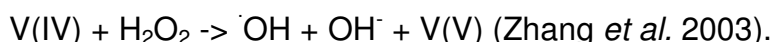
Humans are mainly exposed to vanadium oxides from anthropogenic sources (combustion and industrial processes). Approximately 70.000 to 210.000 tonnes per year have been emitted into the atmosphere during the 1990s worldwide (Nriagu 1998). The general population is exposed to concentrations of vanadium oxides of 1 - 40 ng/m^3 in rural air and to 50 - 200 ng/m^3 in cities. Blood levels of 0.02 - 0.1 $\mu g/l$ have been reported (WHO Regional Office for Europe Copenhagen 2000; IARC 2006).

Occupational exposure is relevant for individuals working with processing and refining of vanadium-rich ores and slags, production of vanadium and vanadium-containing products, cleaning of oil-fuelled boilers and furnaces, or persons who are handling catalysts in the chemical industry (IARC 2006). In these settings, vanadium oxide concentrations in the air are in the low mg/m^3 range, with peak concentrations of up to several hundred mg/m^3 . Biomonitoring of workers exposed to vanadium oxides revealed a 7-fold higher vanadium concentration in the blood than for non-exposed individuals (Ehrlich *et al.* 2008).

1.5.3 Generation of ROS by vanadium oxides

Most of the effects of vanadium oxides have been attributed to their capacity of producing ROS.

Vanadium compounds entering the cell are usually in the (V)-oxidation state and become reduced intracellularly (Hansen *et al.* 1982; Sabbioni *et al.* 1993). This reduction generates superoxide radical ($O_2^{\cdot-}$) and hydrogen peroxide (H_2O_2). Further radicals can be produced in Fenton-like reactions catalyzed by vanadium:



As the product is V(V), a new series of reductions and oxidations may start over. This redox-cycling results in a high amount of ROS that the cell has to cope with (Zychlinski *et al.* 1991; Leonard *et al.* 1994; Sit *et al.* 1996).

1.5.4 Biological effects and toxicity

In the aqueous environment inside an organism or a cell, vanadium oxides are present usually as vanadate ions, mostly as tetravalent (IV) vanadyl (VO^{2+}) and pentavalent (V) vanadate (HVO_4^- , VO_3^- and / or $H_2VO_4^-$) (Evangelou 2002). Various biological effects have been described and attributed to these soluble vanadium oxides species. The inhibition of the Na^+/K^+ ATPase by vanadate has been discovered in 1977 by Cantley *et al.* (Cantley *et al.* 1977). Since then, inhibition of phosphoenzyme ion-transport ATPases, acid and alkaline phosphatases, H^+/K^+ ATPase, phosphotyrosyl protein phosphatase, myosin ATPase, phosphofructokinase, adenylate kinase and cholinesterase has been described (Nechay *et al.* 1986). The mechanism of inhibition is based upon the structural similarity of the vanadate ion to phosphate (Cantley *et al.* 1978a; Crans *et al.* 1995). Binding of vanadate in the catalytical centre is supposed to result in the oxidation of essential amino acid (e.g. cysteine) residues and the consequent inhibition of the enzymatic function (Herrlich *et al.* 2000).

Phosphatase inhibition is also responsible for another vanadate-mediated effect. If phosphatase function lacks, the phosphorylation of the epidermal growth factor receptor (EGF-R) and the insulin receptor after ligand-binding persists (Tamura *et al.* 1984; Kadota *et al.* 1987a; Kadota *et al.* 1987b). This leads to enhanced activity of downstream protein kinases and stimulates cell proliferation. Consequently, glucose transport activity and glucose metabolism are increased (Becker *et al.* 1994;

Barceloux 1999). This is the so-called “insulin-like effect” of vanadium oxides (Zhao *et al.* 1996; Samet *et al.* 1998; Wang *et al.* 2000).

The insulin-like effect occurs only at low vanadium concentrations. At higher concentrations, the pro-proliferative action of vanadate is masked by the cytotoxicity of vanadium compounds. The reported threshold concentration lies between 10^{-10} M and 0.01 mM (Hanuske *et al.* 1987; Cortizo *et al.* 1995; Rehder *et al.* 2002). Fifty percent toxicity and inhibitory concentration (IC₅₀) respectively for vanadate have been reported to range between 100 μ M (Bracken *et al.* 1985b) and 1.27 ± 0.28 mM (Yang *et al.* 2004).

Induction of cell cycle arrest has also been reported after exposure of cells to vanadate. It has been shown that vanadate-mediated ROS formation activates ERK and p38. Consequently, p21 and Cdc2 are upregulated and Cdc25C is degraded, which finally leads to cell cycle arrest at the G2/M phase (Zhang *et al.* 2003).

1.5.5 Genotoxicity of vanadium oxides

Induction of different kinds of DNA damage have been observed after exposure to vanadium oxides. Incubation of isolated DNA with V(IV) induced hydroxylation of guanine yielding 8-oxo-G and subsequent DNA strand breakage (Shi *et al.* 1996; Lloyd *et al.* 1998). In different *in vitro* cell systems, DNA strand breaks, micronuclei, sister chromatid exchanges and chromosomal aberrations were found (Owusu-Yaw *et al.* 1990; Migliore *et al.* 1993; Zhong *et al.* 1994; Rojas *et al.* 1996; Ivancsits *et al.* 2002). Chromosome aberrations, sister chromatid exchanges and DNA strand breaks occurred in human peripheral lymphocytes and leukocytes, i.e. *ex vivo* (Rodriguez-Mercado *et al.* 2003). *In vivo* exposure of mice to vanadium compounds yielded DNA strand breaks and reprotoxic effects (Altamirano-Lozano *et al.* 1996; Altamirano-Lozano *et al.* 1999). Moreover, aneugenic effects due to disturbance of spindle formation and chromosome segregation have been described for vanadium compounds in lysed mitotic PtK cells (rat kangaroo) and cultured human lymphocytes respectively (Cande *et al.* 1978; Ramirez *et al.* 1997; IARC 2006). In occupationally exposed workers, an increase in oxidative DNA damage, in induction of micronuclei, nucleoplasmatic bridges and nuclear buds has been observed (Ehrlich *et al.* 2008). The inhibition of the repair of DNA double strand breaks and bleomycin-induced DNA damage by vanadium pentoxide has been reported as well (Ivancsits *et al.* 2002; Ehrlich *et al.* 2008).

Concerning tumorigenesis, an inhalation study (V_2O_5 at concentrations of 0, 1, 2 and 4 mg/m³, 6 h per day, 5 days/week for 104 weeks) revealed an increase in the incidence of alveolar and bronchiolar neoplasms as well as a significant increase in hyperplasia of alveolar/bronchial epithel in mice of both sexes and male rats (Ress *et al.* 2003). In contrast, in humans, no correlation between exposure to vanadium oxides and cancer incidence could be established yet. Thus, vanadium pentoxide is classified as “possibly carcinogenic to humans (group 2B)” (IARC 2006).

1.6 Objective of this work

Little is known about the genotoxicity of many of the novel nanomaterials that are produced nowadays. However, the results of studies with particulate matter raise concern that inhalative exposure to nanomaterials may lead to carcinogenesis. Moreover, the enhanced ability of nanomaterials to generate ROS that has been observed for many nanomaterials suggests an elevated genotoxic potential via oxidative DNA damage.

The aim of this work was to examine the genotoxic potential of synthetic nanomaterials in a human alveolar epithelial cell line (A549) as a model for inhalative exposure. I wanted to analyze and compare the biological and toxicological effects of different nanosized vanadium oxides (vanadium trioxide and vanadium pentoxide) and the same material in their bulky size. A set of different vanadium compounds, including soluble vanadate ions, was chosen to reveal underlying mechanisms or different modes of action of toxicity.

After determination of the physico-chemical properties of the vanadium oxide materials, the cellular response to these substances, including uptake and effects on cell viability and proliferation, were examined. The generation of reactive oxygen species was analyzed for particles alone and in combination with cells. Genotoxicity testing was then performed at non-cytotoxic concentrations. The following genotoxicity endpoints were examined: DNA base modifications (8-oxo-guanine formation; detection via a FITC-coupled probe and flow-cytometrical analysis), DNA strand breaks (comet assay) and the induction of clastogenic / aneugenic effects (micronucleus test). Moreover, effects on cell cycle progression were assessed using a flow cytometry-based analysis of the cell cycle.

As vanadium oxides find only limited application, I further compared their genotoxic effects to those of frequently, at large-scale produced nanomaterials (carbon black, titanium dioxide, zinc oxide) using the comet assay and the micronucleus test.

In conclusion, the main questions to be answered were:

1. Are nanomaterials genotoxic? What kind of DNA damage is induced? What are the mechanisms and consequences of genotoxicity?
2. Are there differences in the effects exerted by bulk and nanomaterials of the same chemical origin? Are there differences in the biological effects exerted by different vanadium oxides?
3. What could be the reason for different effects?

2 Materials and Methods

2.1 Material

2.1.1 Technical equipment

Product	Manufacturer
Analytical Scale Sartorius 1602 MP Casy [®] 1	Sartorius AG Mechatronik, Göttingen
CCD Camera Kappa DX 4	Kappa opto-electronics, Gleichen
Centrifuge 5415 C, 5417R	Eppendorf AG, Hamburg
Cryo 1 °C Freezing Container	Nalgene [™] , Labware, USA
Electrophoresis PowerPac Basic	Bio-Rad Laboratories GmbH, München
Electrophoresis Power Supply EPS 500/400	Pharmacia Biotech, Uppsala, Sweden
Flow Bench Lamin Air [®] HB2460	Heraeus Christ, Fellbach
Flow Cytometer BD LSR II	Becton Dickinson, Heidelberg
Fluorescence Microscopes DM IRE2 and Leitz DM IL	Leica Microsystems, Wetzlar
Fluorescence Reader FL600	MWG Biotech AG, Ebersberg
ICP-OES OPTIMA 4300 DV	Perkin Elmer, Waltham, Massachusetts, USA
Incubator CB 210	WTB Binder Labortechnik GmbH, Tuttlingen
Microplate Absorption Reader	VersaMax, Molecular Devices, Sunnyvale, CA, USA
Pipets „Research“	Eppendorf AG, Hamburg
Scale Mettler PC180	Mettler Waagen GmbH, Gießen
Sonifier B15	Branson, G. Heinemann, Schwäbisch Gmünd
Transmission Electron Microscope EM 109 T	Carl Zeiss AG, Oberkochen
UV-lamp NU-KL 15	Konrad Benda Laborgeräte, Wiesloch

2.1.2 Software

Product	Provider
CellQuest Pro (Flow Cytometer)	BD Biosciences, Heidelberg
ChemBioDraw Ultra 11.0	CambridgeSoft, Cambridge, MA, USA
Improvision Volocity 4 (Fluorescence Microscope)	Improvision, Coventry, UK

Lambda KC4 2.7 (Fluorescence Reader)	MWG Biotech AG, Ebersberg
ModFit LT (Flow Cytometer)	Verity software house, Topsham, USA
Sigma Plot 2002	SPSS Inc., Chicago, Illinois, USA
SOFTmax Pro 3.1 (Microplate Absorption Reader)	VersaMax, Molecular Devices, Sunnyvale, CA, USA
VisComet (Comet Assay)	Impuls computergestuetzte Bildanalyse GmbH, Gilching, Germany

2.1.3 Consumables

Product	Provider
Cell Culture Flasks (75 cm ²)	Sarstedt, Nürnberg
75-mesh Copper Grids	Plano, Wetzlar
Cover Slips	Carl Roth GmbH & Co, Karlsruhe
Eppendorf Tubes (0.5 ml, 1.5 ml, 2 ml)	Eppendorf AG, Hamburg
Falcon Tubes (15 ml, 50 ml)	Greiner bio one, Frickenhausen
Lab-Tek Chambered Coverglass	Nalge Nunc International, Rochester, NY, USA
Microcon Ultracel YM-100 centrifugal filter device	Millipore, Billerica, MA, USA
Microscope Slides Super Frost	Carl Roth GmbH & Co, Karlsruhe
Multiwell plates (6, 96)	Nalge Nunc International, Rochester, NY, USA
Pipet tips	Corning Incorporated, Schiphol-Rijk, The Netherlands

2.1.4 Chemicals

Chemical substance	Provider
2',7'-Dichlorodihydrofluorescein-diacetate (H ₂ DCF-DA)	Invitrogen, Karlsruhe
3-(4,5-dimethylthiazol-2-yl)-2,5-diphenyltetrazolium bromide (MTT)	Sigma-Aldrich Chemie, Taufkirchen
Acridinorange	Sigma-Aldrich Chemie, Taufkirchen
Agarose (normal melting point)	PeqLab, Erlangen
AlamarBlue™	AbD Serotec, Oxford, UK
Aprotinin	Sigma-Aldrich Chemie, Taufkirchen
BCA reagent	Pierce, Rockford, USA
Bovine serum albumin (BSA)	Sigma-Aldrich Chemie, Taufkirchen
Casyton®	Schärfe Systems, Reutlingen
Colchicin	Sigma-Aldrich Chemie, Taufkirchen
Copper sulfate (CuSO ₄)	Merck KGaA, Darmstadt
CyStain DNA 1-step	Partec, Münster

Cytochalasin B	Sigma-Aldrich Chemie, Taufkirchen
Diethylene glycol (DEG)	Sigma-Aldrich Chemie, Taufkirchen
Dihydrorhodamine 123 (DHR)	Invitrogen, Karlsruhe
Dimethyl sulfoxide (DMSO)	Sigma-Aldrich Chemie, Taufkirchen
Ethanol 99.9%	Carl Roth GmbH & Co, Karlsruhe
Ethidium bromide	Sigma-Aldrich Chemie, Taufkirchen
Ethylenediaminetetraacetic acid (EDTA) disodiumsalt dihydrate	Carl Roth GmbH & Co, Karlsruhe
Hanks' Balanced Salt Solution (HBSS)	Invitrogen, Karlsruhe
Hydrochloric acid	Carl Roth GmbH & Co, Karlsruhe
Hydrogen peroxide	Merck KGaA, Darmstadt
Isopropanol	Carl Roth GmbH & Co, Karlsruhe
KH ₂ PO ₄	Carl Roth GmbH & Co, Karlsruhe
Leupeptin	Sigma-Aldrich Chemie, Taufkirchen
Low Melt Agarose	Carl Roth GmbH & Co, Karlsruhe
Methyl methanesulfonate (MMS)	Sigma-Aldrich Chemie, Taufkirchen
Na ₂ HPO ₄ ·2H ₂ O	Carl Roth GmbH & Co, Karlsruhe
Nitric acid (HNO ₃)	Carl Roth GmbH & Co, Karlsruhe
N-Lauroylsarcosinat	Sigma-Aldrich Chemie, Taufkirchen
Paraformaldehyde (PFA)	Sigma-Aldrich Chemie, Taufkirchen
Phenylmethylsulfonyl fluoride (PMSF)	Sigma-Aldrich Chemie, Taufkirchen
Phosphate buffered saline (PBS)	Invitrogen, Karlsruhe
Sodium deoxycholate	Sigma-Aldrich Chemie, Taufkirchen
Sodium dodecyl sulfate (SDS)	Carl Roth GmbH & Co, Karlsruhe
Sodium chloride	Carl Roth GmbH & Co, Karlsruhe
Sodium hydroxide pellets	Merck, Darmstadt
Triton X-100	Carl Roth GmbH & Co, Karlsruhe
Tris-HCl	Carl Roth GmbH & Co, Karlsruhe
Tris(hydroxymethyl)aminomethane (TRIS)	Carl Roth GmbH & Co, Karlsruhe
Vanadium (III) oxide	Sigma-Aldrich Chemie, Taufkirchen
Vanadium (V) oxide	Sigma-Aldrich Chemie, Taufkirchen

2.1.5 Kits

Product	Provider
Biotrin OxyDNA Test	BD Biosciences, Woburn, USA
Cell proliferation ELISA, BrdU Kit	Roche Applied Science, Mannheim
Cytotoxicity Detection Kit (LDH)	Roche Applied Science, Mannheim
XTT Kit	Xenometrix, Allschwil, Switzerland

2.1.6 Bulk and nanomaterials

Tab. 1 Bulk and nanomaterials used in this work

Material	Abbreviation	Characteristics	Provider	References
Bulk vanadium trioxide	bV ₂ O ₃	Specific surface 1.9 m ² /g [#]	Sigma-Aldrich	-
Nano vanadium trioxide	nV ₂ O ₃	Needle-like structure Average diameter 25 nm Length 100 – 1.000 nm Specific surface 74.9 m ² /g	C. Feldmann	1,2
Bulk vanadium pentoxide	bV ₂ O ₅	Specific surface 4.9 m ² /g [#]	Sigma-Aldrich	-
Nano vanadium pentoxide	nV ₂ O ₅	rod-shaped spherical diameter 170 – 180 nm	C. Feldmann	2
Titanium dioxide	TiO ₂	NanoCare reference material mean size 21 nm	NanoCare material n° 1.2	3
Carbon black	CB	NanoCare reference material Mean diameter 14 nm	NanoCare material n° 2.0	-
Zinc oxide	ZnO	mean size 40 nm	NanoCare material n° 9.0	-

1: (Feldmann 2003); 2: (Worle-Knirsch *et al.* 2007); 3: (Schulze *et al.* 2008).

#: BET-Analysis was done by Hans-Jürgen Schindler, at the Department of High Performance Ceramics, EMPA Dübendorf, Switzerland

2.1.7 Cell culture: cell lines, medium and supplements

In this work, the human alveolar epithelial cell line A549 (ATCC, CCL-185) (Giard *et al.* 1973), obtained from American Type Culture Collection (Rockville, MD), was used as a model of human type II alveolar epithelial lung cells (Lieber *et al.* 1976).

Product	Provider
Accutase	PAA, Pasching, Austria
Dulbecco's modified Eagle's medium (DMEM)	GIBCO® Invitrogen, Karlsruhe
Fetal calf serum (FCS)	GIBCO® Invitrogen, Karlsruhe

Insulin solution	Sigma-Aldrich Chemie, Taufkirchen
L-glutamine	Cambrex, Verviers, Belgium
Penicillin-Streptomycin Liquid	GIBCO [®] Invitrogen, Karlsruhe
Sodium pyruvate	GIBCO [®] Invitrogen, Karlsruhe
Trypsin-EDTA	GIBCO [®] Invitrogen, Karlsruhe

2.2 Methods

2.2.1 Cell culture

2.2.1.1 Culture of A549 cells

A549 cells are growing adherently with a doubling time of approximately 24 hours. The cells were cultivated at 37°C and 5% CO₂ in humidified air in DMEM medium with supplements as given in Tab. 2.

Tab. 2 Content of medium for A549 cells

<p>A549 Medium</p> <p>DMEM</p> <p>10% (v/v) fetal calf serum (FCS)</p> <p>2 mM L-glutamine</p> <p>100 µg/ml penicillin and 100 U/ml streptomycin</p>

Once a week, when cells were approaching 100% confluency, cells were subcultivated. To this end, the medium was removed and cells were washed once with pre-warmed phosphate buffer saline without Ca²⁺ and Mg²⁺ (PBS -/-). Cells were detached from the cell culture flask by incubation with 2 ml trypsin-EDTA. Incubation with trypsin-EDTA was for 5 to 10 min at 37°C. Then, addition of 8 ml fresh cell culture medium stopped trypsinization and cells were transferred to a 50 ml Falcon tube. Cells were spun down for 5 min at 405 x g. Medium was aspirated and cells were resuspended in 20 ml fresh medium.

A 1:100 dilution of the cell suspension was prepared and the cell number was counted using a cell counter (Casy[®]1, Innovatis). In a new culture flask, 2 x 10⁵ cells were seeded in 20 ml medium.

2.2.1.2 Cryoconservation of cells

For long-term storage, cells were kept in liquid nitrogen. The desired number of cells (usually 10^6 cells per ml) were suspended in FCS containing 10% dimethyl sulfoxide (DMSO) and transferred to cryo-tubes. Cells were first frozen at -80°C . To cool down the cells slowly (1°C per minute), a freezing container (Cryo 1°C Freezing Container, NalgeneTM, Labware, USA) was used. Finally, cells were transferred to liquid nitrogen.

To re-cultivate cells stored in liquid nitrogen, the tube containing the cells was put on ice during transport from the N_2 container to the lab. Upon arrival, cells were immediately thawed in a 37°C water bath and transferred to 20 ml pre-warmed cell culture medium in a culture flask. Medium was changed the next day. The cells were cultivated for at least two weeks after thawing before using them for experiments.

2.2.2 Preparation of test substances

2.2.2.1 Preparation of particles

NanoCare nanoparticle suspensions (TiO_2 , CB, ZnO) were prepared according to the standard operating procedure “Preparing suspensions of nanoscale metal oxides for biological testing” published at the NanoCare homepage www.nanopartikel.info. Briefly, test material is weighed into a 10 ml snap-on lid glass and cell culture medium (max. 6 ml) is added to obtain a stock suspension of a concentration of 1 mg/ml. The suspension is stirred on a magnetic stir bar for 1 hour at 900 rpm at room temperature (RT), then, the desired dilutions are prepared. For this purpose, an aliquot is taken out of the stock suspension while stirring. This aliquot is added to the – already stirring – solvent and stirred for another 24 hours.

2.2.2.2 Preparation of vanadium oxides

Vanadium oxide nanomaterials were delivered as suspensions in DEG at concentrations of 14.4 mg/ml (nano V_2O_3) and 0.5 mg/ml (nano V_2O_5) from C. Feldmann (Feldmann 2003). Vanadium oxide bulk materials (CAS numbers: 1314-34-7 (V_2O_3) and 1314-62-1 (V_2O_5)) were suspended in diethylene glycol (DEG) at 14.4 mg/ml (V_2O_3) and 5 mg/ml (V_2O_5) and sonified (Sonifier B15, Branson) until a homogenous suspension was achieved. Before use, a 1:10 dilution in DEG was

prepared (except for nano V_2O_5) to yield the following concentrations: bulk and nano V_2O_3 1.44 mg/ml, bulk and nano V_2O_5 0.5 mg/ml.

Both bulk and nano vanadium oxides were sonified (30 pulses at 40% output) prior to withdrawal of the required amount of substance. After centrifugation (21.000 x g, 15 min), excess DEG was removed and the vanadium oxides were resuspended in water or cell culture medium.

2.2.2.3 Preparation of vanadate solution

A solution of soluble vanadium oxide species (for comparison of the effects of soluble ionic species versus undissolved vanadium oxides) was prepared from 1 mg of bulk V_2O_5 . The bulk vanadium pentoxide was suspended in DEG and sonified. After centrifugation (21.000 x g, 15 min), excess DEG was removed. The vanadium oxide was resuspended in 5 ml Millipore water in a 50 ml glass volumetric flask and stirred until dissolution. Aliquots of the solution were filtered by centrifugation (13 min at 14.000 x g) using a Microcon Ultracel YM-100 centrifugal filter device (Millipore), pooled and analyzed by inductively coupled plasma optical emission spectrometry (ICP-OES) (see section 2.2.3.2) to determine the vanadium concentration.

2.2.3 Characterization of test materials

2.2.3.1 Preparation of nanomaterials for characterization by transmission

electron microscopy

1 ml of the stock solution of vanadium oxide nanomaterials was spun at 21.000 x g for 15 min. The DEG was removed, the pellet resuspended in 50 μ l H_2O and spun at 1300 x g for 10 min. The supernatant was discarded and the pellet once again resuspended in 50 μ l H_2O and sonified (30 pulses at 40% output). A 1:10 dilution in H_2O was prepared and dropped onto 75-mesh formvar-coated copper grids, dried over night and analyzed with a Zeiss 109T transmission electron microscope.

2.2.3.2 Determination of the solubility of vanadium oxides

Reaction tubes were cleaned in subboiled nitric acid (HNO_3) and rinsed with deionized water ("Millipore- H_2O , resistivity < 20 $M\Omega \cdot cm$) to minimize contamination. Vanadium oxides were prepared as described above (see section 2.2.2.2) and

suspended in Millipore-H₂O at a concentration of 1 mg/ml. After sonification, vanadium oxide suspensions were incubated at 37°C for 1, 3.5, 24, 48 and 144 hours. At the given timepoints, the vanadium oxide suspensions were sedimented by centrifugation (14.000 x g, 15 min). 200 µl of the supernatant were applied to a Microcon Ultracel YM-100 centrifugal filter device (Millipore) and spun for 13 min at 14000 x g to retain nanomaterial remaining in the supernatant. The flow-through was diluted in diluted subboiled HNO₃ (Acid + Millipore-H₂O = 1 + 4) and analyzed by ICP-OES (OPTIMA 4300 DV, Perkin-Elmer) in comparison with matrix matched calibration solutions covering the concentration range of the samples. Three emission lines of vanadium have been used: 311.071 nm, 309.310 nm, and 292.402 nm. The detection limit calculated by 6 times of the standard deviation of 30 acid blanks measured between the samples varies insignificantly between 0.006 mg/l and 0.007 mg/l.

2.2.4 Analysis of vanadium oxide uptake into cells

A549 cells were seeded in 6-well plates at a density of 1.5 million cells per well one day before treatment. Cells were exposed to 10 µg/cm² of bulk and nano V₂O₃, V₂O₅ and vanadate, respectively, for 24 hours at 37°C. After treatment, medium was removed and the cells were thoroughly washed with PBS-/- . Cells were harvested by trypsinization and pelleted by centrifugation (405 x g, 5 min). The cell pellet was lysed in 100 µl RIPA buffer (see Tab. 3) supplemented with 20 µg/ml aprotinin, 20 µg/ml leupeptin and 1 mM phenylmethylsulfonyl fluoride (PMSF). Lysis was performed for 1 hour on ice. The protein content was determined by the bicinchoninic acid (BCA) assay (Pierce, see section 2.2.5). 95 µl of the cell lysate were dissolved in 4 ml subboiled HNO₃ and 0.5 ml subboiled HCl in silica tubes and subjected to microwave digestion at 250°C and a pressure of 80 bar prior to quantification by ICP-OES (see section 2.2.3.2). To account for varying cell numbers, vanadium content was normalized by using the protein concentration of the respective samples.

Tab. 3 Content of RIPA lysis buffer

RIPA lysis buffer
150 mM NaCl
20 mM Tris-HCl pH 7.4
0.5% (w/v) sodium-deoxycholate
5 mM sodium-EDTA
0.1% (v/v) SDS
1.0% (v/v) Triton-100

2.2.5 Determination of the protein concentration (BCA assay)

Protein concentrations were determined with the BCA assay which is based on the biuret reaction (Smith *et al.* 1985). This reaction involves the chelation of proteins and copper (Cu^{2+}) ions under alkaline conditions, yielding a blue complex. Subsequently, a reduction of the Cu^{2+} ions to Cu^{1+} ions, and the colorimetric detection of Cu^{1+} ions by bicinchoninic acid (BCA) occurs. BCA and Cu^{1+} form a purple complex with a maximum absorption at 562 nm which can be detected photometrically. The first complex formation is directly proportional to the number of peptide bonds, the second to the number of Cu^{1+} ions; thus, the absorption at 562 nm is proportional to the protein concentration. For quantitation of the protein concentration, known concentrations of bovine serum albumin (BSA) were used to generate a standard curve from which the concentration of the unknown protein samples could be derived. The assay was performed in a 96-well plate. 10 μl of the protein standards (0, 0.1, 0.5, 1.0, 1.5, 2.0, 2.5, 3.0 mg/ml BSA) and 2 to 5 μl of the samples were applied to the wells in duplicates. The BCA reagent was prepared by mixing BCA solution and 4% copper sulfate (CuSO_4) solution at the ratio 50:1. 200 μl of the BCA reagent were added to each well; then, the plate was incubated for 30 min at 37°C. Photometrical measurement of the absorption (microplate absorption reader: VersaMax, Molecular Devices) at 562 nm occurred after the samples had cooled down to room temperature. Protein concentrations were determined from the standard curve using the SOFTmax Pro 3.0 software.

2.2.6 Cell viability assays

To assess the biological effects of novel chemical substances, a number of assays probing cell viability are used. In this work, different assays were used to analyze cell proliferation and acute toxicity (including metabolic activity or integrity of the cell membrane). Some of these assays have overlapping applications, as assays probing metabolic activity also detect cell proliferation (more cells also means more overall metabolic activity and thus a stronger signal).

2.2.6.1 Proliferation assay I (cell number)

This assay assesses cell proliferation by detecting alterations in the cell number of treated samples in comparison to untreated control cells.

A549 cells were seeded in 6-well plates at a concentration of 10^5 cells per well and cultivated over night. Cells were treated with bulk and nano vanadium oxides (1, 2 and $10 \mu\text{g}/\text{cm}^2$) or $10 \mu\text{l}$ DEG in 2 ml medium as solvent control for 24, 48 and 72 hours. At the given timepoints, cells were harvested by trypsinization, and a $200 \mu\text{l}$ aliquot was diluted 1:100 and counted using the Casy®1 cell counter.

2.2.6.2 Proliferation assay II (AlamarBlue™ assay)

This assay serves both at analysis of cell proliferation (Ahmed *et al.* 1994; de Fries *et al.* 1995) and cytotoxicity (Nociari *et al.* 1998). The indicator dye AlamarBlue™ comprises an oxidation-reduction indicator that changes color and becomes fluorescent due to mitochondrial reduction in viable cells. The more cells are present, the more dye is converted and the stronger is the fluorescence, which is measured at at 560 nm excitation and 620 nm emission wavelengths.

10.000 cells were seeded in $200 \mu\text{l}$ medium per well of a 96-well plate and grown over night. The next day, cells were treated with bulk and nano vanadium oxides at concentrations of 1, 2, 10 and $20 \mu\text{g}/\text{cm}^2$. DEG ($40 \mu\text{l}$ in 8 ml medium) served as negative control, insulin ($10 \mu\text{g}/\text{ml}$) as a positive control. Cells were incubated for 24 and 48 hours. After incubation, AlamarBlue™ dye was added to the cells to a final ratio of 1:10 ($22 \mu\text{l}$ to $200 \mu\text{l}$ medium). The cells were incubated further for another 1 to 2 hours and finally analyzed in the fluoreader (FL600, MWG Biotech; excitation: 560 nm; emission: 620 nm).

2.2.6.3 Proliferation assay III (BrdU assay)

The incorporation of a base (thymidin) analogue (5-bromo-2'-deoxy-uridine, BrdU) into the DNA of proliferating cells during DNA synthesis is the principle of this proliferation assay. BrdU can be later on detected by a BrdU-specific antibody. In the Cell proliferation ELISA BrdU Kit provided by Roche Applied Science, this antibody is conjugated to a peroxidase which catalyzes the conversion of a colorimetric substance. Absorbance of this substance is then measured photometrically at 450 nm wavelength.

10.000 cells were seeded in 200 µl medium per well of a 96-well plate and grown over night. The next day, cells were treated with vanadium oxides at concentrations of 1, 2, 10 and 20 µg/cm² for 24 and 48 hours. DEG (10 µl in 2 ml) served as solvent control, insulin (10 µg/ml) as a positive control. Each concentration was run in quadruplicates. After incubation, cells were labeled with 10 µM BrdU in culture medium for 2 hours at 37°C. The labeling medium was removed and cells were fixed and the DNA partly denatured by addition of the FixDenat solution provided with the kit for 30 min at RT. The FixDenat solution was aspirated and the antibody-solution (prepared according to the protocol of the manufacturer) applied to the cells for 90 min at RT. Thereafter, cells were washed three times with the provided Washing solution. Then, 100 µl of the Substrate solution were added per well and incubated at RT for approximately 10 min (the color reaction was visually controlled to assure sufficient coloration for photometric detection). Absorbance was measured at a wavelength of 450 nm (reference wavelength: 690 nm).

2.2.6.4 Toxicity assay I (MTT assay)

The MTT assay analyzes the metabolic activity of cells via conversion of the yellow tetrazolium salt 3-(4,5-dimethylthiazol-2-yl)-2,5-diphenyltetrazolium bromide (MTT) (see Fig. 7). In the mitochondria of viable and metabolically active cells, succinate-dependent dehydrogenases convert the yellow salt to water-insoluble blue formazan crystals. Prior to the photometrical measurement, these crystals are solubilised in isopropanol. To minimize possible influence of the red pH-indicator phenol-red in the cell culture medium, isopropanol is acidified by 1% (v/v) hydrochloric acid (HCl) which changes the color of phenol-red to yellow. Measurement of the absorption of the blue formazan is performed at 555 nm.

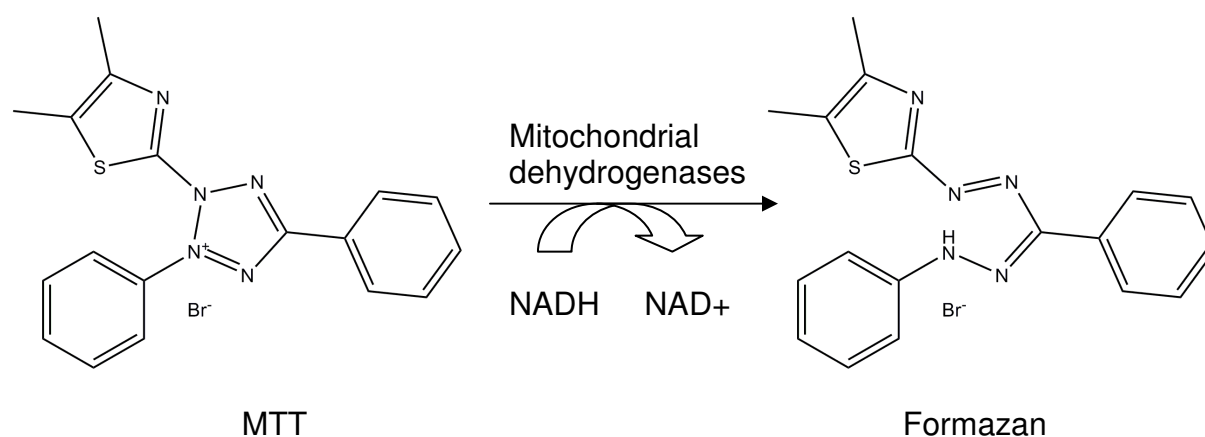


Fig. 7 Conversion of MTT to formazan in the MTT assay.

Mitochondrial dehydrogenases convert the yellow MTT salt to blue, water-insoluble formazan.

10.000 cells were seeded in 200 μ l medium per well of a 96-well plate and grown over night. The next day, cells were treated with vanadium oxides at concentrations of 1, 2, 10 and 20 μ g/cm² for 24 and 48 hours. DEG served as solvent control (10 μ l in 2 ml medium). Each concentration was run in quadruplicates. After treatment, cells were washed twice with PBS-/- and incubated for 2 hours with medium containing 10% (v/v) of a MTT stock solution of 5 mg/ml in PBS, then spun down (350 x g, 5 min). The medium was removed and the formazan crystals were dissolved in isopropanol containing 1% HCl. After another centrifugation step, the supernatant was transferred to a new 96-well plate and absorption measured with the photometer at 555 nm.

2.2.6.5 Toxicity assay II (XTT assay)

The XTT assay resembles the MTT assay as it also is based upon conversion of a tetrazolium salt by mitochondrial dehydrogenases in viable cells. But in contrast to the MTT salt which yields water-insoluble crystals, the product of the conversion of XTT (2,3-bis[2-methoxy-4-nitro-5-sulfopheny]-2H-tetrazolium-5-carboxyanilide inner salt) is a soluble orange formazan (see Fig. 8). Thus, the solubilization step is not needed. Photometric quantitation occurs at 450 nm (reference wavelength 690 nm).

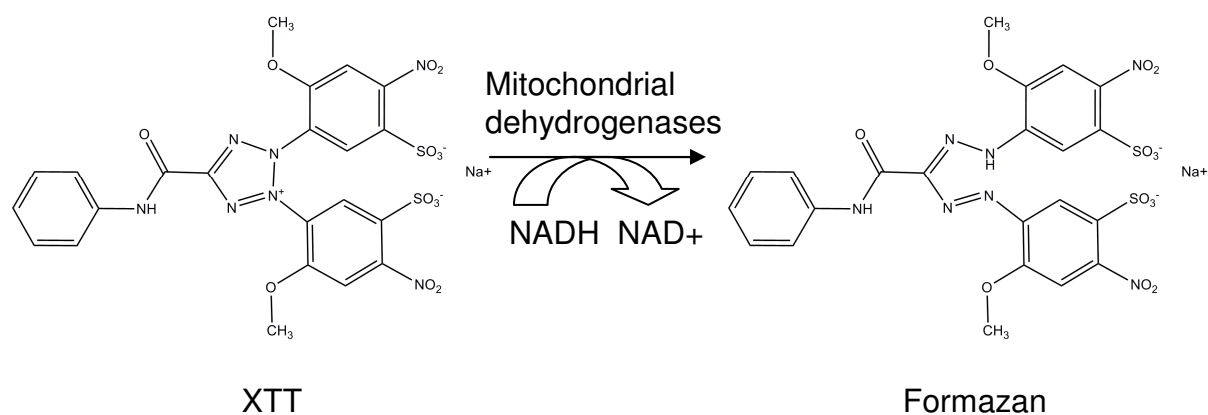


Fig. 8 Conversion of XTT to formazan in the XTT assay.

Mitochondrial dehydrogenases convert the yellow XTT salt to an orange, water-soluble formazan.

10.000 cells were seeded in 200 μl medium per well of a 96-well plate and grown over night. The next day, cells were treated with vanadium oxides at concentrations of 1, 2, 10 and 20 $\mu\text{g}/\text{cm}^2$ for 24 hours. DEG served as solvent control (10 μl in 2 ml medium). Each concentration was run in quadruplicates. After incubation, cells were washed with PBS $^{-/-}$ and supplied with fresh medium. XTT solutions provided in the XTT Kit of Xenometrix were heated to 37 $^{\circ}\text{C}$ in the water bath and mixed 1:100 (XTT II:XTT I). Per well, 50 μl of the XTT-mixture was added. After 2 to 3 hours of incubation at 37 $^{\circ}\text{C}$, absorption was measured photometrically at 450 nm (reference wavelength 690 nm).

2.2.6.6 Toxicity assay III (Lactate dehydrogenase assay)

The cytotoxicity endpoint used by the lactate dehydrogenase (LDH) viability assay is membrane integrity. LDH is an intracellular enzyme which is released by damaged or dead cells as a result of membrane leakage. Activity of LDH in the supernatant is determined indirectly in a two-step process comprising two redox-reactions (see Fig. 9). Firstly, LDH oxidizes lactate to pyruvate; the co-enzyme nicotinic adenine dinucleotide (NAD^+) is reduced to NADH/H^+ . Secondly, the yellow tetrazolium salt INT (2-[4-iodophenyl]-3-[4-nitrophenyl]-5-phenyltetrazoliumchloride) is reduced to a red formazan by transfer of hydrogen and electrons from the NADH/H^+ , which is catalyzed by diaphorase. This color reaction can be quantitated photometrically at a wavelength of 490 nm (reference wavelength 690 nm).

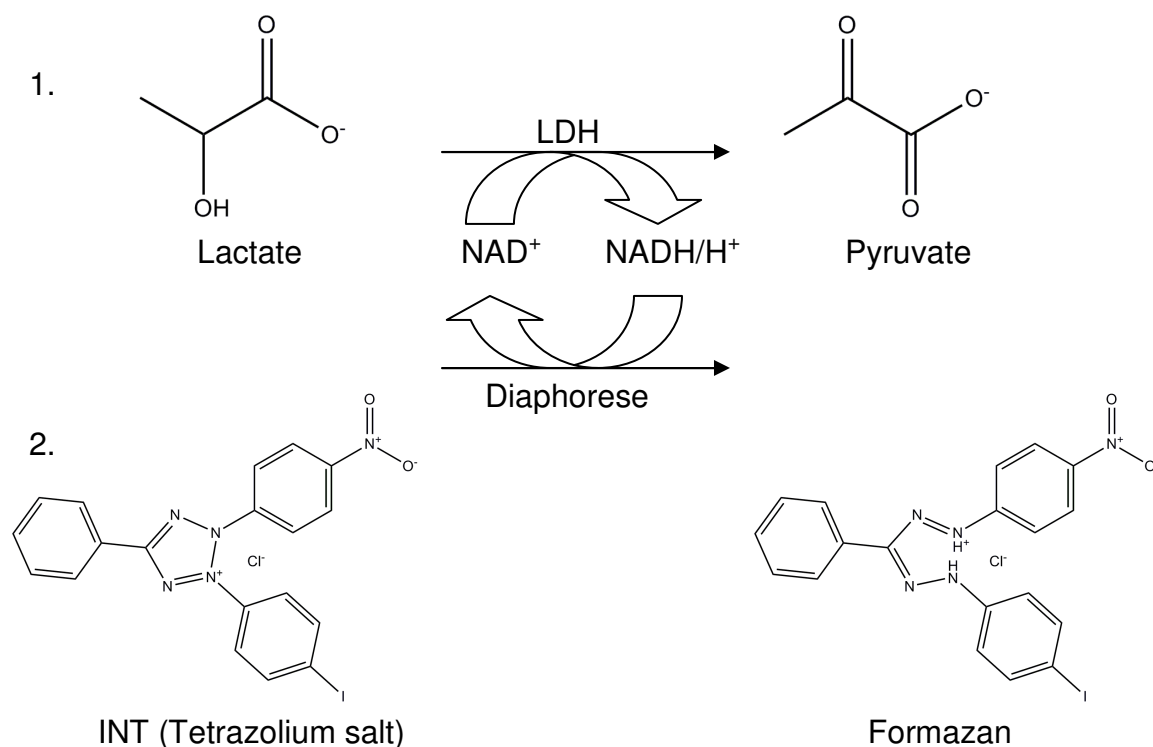


Fig. 9 Redox-reactions in the LDH assay.

A two-step reaction is involved in the colorimetric detection of LDH: Firstly, the oxidation of lactate to pyruvate by LDH generates NADH/H⁺ (1.). Secondly, the tetrazolium salt INT is reduced to the red formazan; this reaction re-oxidizes NADH/H⁺ to NAD⁺(2.).

The LDH assay can be performed in combination with the MTT assay, as 25 μ l of the supernatant of the samples are sufficient. Thus, treatment of the cells is the same as described in section 2.2.6.4. However, 1 hour prior to withdrawal of the supernatant, 8 wells of hitherto untreated cells were treated with Triton X-100 (final concentration 1% (v/v)). Treatment with the detergent Triton X-100 results in complete cell lysis and thus maximum LDH release which serves as a positive control.

75 μ l of PBS/- were pipetted into the wells of a new 96-well plate. The supernatants of the treated cells were added to the wells with PBS. One row with 100 μ l PBS only served as blank. Reagent I and Reagent II included in the Cytotoxicity Detection (LDH) Kit from Roche Applied Science were mixed (250 μ l + 11.25 ml) and 75 μ l of this mixture applied to each well. Incubation was performed at RT in the dark. After a sufficient color reaction had occurred, the reaction was stopped by addition of 50 μ l 1 N HCl to each well. Absorption was measured photometrically at a wavelength of 490 nm (reference wavelength 690 nm). In contrast to the former toxicity tests, where a high absorption was indicative for high cell viability, in the LDH assay, high absorption means high LDH release and thus cytotoxicity.

2.2.7 Detection of reactive oxygen / nitrogen species (ROS / RNS)

2.2.7.1 2',7'-dichlorofluorescein (DCF) assay

This assay detects a wide range of reactive oxygen and nitrogen species including hydrogen peroxide, superoxide anion, hydroxyl radical and peroxynitrite. It uses the non-fluorescent dye 2',7'-dichlorodihydrofluorescein-diacetate (H₂DCF-DA). H₂DCF-DA is uncharged and can thus enter the cell; once internalized, the diacetate is cleaved off by esterases yielding a charged molecule which is sequestered inside the cell. In presence of ROS, the nonfluorescent dye is oxidized to the fluorescent 2',7'-dichlorofluorescein (DCF) (see Fig. 10) (Wan *et al.* 1993). Fluorescence can be measured at a wavelength of 530 nm (excitation 488 nm).

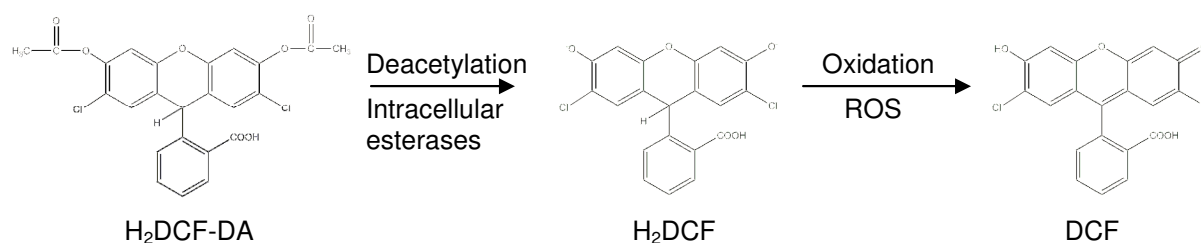


Fig. 10 Conversion of H₂DCF to DCF in the DCF assay.

The uncharged H₂DCF-DA molecule enters the cell and is deacetylated by intracellular esterases. The resulting charged H₂DCF is sequestered inside the cell and oxidized to the fluorescent DCF in the presence of ROS.

Cells were seeded in 96 well plates at 25.000 cells per well one day before treatment. Cells were exposed to vanadium oxides at concentrations of 1, 2, 10 and 20 µg/cm² for 24 h at 37°C. Hydrogen peroxide (0.5 mM) was used as a positive control, DEG as solvent control (10 µl in 2 ml medium). Each sample was run in quadruplicates. After treatment, medium was removed and cells were washed once with pre-warmed Hank's Balanced Salt Solution (HBSS). Cells were incubated for 40 min at 37°C with 50 µM H₂DCF-DA and then washed with HBSS to remove excess dye. Fluorescence was then analyzed in the fluoreader (FL600, MWG Biotech) at a wavelength of 530 nm (excitation 488 nm).

2.2.7.2 Dihydrorhodamine (DHR) assay

The DHR assay is based upon the same working principle as the DCF assay (see section 2.2.7.1) yet uses another dye, dihydrorhodamine123 (DHR). This non-fluorescent dye is oxidized in the presence of ROS (mainly by superoxide anion,

hydrogen peroxide and peroxyxynitrite) to the fluorescent rhodamine123 which accumulates in mitochondrial membranes (Emmendorffer *et al.* 1990; Henderson *et al.* 1993; Royall *et al.* 1993) (see Fig. 11). The green rhodamine fluorescence can be measured at a wavelength of 530 nm (excitation 488 nm).

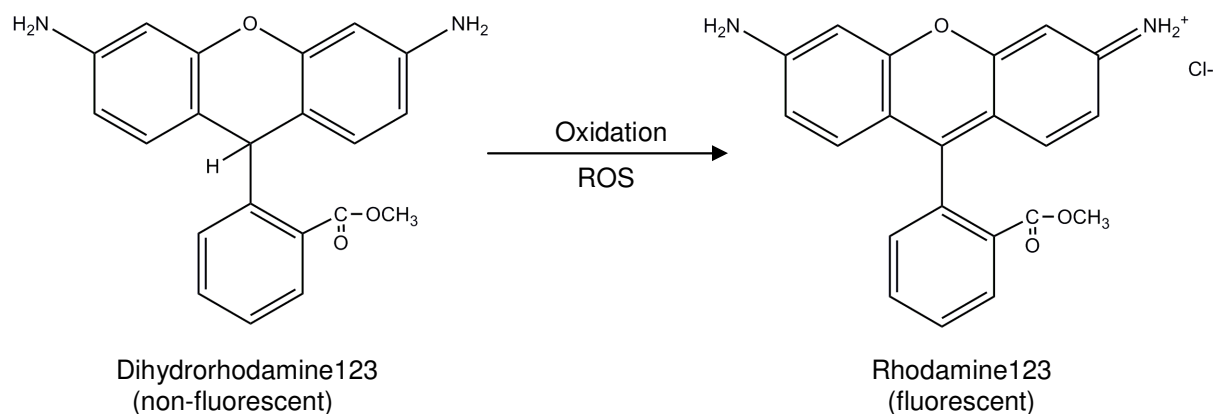


Fig. 11 Oxidative conversion of dihydrorhodamine123 to rhodamine123 by ROS.

The non-fluorescent dihydrorhodamine123 gets oxidized in the presence of ROS. Product is the fluorescent rhodamine 123.

Cells were seeded in 96 well plates at a density of 25.000 cells per well one day before treatment. For microscopic analysis, 10⁵ cells were seeded in a 4-well chamber slide instead. Cells were exposed to vanadium oxides at concentrations of 1, 2, 10 and 20 µg/cm² (15 µg/cm² for chamber slides) for 24 h at 37°C. Hydrogen peroxide (0.5 mM) was used as a positive control, DEG as solvent control (10 µl in 2 ml medium). Each sample was run in quadruplicates. After treatment, medium was removed and cells were washed once with pre-warmed HBSS. Per well, 100 µl of 10 µM dihydrorhodamine123 in HBSS were added and cells were incubated for 45 min at 37°C. Afterwards, the DHR solution was removed and cells were washed twice with HBSS. 100 µl of HBSS were added and fluorescence (485/530 nm) was measured using the fluoreader (FL600, MWG-Biotech) after 0, 1, 2, and 3 hours.

The assay was also performed without cells, i.e. with vanadium oxides in cell culture medium. In this case, a 96-well plate without cells was supplied with the same concentrations of vanadium oxides as described above and incubated likewise. After incubation, the dye was directly added to the medium containing the vanadium oxides, incubated for another 40 min at 37°C and then measured.

2.2.8 Genotoxicity assays

Genotoxicity assays serve to detect and to analyze possibly harmful alterations of the DNA including mutations, strand breaks, chromosome breaks or chromosome aberrations.

2.2.8.1 Comet assay (single cell gel electrophoresis)

The comet assay is a simple and fast test for the detection of DNA damage. It has been described first by Singh *et al.* (Singh *et al.* 1988). For the comet assay, a small number of cells are embedded into a thin agarose layer, lysed, subjected to electrophoresis and stained with a fluorescent DNA-intercalating dye. The more the chromosomal DNA in the nucleus is damaged, the higher is the migration of the DNA fragments during electrophoresis, producing a comet-like structure with a “head” (genomic unfragmented DNA) and a “tail” (migrated DNA fragments).

The most widely used comet assay with alkaline lysis detects mainly single-strand breaks and alkali-labile sites; neutral lysis conditions can be chosen for monitoring of double strand breaks. Different other variations have been described, e.g. for the detection of crosslinks, single strand nicks or specific classes of base damage.

The advantage of the comet assay consists in its simple and fast performance, its sensitivity, the possibility to analyze DNA damage in single cells and the need for low numbers of cells. Moreover, the comet assay works well for nearly any eukaryotic cell population, no matter if they are dividing or not. It is therefore widely used in genotoxicity testing (Speit *et al.* 1999).

The alkaline comet assay was performed basically as described by Singh *et al.* (Singh *et al.* 1988). Cells were seeded in 6-well plates at a density of 250.000 cells per well one day before treatment and exposed to 1 and 2 $\mu\text{g}/\text{cm}^2$ of vanadium oxides and vanadate for 24, 36 and 48 hours. DEG (10 μl in 2 ml medium) was used as solvent control. Methyl-methane sulfonate (MMS, 1 mM) was used as a positive control and added 1 hour prior to the end of incubation. Then, the medium was removed, cells were washed once with PBS and harvested using accutase. Cells were suspended in 0.5 ml of cell culture medium. 80 μl of the cell suspension were mixed with 320 μl of 37 °C warm 0.5% (w/v) low-melting agarose in PBS. 180 μl of the agarose-cell solution were applied to microscope slides precoated with 1.5% (w/v) agarose (PeqGold Universal Agarose, PeqLab) in PBS. Each sample was run in duplicates. A cover slip was placed on the slide, agarose was allowed to solidify

(5 min at 4°C) and cover slips were removed before putting slides into a lysis solution for 1 hour at 4°C (see Tab. 4). Slides were then put into a horizontal electrophoresis tray containing the alkaline electrophoresis buffer allowing unwinding of the DNA for 20 min (see Tab. 4). Thereafter, electrophoresis (25 V, 300 mA) was performed for 20 min. After electrophoresis, slides were neutralized in TRIS buffer (see Tab. 4), rinsed in H₂O and dehydrated in 99% ethanol and dried over night. DNA was stained with ethidiumbromide (20 µg/ml) and comets were analyzed using a Leitz DM IL microscope (Leica) equipped with a Kappa DX 4 camera (Kappa opto-electronics) and the software “Viscomet” (Impuls computergestuetzte Bildanalyse GmbH) (see Fig. 12). Excitation wavelength was 510 to 560 nm. Per slide, 50 randomly chosen comets were analyzed blinded.

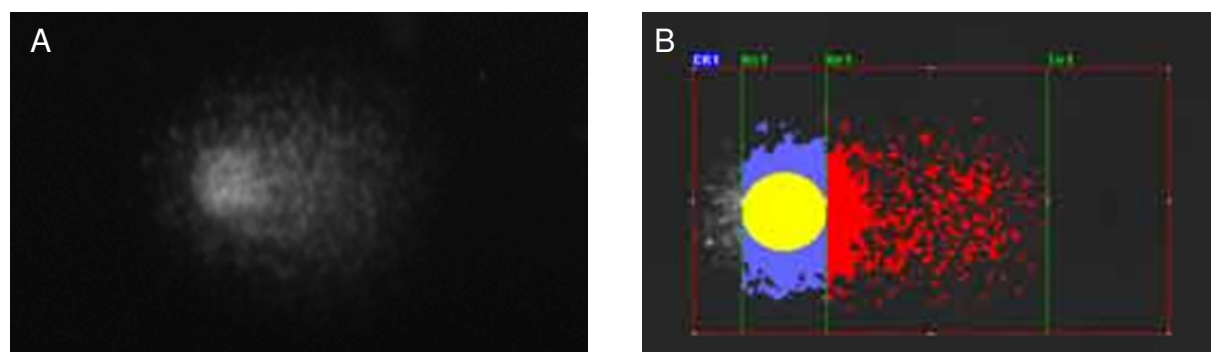


Fig. 12 Analysis of comets using the “Viscomet” software.

(A) Microscopic image of a cell with DNA damage (magnification 400x). (B) The Viscomet Software quantifies fluorescence intensities and determines head (yellow) and tail (red) regions of the comet and their percentage of DNA. The blue region (“body”) is not included into the analysis.

Tab. 4 Content of buffers and solutions used in the comet assay

Name/Purpose	Content
Normal melting point agarose solution	1.5% (w/v) agarose in PBS
Low melting point agarose solution	0.5% (w/v) low-melting agarose in PBS
Lysis Buffer	2.5 M NaCl 100 mM EDTA 10 mM TRIS 1% Na-Laurolysarcosinat Adjust pH to pH 10

Lysis Solution	Freshly prepared before use: Add 10% (v/v) DMSO 1% (v/v) Triton-X-100 to 66.75 ml Lysis Buffer
NaOH Solution	5 M NaOH (pellets) in H ₂ O
EDTA Solution	0.2 M Na ₂ -EDTA·2H ₂ O Adjust pH to pH 10
Electrophoresis Buffer	Freshly prepared before use: 0.3 M NaOH 1 mM EDTA
Neutralization Buffer	0.4 M TRIS, adjust pH to pH 7.5

2.2.8.2 Micronucleus test

The micronucleus test has been developed by J.A. Heddle in 1973 (Heddle 1973) and has since then become a widely used, powerful tool for the analysis of genotoxicity at the chromosomal level. Chromosomal aberrations are frequent in cancer cells and their assessment may provide insight into causes and consequences of the deregulation occurring in tumor cells.

Micronuclei contain chromosomal fragments arising from chromosomal breaks or whole chromosomes that failed to be distributed during mitosis. In telophase, the fragments or whole chromosomes are enveloped by a nuclear membrane and hence gain the appearance of a small nucleus.

The method is applied to assess naturally occurring genetic damage as well as the genotoxicity of chemicals and exposure to irradiation. The micronucleus test is responsive to a variety of genotoxic effects, ranging from double-strand breaks to inhibition of spindle formation. Even minor lesions such as base-base mismatches or epigenetic modifications such as hypomethylation can be detected if they yield chromosomal breakage during processing of the lesion by the cell or changes impairing the equal distribution of chromosomes during mitosis.

To perform a micronucleus test, cells are placed or grown on a microscope slide, fixed with ethanol, stained and analyzed by microscopy. Mostly, a cytokinesis blocker

(cytochalasin B) is used to be able to score only cells which have undergone exactly one cell division. These cells are marked by the existence of two nuclei. Usually, the number of binucleated cells with micronuclei in 1.000 binucleated cells is determined. Additional parameters such as the number of apoptotic or mitotic cells and nucleoplasmatic bridges (see Fig. 13) may be scored to get a more complete view of the effect of the toxic agent (Fenech 2000).

The micronucleus test has been established and validated in our lab by using different genotoxic agents (H_2O_2 , MMS) at different concentrations. MMS at a concentration of $150\ \mu M$ yielded a significant increase in binucleated cells with micronuclei in comparison to control cells and was used in subsequent experiments as a positive control.

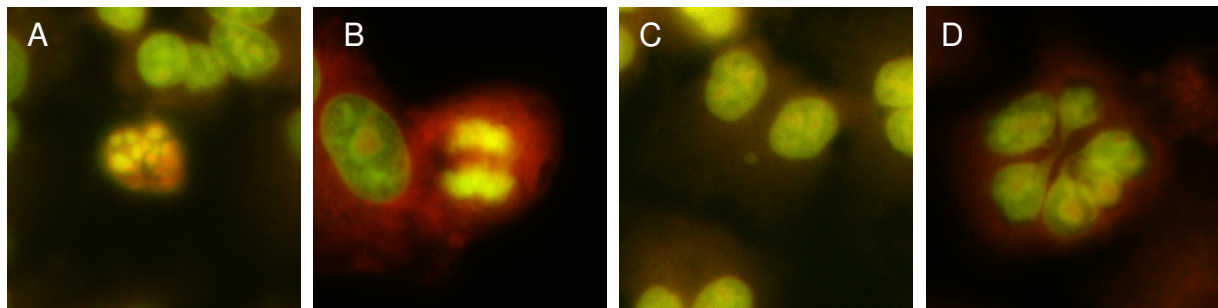


Fig. 13 Examples of parameters scored in the micronucleus test.

(A) Apoptotic cell. (B) Mitotic cell (anaphase). (C) Binucleated cell with micronucleus. (D) Cell with segmented nuclear morphology and nucleoplasmic-bridge-like structures. Staining: Acridinorange. Magnification: 630x.

Cells were seeded in a 4-well chamber slide at a density of 100.000 cells per well and grown over night. Cells were treated with 1 and $2\ \mu g/cm^2$ vanadium oxides for 24 hours. DEG ($10\ \mu l$ in 2 ml medium) was used as a solvent control, MMS ($150\ \mu M$) as a positive control. To each sample, $4\ \mu g/ml$ cytochalasin B were added to induce binucleated cells. Each sample was run in duplicates. After incubation at $37^\circ C$ for 24 hours, medium was removed and cells were fixed with 1 ml $-20^\circ C$ cold absolute ethanol and stored at $-20^\circ C$ until staining and evaluation.

To stain the cells, ethanol was aspirated and cells dried for several minutes. Acridinorange, a dye which stains RNA red and DNA green, was used at a concentration of 0.2 mM in Sørensen's buffer (see Tab. 5). Cells were stained for 10 min, then washed twice with Sørensen's buffer for 5 min. Finally, 0.5 ml Sørensen's buffer were added to each well and cells were analyzed at the Leitz DM IL microscope (Leica) using a filter allowing an excitation wavelength of 450 nm – 490 nm and the detection of an emission at a wavelength of 590 nm.

The following parameters were counted: In the first run, the number of mono-, bi- and polynucleated cells, the number of apoptotic and mitotic cells and the number of cells with segmented nuclei. In the second run, the number of binucleated cells with micronuclei in at least 1.000 binucleated cells.

Tab. 5 Content of solutions and buffers used in the micronucleus test

Name	Content
0.06 M KH_2PO_4	4.54 g KH_2PO_4 in 0.5 l H_2O
0.06 M $\text{Na}_2\text{HPO}_4 \cdot 2\text{H}_2\text{O}$	5.938 g $\text{Na}_2\text{HPO}_4 \cdot 2\text{H}_2\text{O}$ in 0.5 l H_2O
Sørensen's buffer pH 6.8	Freshly prepared before use 24.6 ml 0.06 M $\text{Na}_2\text{HPO}_4 \cdot 2\text{H}_2\text{O}$ 50.8 ml 0.06 M KH_2PO_4
Acridinorange Stock Solution	1 mM acridinorange in H_2O
Acridinorange Staining Solution	Freshly prepared before use Dilute Acridinorange Stock Solution 1:5 in Sørensen's buffer

2.2.8.3 Biotrin OxyDNA test

Oxidized DNA bases are an important mutagenic DNA lesion. This assay was used to analyze the content of oxidized guanine (8-oxo-guanine) in the DNA. The Biotrin OxyDNA Test kit from BD Biosciences provides a fluorescein isothiocyanate (FITC)-coupled probe specifically binding to 8-oxo-guanine. The green fluorescent FITC can be detected either by microscopy or flow cytometry after excitation at 488 nm.

A549 cells were seeded in 6-well plates at a density of 500.000 cells per well one day before treatment. Cells were treated for 24 hours with vanadium oxides at a concentration of 1 and 2 $\mu\text{g}/\text{cm}^2$. After treatment, medium was removed and cells were washed once with PBS. Cells were detached with accutase, suspended in PBS and pelleted by centrifugation (405 x g, 5 min). The pellet was resuspended in 0.5 ml

PBS, then, 0.5 ml ice-cold 4% (w/v) paraformaldehyde in H₂O was added and cells incubated for 15 min on ice. Cells were pelleted again by centrifugation and washed twice with PBS. Thereafter, ice-cold 70% (v/v) ethanol was added for 30 minutes. Afterwards, cells were washed once with PBS, once with Wash Solution provided in the Biotrin OxyDNA Test (BD Biosciences) and then incubated with 100 µl FITC-conjugated anti-8-oxo-guanine-probe for 30 minutes at 37°C. After two washing steps with Wash Solution, cells were suspended in PBS and analysis was performed by flow cytometry (BD LSR II, Becton Dickinson).

For microscopy, cells were grown in 4-well chamber slides at a density of 100.000 cells per well and treated likewise. The protocol in this case does not require cell harvesting, and instead of centrifugation, solutions could be aspirated to be removed, as cells are attached to the slides. After the final washing step, the chambers were removed, mounting medium was applied and the slides were covered by cover slips and stored in the dark until analysis.

2.2.9 Cell cycle analysis

Alterations in the cell cycle can be the consequence of toxic or DNA-damaging effects of a noxa. The content of DNA in the cells during the different phases of the cell cycle is varying: It is 1n during G₀/G₁-phase, increases from 1n to 2n during S-phase and is finally 2n in G₂/M-phase before the onset of mitosis. After mitosis, each daughter cell has 1n. These cycling DNA-levels and thus cell cycle progression can be monitored using a DNA-staining dye such as 4'-6-diamidino-2-phenylindole (DAPI). In the flow cytometer, the fluorescence signal of a cell with 1n is half of the fluorescence signal of a cell with 2n (the signal of DNA-synthesizing cells is in-between); hence, cells in G₀/G₁-phase and G₂/M-phase can be quantified separately and their ratio can be compared.

A549 cells were seeded in 6-well plates at a density of 500.000 cells per well one day before treatment. Cells were exposed to vanadium oxides at concentrations of 2 and 10 µg/cm² for 24 hours. Colchicin (25 µM) was used as a positive control for G₂/M arrest. After treatment, medium was transferred to a 15 ml tube. Cells were washed with PBS which was also transferred to the same 15 ml tube. Cells were detached with 0.2 ml accutase, suspended in 0.8 ml media and transferred to the 15 ml tube. After centrifugation (405 x g, 5 min), the supernatant was discarded and cells were resuspended in ice-cold PBS. All following steps were performed at 4°C. Cells were

centrifuged once again, washed with PBS and resuspended in 1 ml cold PBS. 3 ml of ice-cold 99% ethanol were added dropwise while vortexing. Cells were fixed for one to two hours on ice, then pelleted by centrifugation. The supernatant was removed and cells were stained protected from light with 0.5 ml CyStain DNA 1step (Partec) over night at 4°C. Analysis was performed by flow cytometry using UV excitation. Data was quantified using ModFit LT software (see Fig. 14).

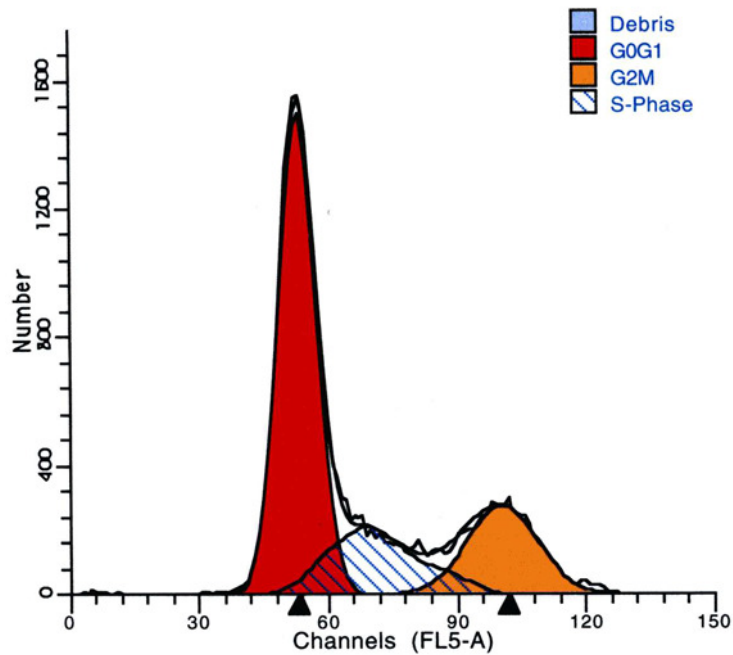


Fig. 14 Quantification of cell cycle analysis using ModFit LT software.

The data acquired by flow cytometry were quantified with the ModFit LT Software. A model is generated (smooth line) and the areas under the curve for the cell cycle phases calculated. The example shows the distribution of cell cycle phases in control cells.

3 Results

The aim of my work was to examine the genotoxic potential of synthetic metal oxide nanomaterials. The experiments were performed in a human alveolar epithelial cell line (A549), as a model of inhalative exposure, which is the most important way of exposure for nanomaterials. I used different vanadium oxides, both bulk and nano-sized material as well as soluble vanadate ions, to be able to compare the biological effects of the different closely “related” substances. Moreover, the use of a set of vanadium oxides of different physical and chemical composition was supposed to enable conclusions about possible mechanisms responsible for the observed effects. At first, the physico-chemical characteristics of the vanadium oxides were determined. Then, the amount of vanadium taken up into cells was analyzed and the effects of vanadium oxides on cell viability and proliferation were examined. Assessment of cell viability is important as one has to exclude to use cytotoxic concentrations during genotoxicity testing. Consequently, the ability of vanadium oxides to generate reactive oxygen species was analyzed, as genotoxicity can be due to oxidative stress. Genotoxicity testing included assays probing DNA mutations, DNA strand breaks and chromosome breaks / disturbance of mitosis. DNA damage can lead to cell cycle arrest, thus, the consequences of vanadium oxide treatment for cell cycle progression were examined.

Besides the vanadium oxides, which find only limited application e.g. as catalysts, three nanomaterials produced at large scale (carbon black, titanium dioxide, zinc oxide) have also been subjected to genotoxicity testing. The population is exposed more and more to those nanomaterials e.g. in cosmetics, printer toners or paint; thus, knowledge about a possible DNA-damaging capacity is required. Moreover, the comparison of different nanomaterials may help to elucidate the mechanisms of genotoxicity.

3.1 Characterization of vanadium oxides

3.1.1 Metric characterization

When studying novel nanomaterials, the characterization of their physico-chemical properties is essential. This is to be able to compare different studies and moreover, to be able to derive possible correlations between observed effects and the characteristics of the material.

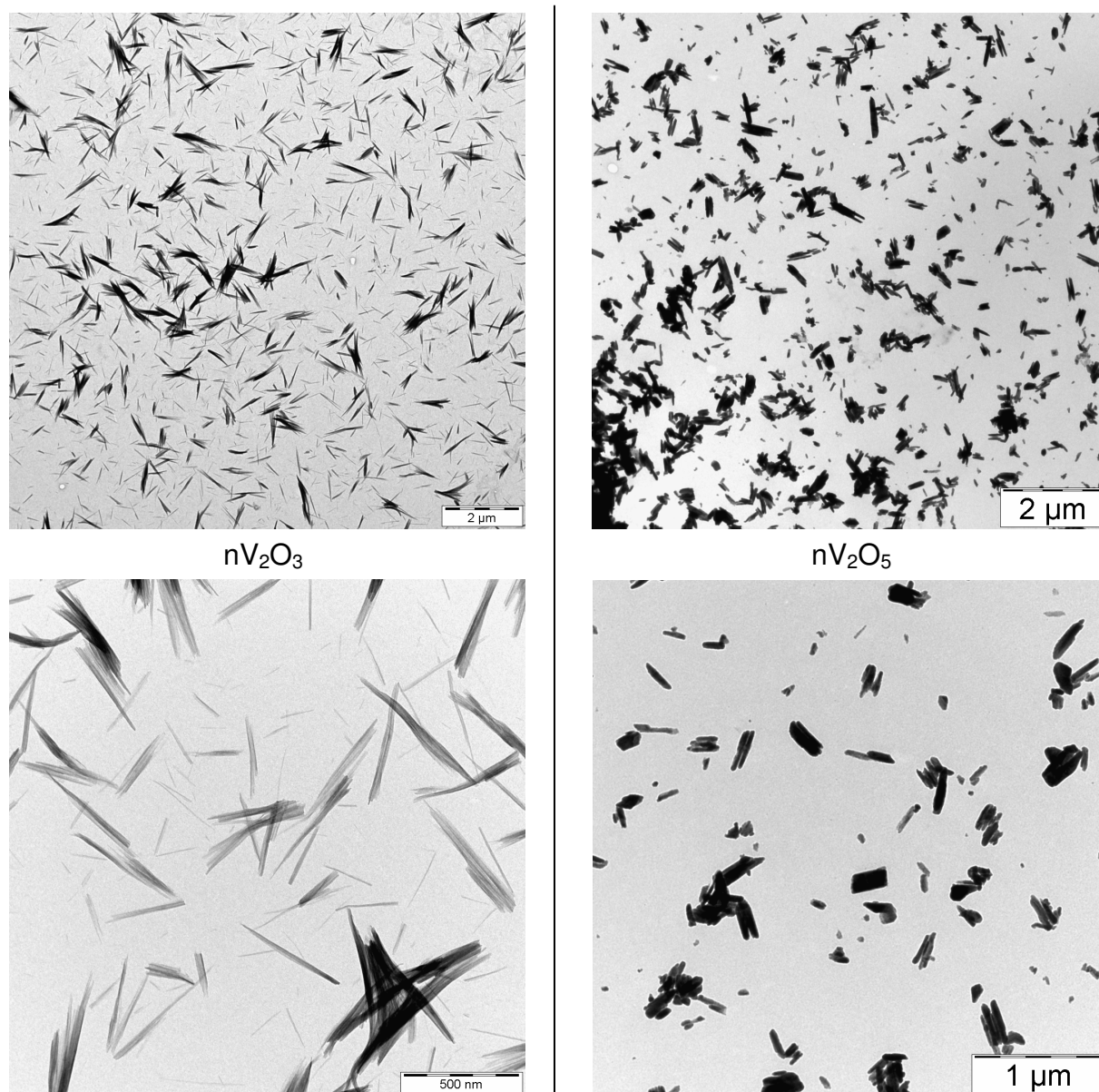


Fig. 15 Transmission electron micrographs of nano vanadium oxides.

The TEM images of aqueous preparations of nano V_2O_3 (at the left) and nano V_2O_5 (at the right) show the needle-like (V_2O_3) and the rod-like shape (V_2O_5) of the nanomaterials respectively. Figures of V_2O_3 were kindly provided by Katrin Kern.

Optical characterization was done by transmission electron microscopy (TEM). TEM images (Fig. 15) show needle-like structures of 100 to 1.000 nm in length and an average diameter of 25 nm for nano V_2O_3 . The fibers are often found in bundles (Worle-Knirsch *et al.* 2007). Nano V_2O_5 are rod-like shaped nano-objects of different size. They are up to several hundred nanometer in length and usually have a diameter of less than 50 nm. Like nano V_2O_3 , the V_2O_5 nanofibers are often seen as agglomerates.

The spherical diameter of nano V_2O_3 is approximately 70 nm, the one of nano V_2O_5 is approximately 170 nm (data provided by the manufacturer C. Feldmann). Brunauer-Emmet-Teller (BET)-analysis yielded a specific surface of $1.9 \text{ m}^2/\text{g}$ for bulk V_2O_3 , $4.8 \text{ m}^2/\text{g}$ for bulk V_2O_5 and $74.9 \text{ m}^2/\text{g}$ for nano V_2O_3 . Thus, the specific surfaces of nanomaterials are 15 to 38-fold higher than the specific surfaces of bulk materials. A summary of these data can also be found in Tab. 1.

3.1.2 Solubility of vanadium oxides

A feature that distinguishes V_2O_3 and V_2O_5 is solubility. In literature, the solubility of vanadium trioxide in water is given as “hardly soluble, ca. 0.1 g/l” (BGIA GESTIS database), whereas the solubility of vanadium pentoxide is 1-8 g/l in water (IARC 1997), thus at least ten-fold higher than for the trioxide. The solubility of nanomaterials in comparison to their bulk counterparts is supposed to be greater, as the increased surface to mass ratio facilitates dissolution (Borm *et al.* 2006). Thus, I was interested in probing and comparing the solubility of the four different vanadium oxide species (bulk V_2O_3 , nano V_2O_3 , bulk V_2O_5 and nano V_2O_5).

To this end, vanadium oxides were suspended in water and incubated at 37°C . At several time points, undissolved material was spun down and an aliquot of the supernatant was filtered to remove residual insoluble material. The amount of vanadium in the samples was analyzed by inductively coupled plasma optical emission spectrometry (ICP-OES). This method is based on the excitation of atoms in an argon-plasma. When the excited atoms return to a lower energy state, they emit the excess energy as photons of characteristic wavelengths. These spectra can be used both to identify elements and to quantify their amount in a sample.

Fig. 16 displays the results of the analysis of the solubility of vanadium oxides over time. Solubility of bulk V_2O_3 is low with approximately 15 mg/l and does not increase

over time. In contrast, nano V_2O_3 was found to have released 30 mg/l soluble vanadium oxide species after 3.5 hours, and this increases over time to approximately 60 mg/l after 144 hours. Bulk V_2O_5 starts with approximately 20 mg/l and the amount of soluble species increases rapidly to reach finally 130 mg/l. For nano V_2O_5 , the concentration after 3.5 hours is already 110 mg/l and goes up to nearly 160 mg/l.

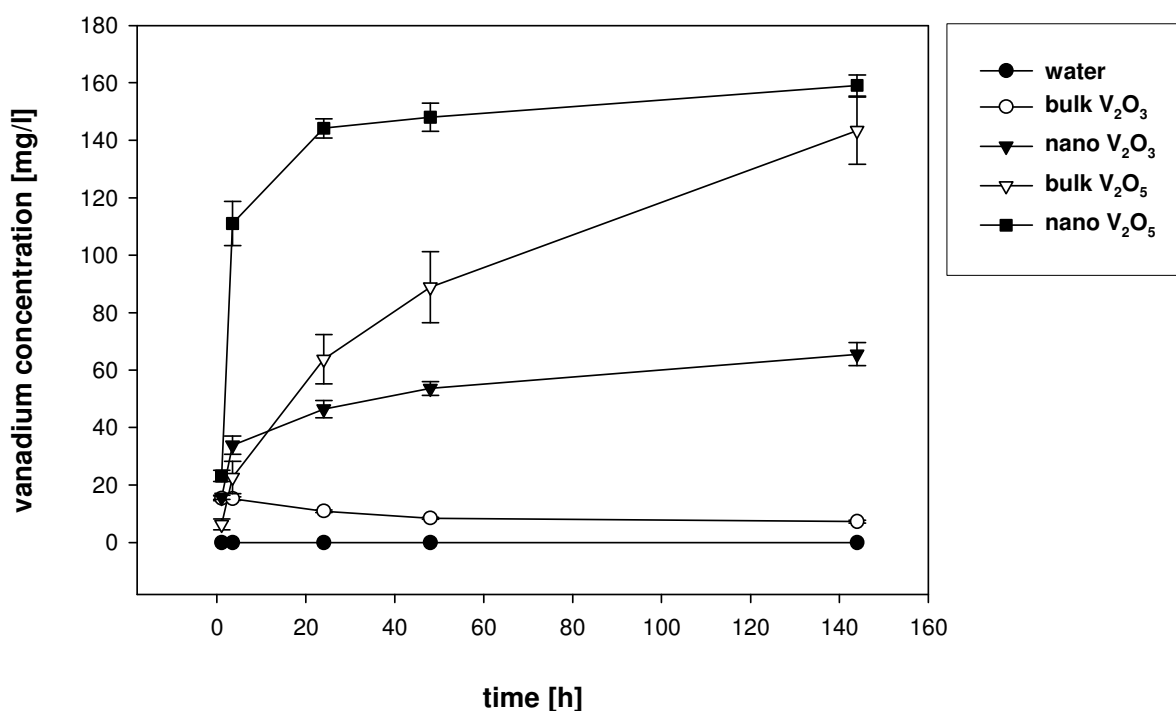


Fig. 16 Solubility of vanadium oxides.

Bulk and nanoscaled V_2O_3 and V_2O_5 (1 mg/ml in H_2O) were incubated at 37°C. At several time points, the amount of soluble vanadium oxide species in the supernatant was determined by ICP-OES. Samples were run in independent duplicates; values are means with standard deviations.

Thus, solubility is lowest for bulk V_2O_3 , intermediate for nano V_2O_3 and bulk V_2O_5 and high for nano V_2O_5 .

To account for the fact that vanadium oxides dissolve over time, a solution of vanadium oxide ions, referred to as “vanadate” in this work, has been included into the subsequent experiments to be able to assess the effect of soluble species separately.

3.2 Vanadium oxides are taken up into cells

Vanadate, which is a structural analogue of phosphate, has been shown to be able to enter cells via phosphate transport system II in fungal cells (Bowman 1983) and the anion transporter in erythrocytes (Heinz *et al.* 1982). As I could show the time-dependent dissolution of vanadium oxide species, I was interested to know if there is also vanadate uptake in A549 cells.

A549 cells were treated with $10 \mu\text{g}/\text{cm}^2$ vanadium oxides for 24 hours, harvested and lysed. The vanadium content in the lysate was determined by ICP-OES. To account for varying cell numbers, the vanadium content was normalized to the protein content of the respective samples.

Fig. 17 shows that vanadium was found in all samples exposed to vanadium oxides. It was $0.1 \mu\text{g}/\text{mg}$ protein for bulk V_2O_3 , ca. $0.25 \mu\text{g}/\text{mg}$ protein for nano V_2O_3 and bulk V_2O_5 , $0.34 \mu\text{g}/\text{mg}$ protein for nano V_2O_5 and $0.57 \mu\text{g}/\text{mg}$ protein for soluble vanadate. Thus, vanadium oxides apparently enter the cell; however, what mechanism or way of uptake is involved remains unclear.

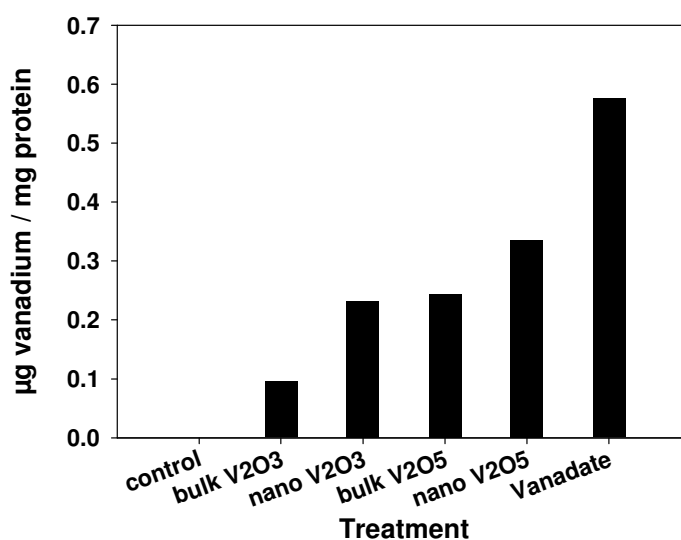


Fig. 17 Uptake of vanadium oxides into cells.

A549 cells were treated with $10 \mu\text{g}/\text{cm}^2$ of different vanadium oxide species for 24 hours. The intracellular vanadium content was analyzed by ICP-OES and normalized to the protein content of the samples.

3.3 Vanadium uptake is correlated to solubility

The results of the vanadium uptake experiment suggested a correlation with solubility, as treatment with the substance of the lowest solubility (bV_2O_3) resulted in the lowest intracellular vanadium concentration, treatment with soluble vanadate ions in the highest intracellular vanadium concentration.

I plotted the percentage of intracellular vanadium concentrations against the log of the percentage of soluble vanadium species at 24 hours. Regression analysis was performed using the SigmaPlot software.

Fig. 18 demonstrates the high correlation between the two parameters; the regression coefficient r^2 was 0.99. Thus, uptake of vanadium into cells is clearly correlated to solubility; the more soluble species are present, the more vanadium is found intracellularly.

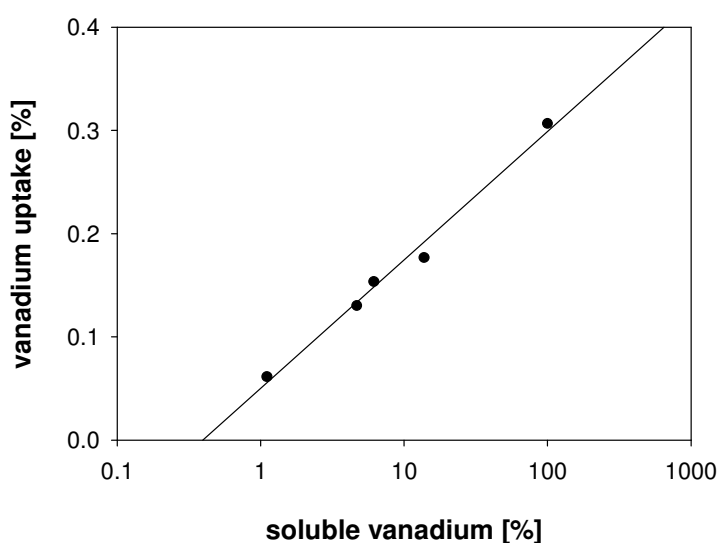


Fig. 18 Correlation of vanadium solubility and uptake.

Vanadium content in A549 cells and solubility of vanadium species were determined using ICP-OES. Percentage of vanadium uptake after 24 h in A549 cells was plotted against the log of the percentage of soluble vanadium species after 24 h. Regression analysis was performed in SigmaPlot 2002 for Windows Version 8.02 (SPSS Inc.).

3.4 Low vanadium oxide concentrations stimulate proliferation

Vanadium oxides enter A549 cells - once internalized, what is their effect on cells? To answer this question, I examined at first the influence of vanadium oxides on cell proliferation. It is known that vanadium oxides exert a biphasic effect on cell proliferation: low concentrations lead to a stimulation of cell proliferation (“insulin-like

effect”), higher concentrations inhibit cell progression or are even cytotoxic (Hanuske *et al.* 1987; Cortizo *et al.* 1995; Cruz *et al.* 1995; Rehder *et al.* 2002).

To assay cell proliferation, three different methods have been applied: 1. Cell count 2. Conversion of a redox-indicator dye by mitochondrial reduction in viable and proliferating cells (AlamarBlue™ assay) 3. Incorporation of BrdU into the DNA of proliferating cells during DNA synthesis and detection of BrdU by an antibody.

Fig. 19 shows the result of BrdU incorporation as a measure of cell proliferation. Insulin as a positive control increased cell proliferation after 24 hours 2.4-fold in comparison to control cells. This was statistically significant. A similar, significant increase was observed when cells were treated with 1 $\mu\text{g}/\text{cm}^2$ bulk V_2O_3 . The other treatments yielded either no stimulation of proliferation or decreased proliferation.

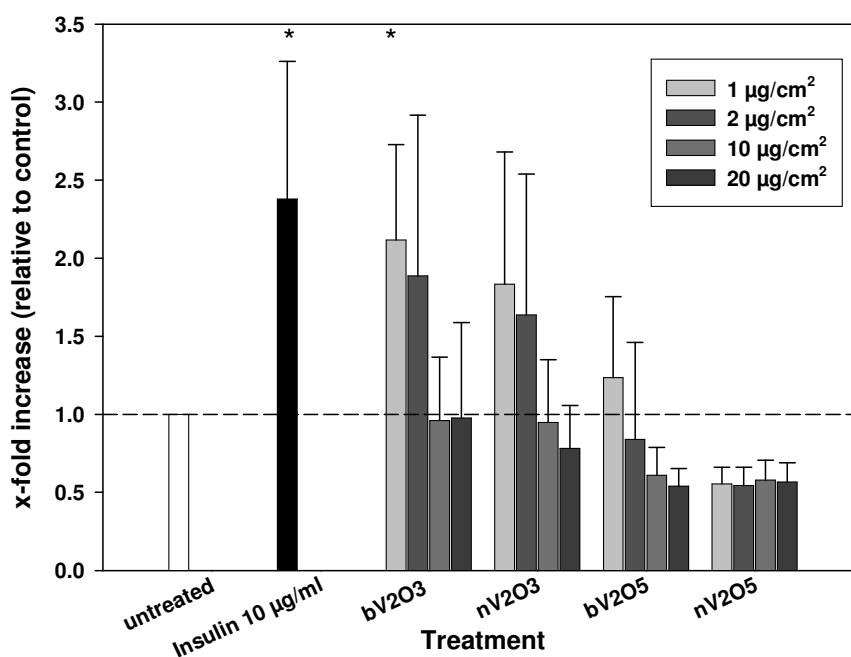


Fig. 19 Low concentrations of vanadium oxides induce cell proliferation.

A549 cells were treated for 24 hours with vanadium oxides (1, 2, 10, 20 $\mu\text{g}/\text{cm}^2$). DEG was used as a solvent control, insulin (10 $\mu\text{g}/\text{ml}$) as a positive control. Cells were labelled with BrdU. BrdU was detected by an antibody catalyzing a colorimetric reaction which was measured photometrically. Values are means of four independent experiments with standard deviations. Student's *t*-Test was performed to determine significant differences (increase) to the control. (*) $p < 0.05$.

The lowest concentration of the vanadium oxide with the lowest solubility (bV₂O₃) led to a stimulation of proliferation, i.e. low concentrations of soluble vanadium oxide displayed a pro-proliferative effect. In contrast, samples which received a higher concentration of better soluble vanadium oxides and hence a higher amount of soluble vanadate showed decreased cell growth.

The results of proliferation analysis by cell count and the AlamarBlue™ assay were similar; therefore, data are not shown here.

3.5 Acute toxicity of vanadium oxides

For the vanadium oxide bulk substances, it is known that cytotoxicity is low for bulk V_2O_3 due to its low water-solubility (WHO Regional Office for Europe Copenhagen 2000), whereas bulk V_2O_5 is cytotoxic at millimolar concentrations (Rehder *et al.* 2002). As cytotoxicity apparently is correlated to solubility, and as I observed a higher solubility for vanadium oxide nanomaterials than for their bulk counterparts, probing and comparing cytotoxicity of the bulk and nanomaterials was the next step. Moreover, these experiments were required to figure out non-cytotoxic concentrations of the vanadium oxides at which genotoxicity testing could be performed.

As earlier studies of our group revealed that nanomaterials can interfere with viability tests and yield false positive results (Worle-Knirsch *et al.* 2006), three different types of tests have been performed: 1. The MTT assay, based upon conversion of a yellow tetrazolium salt to insoluble blue formazan-crystals by mitochondrial dehydrogenases in viable cells. 2. The XTT assay, similar to the MTT assay, but yielding a water-soluble orange formazan. 3. The LDH assay, indirectly detecting cytotoxicity via leakage of the intracellular enzyme LDH into the medium as a result of disturbed membrane integrity in damaged cells. The LDH assay uses as well the conversion of a yellow tetrazolium salt to a soluble, red formazan. In all assays, the amount of the colorimetric product was analyzed photometrically and served as a measure of cell viability/activity.

The MTT assay showed (Fig. 20) that increasing concentrations of vanadium oxides resulted in decreased mitochondrial activity. This was true for all substances tested, but to a different extent. The activity of control cells was set to 100%. At the highest concentration ($62.5 \mu\text{g}/\text{cm}^2$), treatment with bulk V_2O_3 left 84% activity, treatment with nano V_2O_3 74% activity, treatment with bulk V_2O_5 58% activity and treatment with nano V_2O_5 38% activity. The concentration at which 50% of mitochondrial activity (EC_{50}) was retained was $> 62.5 \mu\text{g}/\text{cm}^2$ for bulk V_2O_3 , nano V_2O_3 and bulk V_2O_5 , $31.25 \mu\text{g}/\text{cm}^2$ for nano V_2O_5 and $20 \mu\text{g}/\text{cm}^2$ for vanadate. Hence, cytotoxicity increased with the solubility of the substance. Furthermore, the MTT assay detected the pro-proliferative effect of low vanadium oxide concentrations, too (cellular activity

above 100% for 1 and 2 $\mu\text{g}/\text{cm}^2$ bV_2O_3 and bV_2O_5 ; for 1 $\mu\text{g}/\text{cm}^2$ nV_2O_3 and vanadate).

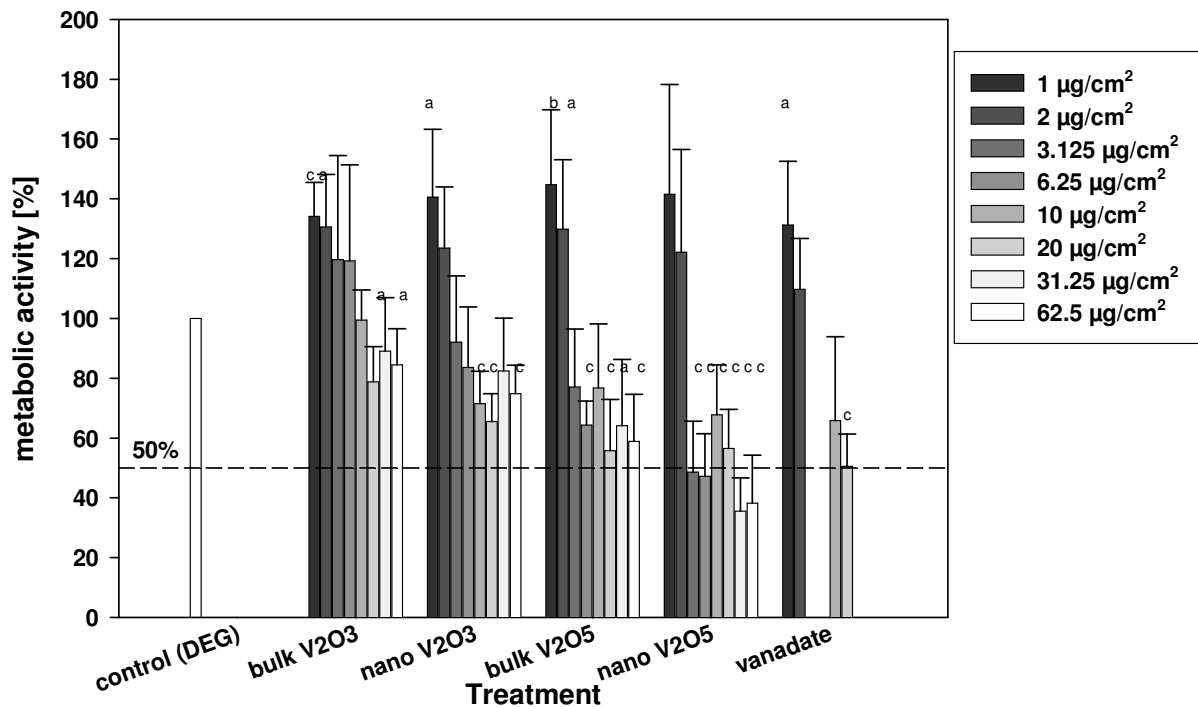


Fig. 20 Metabolic activity of cells decreases with increasing vanadium oxide concentrations.

The MTT assay was performed with A549 cells treated for 24 hours with vanadium oxides at concentrations ranging from 1 $\mu\text{g}/\text{cm}^2$ to 62.5 $\mu\text{g}/\text{cm}^2$. The metabolic activity of control cells was set to 100%. Values are relative to the control and means with standard deviations from three (3.125, 6.25, 31.25, 62.5 $\mu\text{g}/\text{cm}^2$) or four (1, 2, 10, 20 $\mu\text{g}/\text{cm}^2$) independent experiments. Student's *t*-Test was performed to determine significant differences to control. (a) $p < 0.05$; (b) $p < 0.01$; (c) $p < 0.001$.

The XTT assay yielded similar results which are not shown.

In contrast to the MTT and the XTT assay which detect metabolic activity, the LDH assay probes cell viability via the membrane integrity of the cells. No signs of cytotoxicity were observed in the LDH assay after treatment with vanadium oxide species for 24 hours (Fig. 21). After 48 hours of treatment, the LDH release showed a dose-dependent increase for nano V_2O_3 , bulk V_2O_5 and nano V_2O_5 .

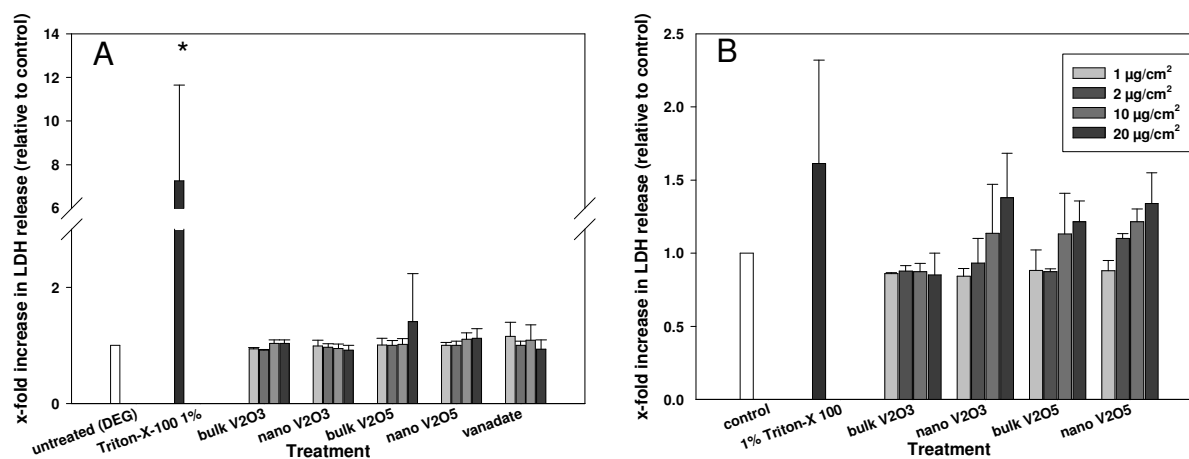


Fig. 21 Cytotoxicity of vanadium oxides measured by the LDH assay.

The LDH assay was performed with A549 cells treated for 24 hours (A) and for 48 hours (B) with vanadium oxides at different concentrations (1, 2, 10, 20 $\mu\text{g}/\text{cm}^2$). LDH release of control cells was set to 1. Values are relative to the control and means with standard deviations from three (24 hours) or two (48 hours) independent experiments. Student's *t*-Test was performed to determine significant differences to control. (*) $p < 0.05$.

Taken together, cell viability assays based upon metabolic activity responded more sensitively to treatment with vanadium oxides; even though, the viability measured by the LDH assay showed the same tendency. Vanadium oxides displayed a dose-dependent cytotoxicity and a correlation of cytotoxicity to the solubility of the substance.

3.6 (Soluble) vanadium oxides generate reactive oxygen species

Generation of reactive oxygen species (ROS) is one of the major threats to cellular integrity. ROS are produced endogenously, e.g. due to electron “leakage” in the mitochondrial electron transport chain. For this reason, cells have different mechanisms to cope with oxygen radicals. Anti-oxidative substances like glutathione or enzymes converting reactive oxygen species into innocuous products (e.g. catalase which catalyzes the reaction of hydrogen peroxide to water and oxygen) are examples for these protective mechanisms. If the cellular ROS load is elevated because of additional production of oxygen radicals by toxic substances or irradiation, the cell may lose its capacity to eliminate ROS effectively. In this case, called “oxidative stress”, the reactive oxygen species are able to oxidize cellular structures, i.e. proteins, lipids or DNA. Oxidative modification of these components often leads to malfunction or degradation and finally cell death.

Generation of ROS has been shown for vanadium oxides. In particular, hydroxyl radicals ($\cdot\text{OH}$), hydrogen peroxide (H_2O_2) and superoxide anions ($\cdot\text{O}_2^-$) are generated via enzymatic and Fenton-type reactions (Zhang *et al.* 2001). The production of reactive oxygen species is supposed to be one of the major mechanisms of cytotoxicity and genotoxicity of vanadium oxides (Evangelou, 2002). Moreover, for nanomaterials, an elevated capacity to produce ROS is suggested because of their high surface reactivity. Thus, examination of the ROS production of bulk and nano vanadium oxides is important.

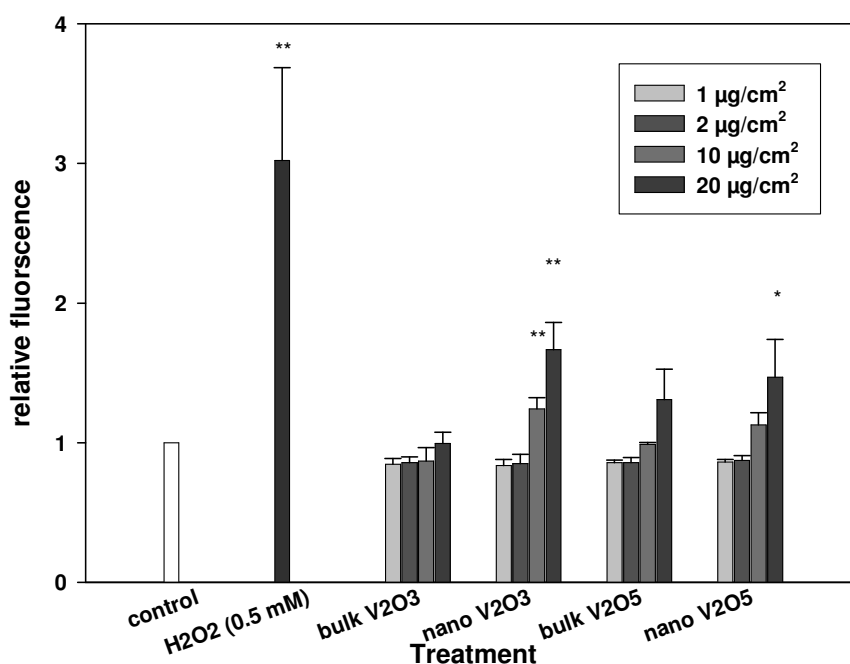


Fig. 22 Soluble vanadium oxides produce reactive oxygen species.

Vanadium oxides (1, 2, 10, 20 $\mu\text{g}/\text{cm}^2$) have been incubated in cell culture medium for 24 hours at 37°C. H_2O_2 in medium (0.5 mM) was used as a positive control. Oxidative conversion of non-fluorescent dihydrorhodamine (DHR) to fluorescent rhodamine was used to measure generation of reactive oxygen species. After incubation, 10 μM DHR was added and the samples were incubated for another 40 min and then analyzed in the fluorometer. The control was set to 1. Values are relative to the control and means with standard deviations of three independent experiments. Significant differences to the control were determined by Student's *t*-Test: (*) $p < 0.05$; (**) $p < 0.01$.

To this end, I used the dihydrorhodamine (DHR) assay which detects mainly superoxide anion and H_2O_2 (Emmendorffer *et al.* 1990; Henderson *et al.* 1993; Royall *et al.* 1993) and the DCF assay, which detects a wider range of reactive oxygen species. Both assays are based upon the oxidative conversion of a dye to a fluorescent product which can be quantified fluorimetrically.

At first, I analyzed the capacity of particles in cell culture medium without cells to generate ROS after 24 hours of incubation at 37 °C.

In Fig. 22 a dose-dependent increase in fluorescence, i.e. in the amount of ROS, can be seen for nano V_2O_3 , bulk V_2O_5 and nano V_2O_5 . Statistical significance was reached for 10 and 20 $\mu\text{g}/\text{cm}^2$ nano V_2O_3 and 20 $\mu\text{g}/\text{cm}^2$ nano V_2O_5 . Thus, the water-soluble substances, and in particular the nanomaterials, were able to produce reactive oxygen species.

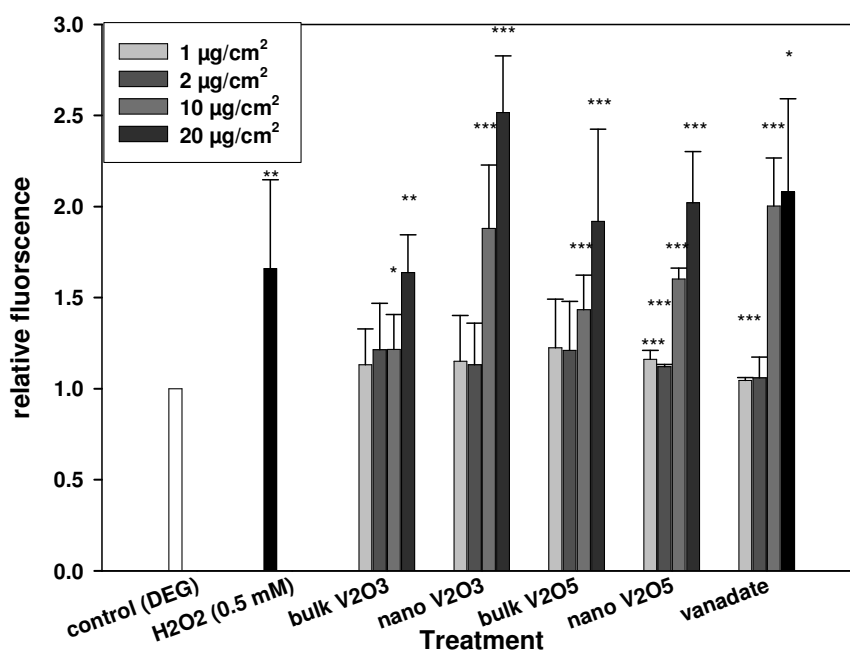


Fig. 23 Vanadium oxides lead to generation of ROS in A549 cells.

A549 cells were exposed to bulk and nano V_2O_3 , V_2O_5 and vanadate at concentrations of 1, 2, 10 and 20 $\mu\text{g}/\text{cm}^2$ for 24 hours. Oxidative conversion of non-fluorescent dihydrorhodamine (DHR) to fluorescent rhodamine was used to measure generation of reactive oxygen species. Hydrogen peroxide (0.5 mM) was used as a positive control. Values are relative values (control was set to 1) and means of three independent experiments with standard deviations. Significant differences to the control were determined by Student's *t*-Test: (*) $p < 0.05$; (**) $p < 0.01$ (***) $p < 0.001$.

Incubation of A549 cells with cell culture medium containing vanadium oxides yielded similar results. Fig. 23 shows that all vanadium oxide species included in the test produced ROS in cells, but for the poorly soluble bulk V_2O_3 , this was only statistically significant ($p < 0.05$ and $p < 0.01$ respectively) at the two highest concentrations (10 and 20 $\mu\text{g}/\text{cm}^2$). In contrast, for the more soluble species, a highly significant increase ($p < 0.001$) was observed at 10 $\mu\text{g}/\text{cm}^2$ (nano V_2O_3 and bulk V_2O_5) or already at the lowest concentration (1 $\mu\text{g}/\text{cm}^2$) for the well soluble nano V_2O_5 and vanadate ions. Thus, cells treated with vanadium oxides, especially with the well-soluble ones, are exposed to reactive oxygen species.

The DCF assay confirmed the results of the DHR assay (data not shown).

3.7 Nano vanadium trioxide, bulk vanadium pentoxide and vanadate induce oxidation of DNA bases

The presence of reactive oxygen species can harm many cellular structures. Oxidation of parts of the DNA is especially dangerous, as this can lead to an accumulation of mutations. The most common oxidative DNA lesion is 8-oxo-guanine (8-oxo-G). Guanine usually pairs with cytosine via three hydrogen bonds; however, 8-oxo-guanine is additionally able to pair with adenine via two hydrogen bonds. If this lesion is not recognized and repaired before DNA synthesis, thymine will be incorporated into the newly synthesized strand opposite to the “wrong” adenine. Consequence is a G:C to T:A transversion (Shibutani *et al.* 1991).

As I observed the generation of reactive oxygen species after exposure of cells to vanadium oxides, the question was if these oxygen radicals affected the DNA. A FITC-coupled probe specific for 8-oxo-guanine was used to detect 8-oxo-G and to analyze its amount by flow cytometry.

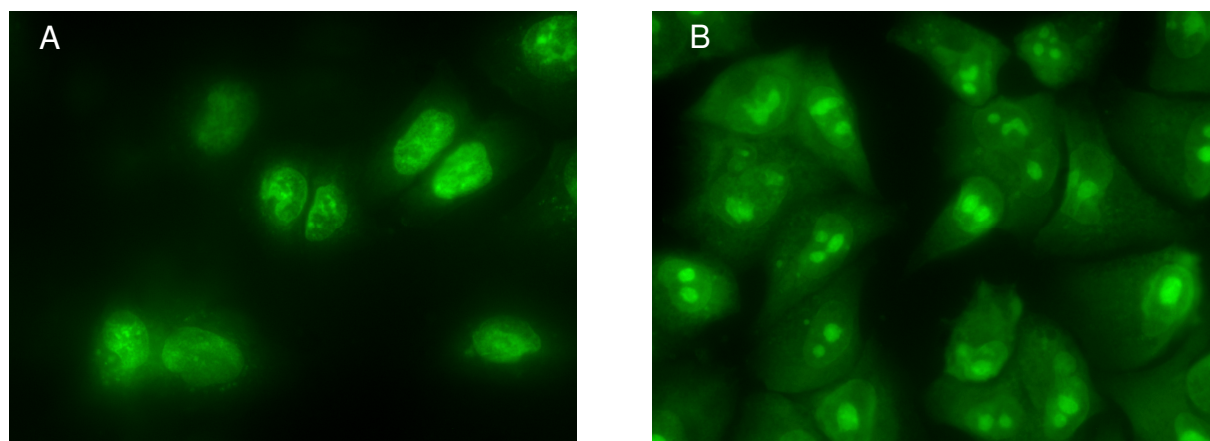


Fig. 24 Detection of 8-oxo-G in cells treated with vanadium oxides by a FITC-coupled probe. A549 cells were grown in chamber slides, treated with DEG as a control (A) and bulk V₂O₅ (2 µg/cm²) (B) for 24 hours, fixed with 4% PFA and stained with a fluorescent probe. Fluorescence was analyzed with the DM IRE2 microscope. Magnification: 630x.

At first, cells were grown, treated, fixed and stained in chamber slides to examine the staining pattern of the FITC-coupled 8-oxo-guanine probe. Fig. 24 shows a modest staining in the nuclear region in control cells.

It has been shown that vanadium(IV), which is generated by intracellular reduction of vanadium pentoxide, induces 8-oxo-G formation in the DNA (Shi *et al.* 1996). Thus, I

expected an increased amount of 8-oxo-G in cells treated with bulk vanadium pentoxide. Indeed, in cells exposed to bulk vanadium pentoxide, the staining is brighter, in particular in the nucleolar region (which contains an especially high content in guanine (Willems *et al.* 1968)). (Moreover, the cytoplasm is also fluorescing more than in control cells. The reason for this cytoplasmic staining may be that reactive oxygen species oxidize bases in the RNA as well and that oxidized RNA bases are recognized by the probe, too.)

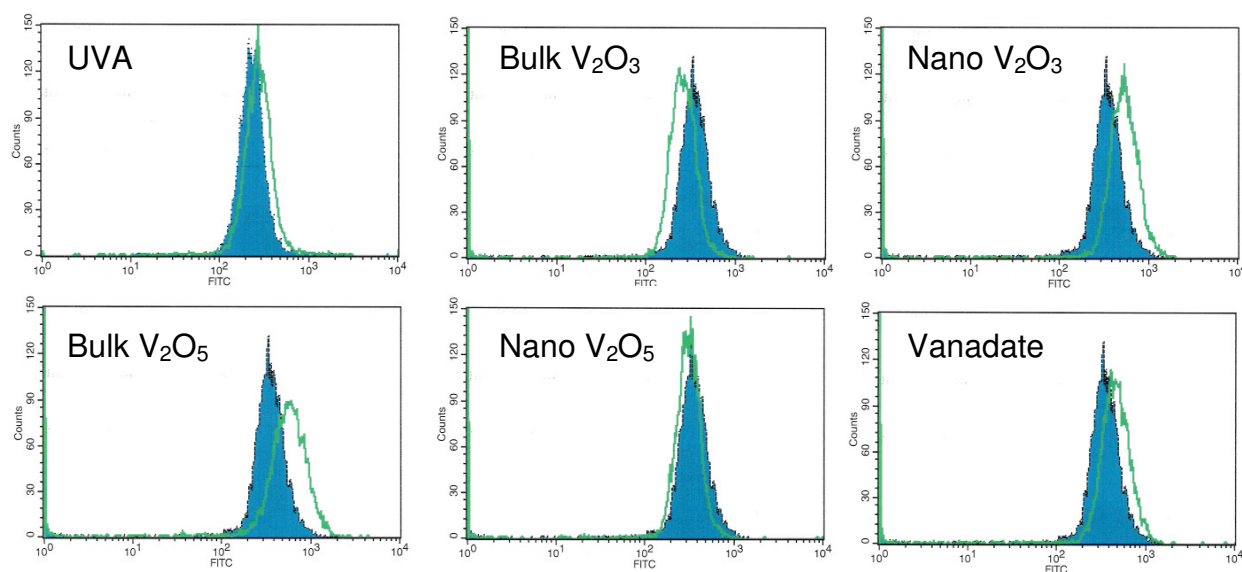


Fig. 25 Changes in 8-oxo-G content after treatment with vanadium oxides.

A549 cells were treated as indicated (positive control 180 J/cm² UVA, vanadium oxides: 2 µg/cm²) for 24 hours, then harvested, fixed and stained with a fluorescent probe specific for 8-oxo-guanine. Fluorescence was analyzed by flow cytometry. Overlays of two histograms are shown. Blue: control cells; green: treated cells.

To quantify the amount of 8-oxo-guanine in cells treated with different vanadium oxide species, cells stained with the probe were analyzed by flow cytometry. In Fig. 25, the results of one representative experiment are shown. A shift to the right in comparison to untreated, stained control cells indicates an increase in fluorescence and thus in 8-oxo-G content, a shift to the left a decrease. An increase in 8-oxo-G was found for the positive control UVA, nano V₂O₃, bulk V₂O₅ and vanadate. It was particularly strong for nano V₂O₃ and bulk V₂O₅. For bulk V₂O₃ and nano V₂O₅, a decrease was observed, which was pronounced for the trioxide and moderate for the nano pentoxide.

To determine the difference between control and treated cell populations, the Kolmogorov-Smirnov statistics included in the CellQuestPro software was applied. This is a two-sample test which determines if two overlaid histograms come from different populations. The calculation computes the summation of the curves and finds the greatest difference between the summation curves. The resulting value $D/s(n)$ is a measure for the difference of two overlaid histograms. The bigger $D/s(n)$, the larger is the difference between two populations.

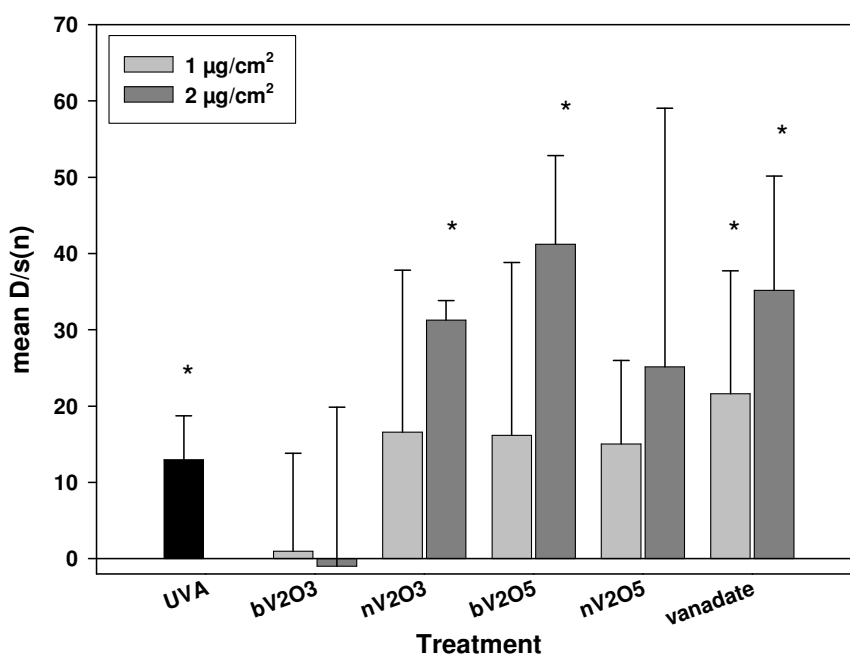


Fig. 26 Analysis of the 8-oxo-G content in cells treated with vanadium oxides.

A549 cells were treated with vanadium oxides ($1 \mu\text{g}/\text{cm}^2$ or $2 \mu\text{g}/\text{cm}^2$) for 24 h and stained with a FITC-coupled probe for 8-oxo-guanine. UVA irradiation ($180 \text{ J}/\text{cm}^2$) was used as positive control. Fluorescence was measured by flow cytometry. Kolmogorov-Smirnov-Statistics (provided with CellQuestPro software, BD Biosciences) was performed to determine the difference in fluorescence of two differently treated cell populations. The $D/s(n)$ value is a measure for the difference of the control and the treated population. Shifts to the right were set as positive values, shifts to the left as negative values. Mean values with standard deviations of three independent experiments are shown in the graph. If the mean value minus standard deviation was >5 , this was considered as significantly different from the control (untreated cells) (*).

I calculated the mean $D/s(n)$ of three independent experiments. Shifts to the left were set as negative values, shifts to the right as positive values. I assumed a significant difference between control and treated cells if the mean value minus the standard deviation was >5 .

The results are displayed in Fig. 26. There is a significant difference between untreated control cells and cells treated with $2 \mu\text{g}/\text{cm}^2$ nano V_2O_3 , bulk V_2O_5 and 1 and $2 \mu\text{g}/\text{cm}^2$ vanadate, but not for treatment with bulk V_2O_3 and nano V_2O_5 . Thus,

the soluble and ROS-producing vanadium oxides induce oxidation of guanine, with exception of nano V_2O_5 . The latter is rather surprising, as nano V_2O_5 generated ROS in comparable amounts to the other substances (nano V_2O_3 , bulk V_2O_5 , vanadate) but this did apparently not lead to an increase in 8-oxo-G content.

3.8 Nano vanadium trioxide and bulk vanadium pentoxide induce DNA strand breaks

Besides being mutagenic, oxidative DNA lesions can also lead to strand breaks. If a repair enzyme such as oxo-guanine-glycosylase (OGG1) excises 8-oxo-G, an abasic site results (Krokan *et al.* 1997), which can lead to a DNA single strand break (reviewed in (Boiteux *et al.* 2004)). Hence, as I observed an increase in the content of 8-oxo-G in the DNA after treatment with some vanadium oxides, I was interested if strand breaks occur in cells exposed to vanadium oxides.

The alkaline comet assay, also called single cell gel electrophoresis, was performed. This method detects DNA strand breaks and alkalilabile sites. Cells are embedded into an agarose gel, lysed and DNA is subjected to an electrical field. The bulky genomic DNA merely migrates, but DNA fragments derived from strand breaks move due to their negative charge towards the cathode. A comet-like structure is formed, with a “head” (undamaged, non-migrating DNA) and a “tail” (DNA fragments migrating towards the cathode). The DNA is stained and analyzed by fluorescence microscopy. The “Viscomet” software was used to determine “head intensity” and “tail intensity”, i.e. the percentage of DNA in the head or the tail. The tail intensity served as a measure of DNA damage.

For time-points earlier than 24 hours (6 hours and 14 hours), no increase in tail intensity was observed after treatment with vanadium oxides (data not shown).

After 24 hours (Fig. 27), treatment with $2 \mu\text{g}/\text{cm}^2$ nano V_2O_3 resulted in a statistically significant increase in tail intensity (5% in contrast to 2% for untreated controls). Treatment for 36 hours showed even more elevated tail intensities. The tail intensity was 15 % for $2 \mu\text{g}/\text{cm}^2$ nano V_2O_3 , 7% for $1 \mu\text{g}/\text{cm}^2$ and 12% for $2 \mu\text{g}/\text{cm}^2$ bulk V_2O_5 . After 48 hours, tail intensity in these samples increased further to 20% ($2 \mu\text{g}/\text{cm}^2$ nano V_2O_3), 9% ($1 \mu\text{g}/\text{cm}^2$ bulk V_2O_5) and 12% ($2 \mu\text{g}/\text{cm}^2$ bulk V_2O_5). Thus, treatment with nano V_2O_3 and bulk V_2O_5 led to a considerable amount of DNA strand breaks, with tail intensities being 5 to 10 times higher than in control cells.

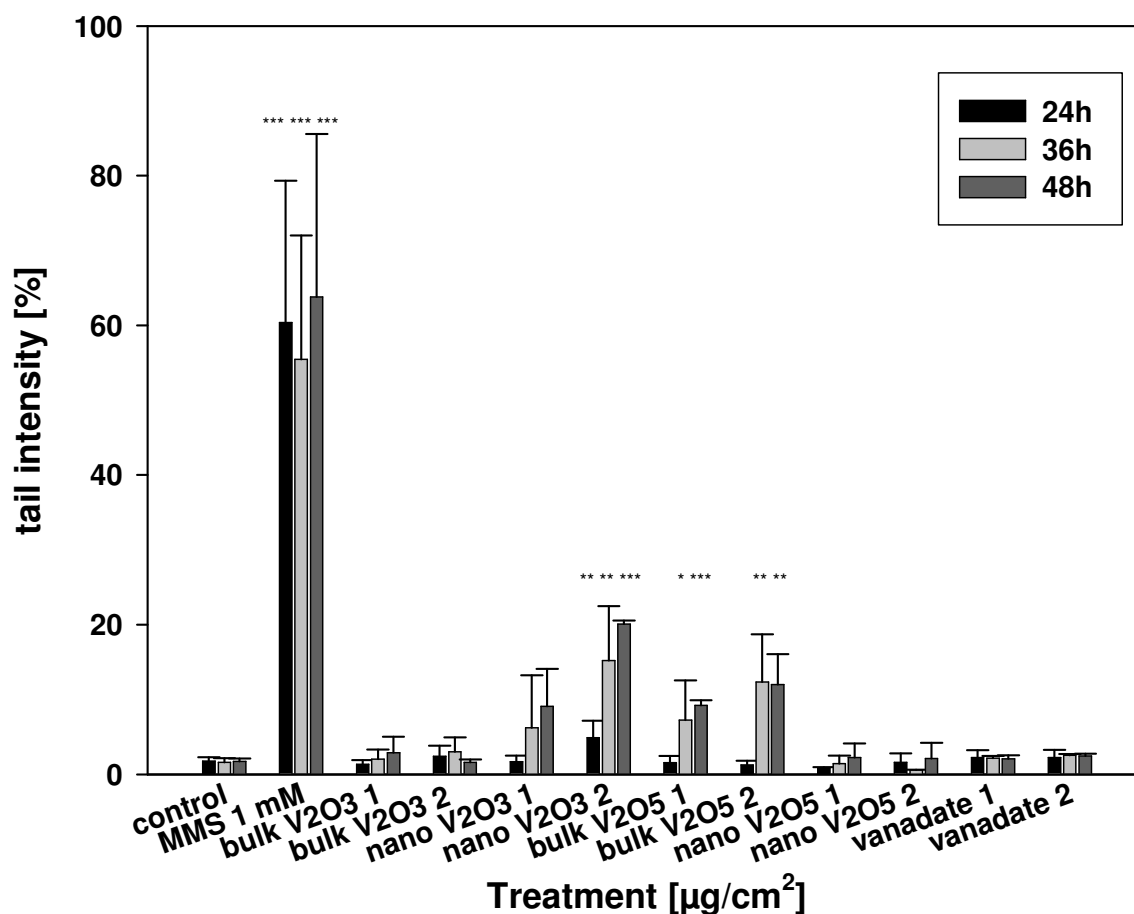


Fig. 27 Nano V₂O₃ and bulk V₂O₅ induce strand breaks in A549 cells.

A549 cells were exposed to vanadium oxides (1 and 2 $\mu\text{g}/\text{cm}^2$) for 24, 36 and 48 hours. Methyl methanesulfonate (MMS, 1 mM) was used as a positive control. An alkaline comet assay was performed to measure the amount of DNA strand breaks (tail intensity indicates percentage of DNA in the tail of the comet). Samples were run in duplicates; per slide, 50 cells were analyzed blinded. Values are means of at least two independent experiments with standard deviations ($n=4$ for controls). Significant differences to the control were determined by Student's *t*-Test: (*) $p<0.05$; (**) $p<0.01$; (***) $p<0.001$.

3.9 No induction of micronuclei by vanadium oxides

After having observed the strand-breaking capacity of several vanadium oxides in the comet assay, I wanted to examine the genotoxicity of vanadium oxides by another common genotoxicity test.

The micronucleus test is a genotoxicity test which detects DNA damage at the chromosomal level. Micronuclei are due to chromosomal breaks or lagging chromosomes (which occur because of aberrations in the centromeric region or disturbance of the mitotic spindle and chromosome separation). Correlation of an increase in the number of micronucleated cells and carcinogenesis has been shown.

Thus, the micronucleus test is one of the most important tests used in genotoxicity testing (Fenech 2000). Besides the induction of micronuclei which serves as a measure for the genotoxic potential of a substance, numerous other parameters can be scored. Examples are the frequency of apoptotic cells (pointing to induction of apoptosis), the frequency of mitotic cells and the nuclear division index (showing possible effects on cell proliferation and mitosis), the number of nucleoplasmatic bridges (a sign for chromosomal rearrangements). Scoring of these additional parameters gives a comprehensive view of the (geno)toxic effects of a substance.

During the first run, I used to score the number of mono-, bi- and polynucleated cells and the number of apoptotic and mitotic cells. The nuclear division index (NDI) was calculated according to the formula given in (Fenech *et al.* 2003): $NDI = (M_1 + 2M_2 + 3M_3 + 4M_4)/N$, where M_1 – M_4 represent the number of cells with 1 to 4 nuclei and N is the total number of viable cells scored. In my samples, tri- or tetranucleated cells occurred very rarely (<0.1%), thus the NDI reflects basically the ratio of mono- to binucleated cells. An NDI of 1 means that no cell division has occurred, whereas an NDI of 2 means all cells have accomplished one cell division.

For control cells, the NDI was 1.7, i.e. the sample contained approximately 70% binucleated and 30% mononucleated cells (Fig. 28). All samples treated with vanadium oxides (except 2 $\mu\text{g}/\text{cm}^2$ bulk V_2O_5) yielded a similar NDI, thus, treatments showed no cytostatic effect. The decrease in NDI for bulk V_2O_5 (1.45) was comparable to that of MMS (1.53), a DNA-alkylating substance which is known to have a cytostatic potential.

The frequency of apoptotic and mitotic cells was approximately 2.5% for both parameters in control cells. In treated cells, these values varied, but never reached statistically significant differences to the control (Fig. 29).

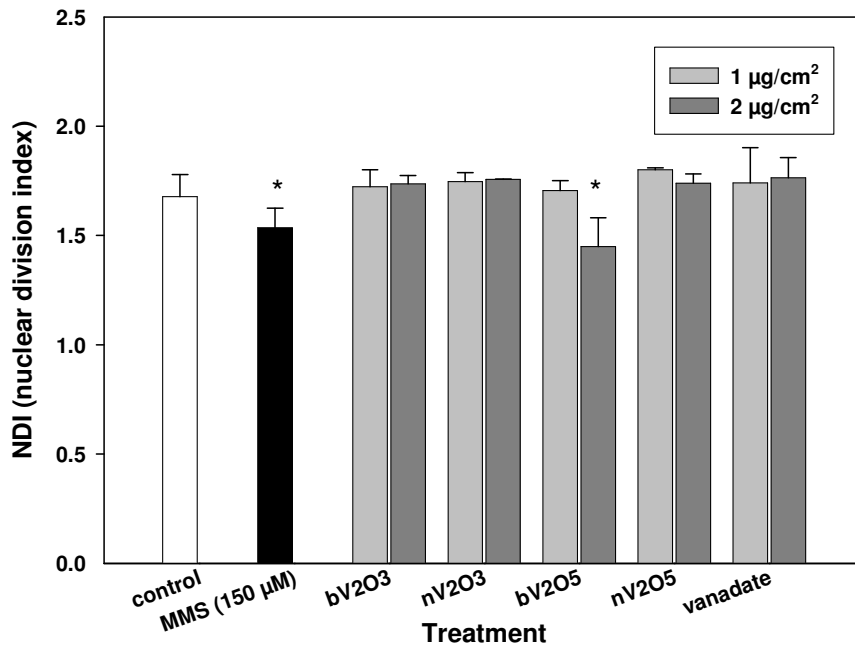


Fig. 28 Effect of vanadium oxides on cell division in the micronucleus test.

A549 were grown and treated for 24 hours in 4-well chamber slides with vanadium oxides (1 and 2 µg/cm²), MMS (150 µM) as a positive control or DEG as a solvent control. Simultaneous incubation with cytochalasin B (4 µg/ml for 24 hours) was used to induce binucleated cells. Cells were fixed with ethanol and stained with acridinorange. The number of mono-, bi- and polynucleated cells was scored blinded and the nuclear division index (NDI) calculated. Values are means of three or six (controls) independent experiments with standard deviations. Student's *t*-Test was performed to determine significant differences from the control. (*) *p*<0.05.

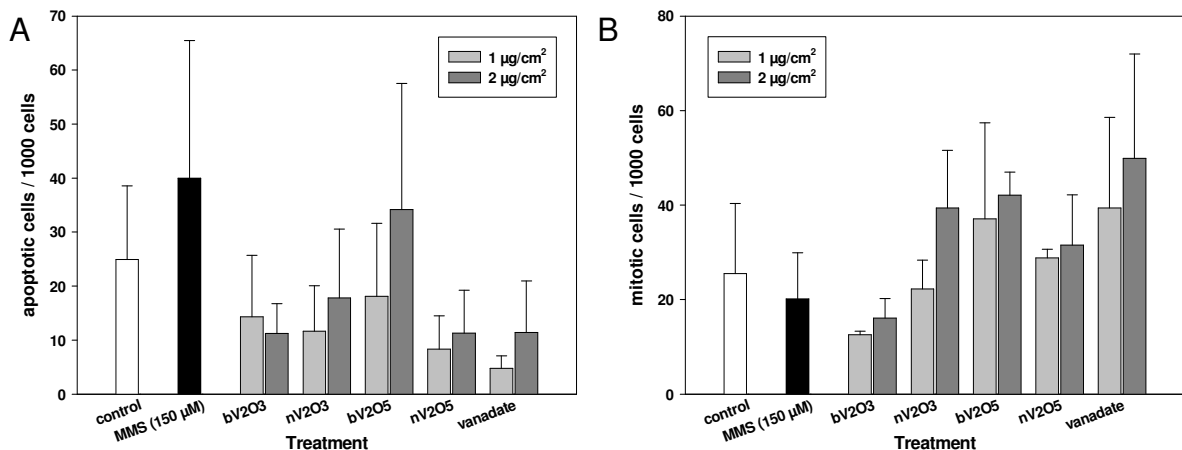


Fig. 29 No induction of apoptosis or mitosis by vanadium oxides in the micronucleus test.

A549 were grown and treated for 24 hours in 4-well chamber slides with vanadium oxides (1 and 2 µg/cm²), MMS (150 µM) as a positive control or DEG as a solvent control. Simultaneous incubation with cytochalasin B (4 µg/ml for 24 hours) was used to induce binucleated cells. Cells were fixed with ethanol and stained with acridinorange. The number of apoptotic (A) or mitotic (B) cells were scored blinded. Values are means of three or six (controls) independent experiments with standard deviations. Student's *t*-Test was performed to determine significant differences from the control.

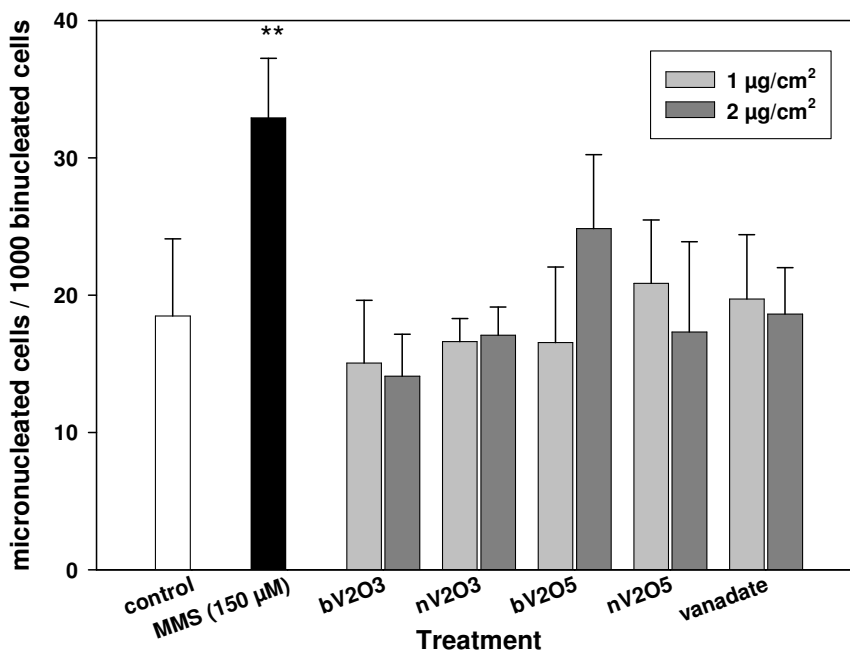


Fig. 30 No induction of micronuclei by vanadium oxides.

A549 were grown and treated for 24 hours in 4-well chamber slides with vanadium oxides (1 and 2 µg/cm²), MMS (150 µM) as a positive control or DEG as a solvent control. Simultaneous incubation with cytochalasin B (4 µg/ml for 24 hours) was used to induce binucleated cells. Cells were fixed with ethanol and stained with acridinorange. The number of binucleated cells and the number of binucleated cells with micronuclei was scored blinded. Values are means of three or six (controls) independent experiments with standard deviations. Student's *t*-Test was performed to determine significant differences from the control. (**) $p < 0.01$.

In the second run, the numbers of binucleated cells in total and those containing one or more micronuclei were scored. Control cells showed a frequency of roughly 2% micronucleated cells (18.5 binucleated cells with micronuclei in 1.000 binucleated cells) (Fig. 30). Treatment with the positive control MMS increased the number of micronucleated cells to 35 per 1.000 binucleated cells, which was statistically significant ($p < 0.01$). In cells treated with vanadium oxides, no statistically significant induction of micronuclei was observed. Only treatment with 2 µg/cm² of bulk V₂O₅ elevated the number of cells with micronuclei to 25 per 1.000 cells; however, this is statistically not significantly different from control cells.

To sum up the results of the micronucleus test, no significant genotoxic potential was observed for vanadium oxides. At the most, there was a tendency for bulk V₂O₅ to affect cell division and DNA integrity, shown as a decrease in the NDI and a slight increase in micronucleus frequency.

3.10 Soluble vanadium oxides change nuclear morphology and mitosis

During scoring for the micronucleus test, I observed cells which displayed a strange nuclear morphology (see Fig. 31). Their nuclei looked segmented, with segments connected by structures resembling nucleoplasmatic bridges. There seemed to be different stages of this morphology; cells with segmented nuclei which were still distinguishable as two nuclei (upper row), and cells whose nucleus or nuclei resembled the petals of a flower (lower row). I started scoring these remarkable structures, too, in order to see if they were related to any treatment.

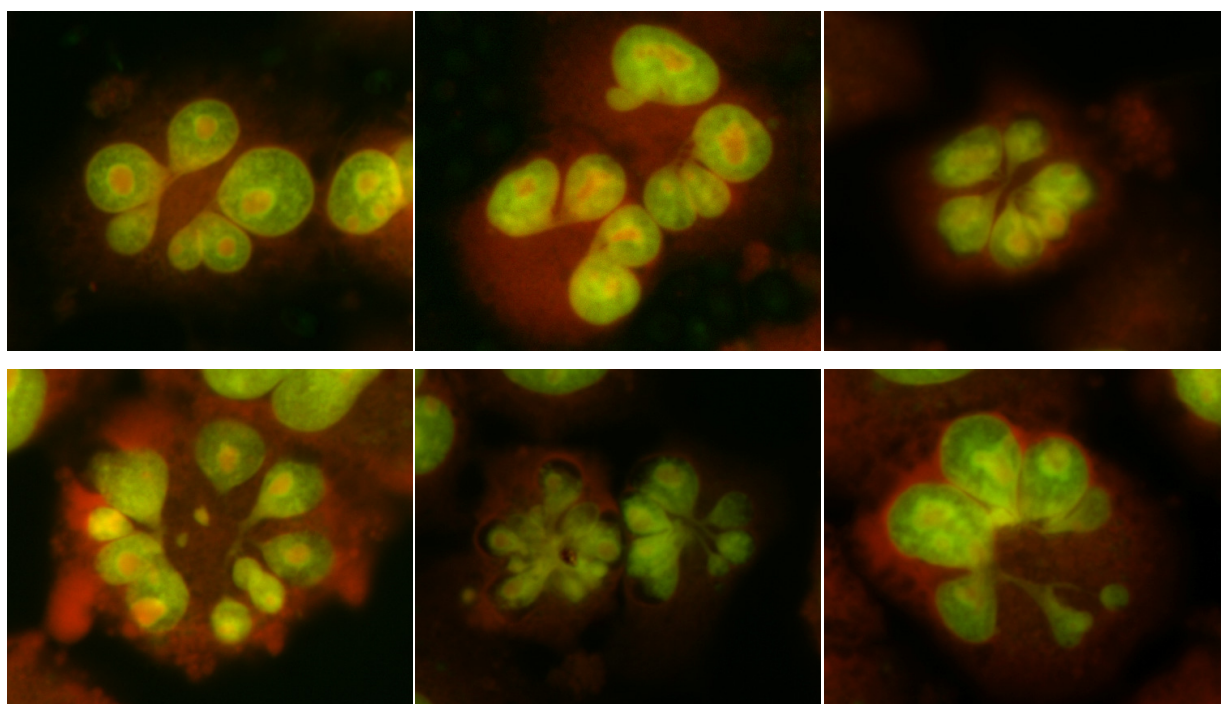


Fig. 31 Altered nuclear morphology in cells treated with vanadium oxides.

A549 cells were grown and treated in 4-well chamber slides with vanadium oxides (1 and 2 $\mu\text{g}/\text{cm}^2$) for 24 hours. Simultaneous incubation with cytochalasin B (4 $\mu\text{g}/\text{ml}$ for 24 hours) was used to induce binucleated cells. Cells were fixed with ethanol and stained with acridinorange and analyzed using fluorescence microscopy. An overlay of red and green fluorescence is shown. Magnification 630x.

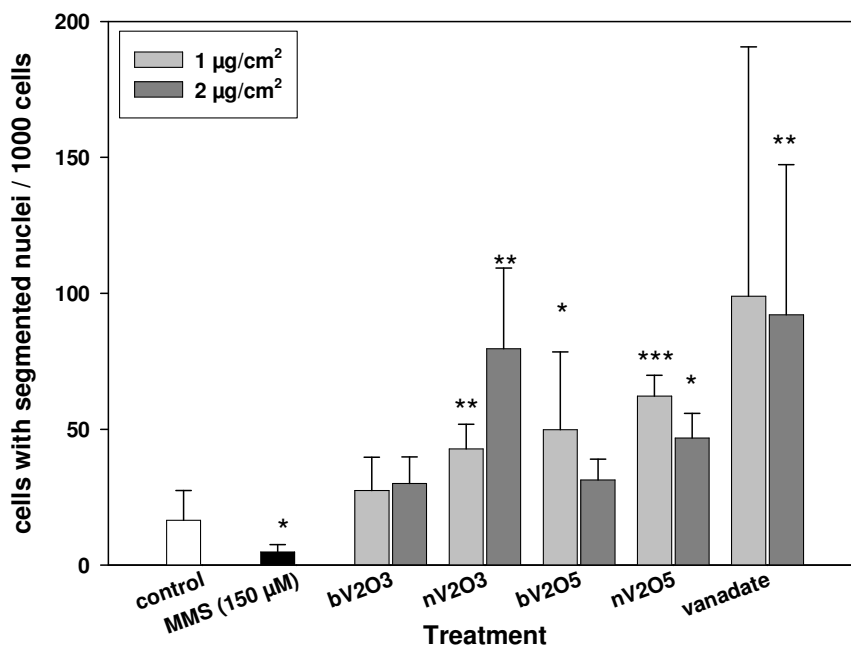


Fig. 32 Soluble vanadium oxides increase the number of cells with segmented nuclei.

A549 cells were grown and treated for 24 hours in 4-well chamber slides with vanadium oxides (1 and 2 µg/cm²). Simultaneous incubation with cytochalasin B (4 µg/ml for 24 hours) was used to induce binucleated cells. Cells were fixed with ethanol and stained with acridinorange and analyzed using fluorescence microscopy. The number of cells with segmented nuclei was scored blinded. Values are means of three independent experiments with standard deviations. Student's *t*-Test was performed to determine significant differences from the control. (*) *p*<0.05; (**) *p*<0.01; (***) *p*<0.001.

Fig. 32 shows the results of this scoring: An altered nuclear morphology was found in 16 of 1.000 cells of untreated control cells. In cells exposed to MMS, less than 5 cells in 1.000 looked changed. Bulk V₂O₃ displayed control levels, but nano V₂O₃, bulk V₂O₅, nano V₂O₅ and vanadate increased the number of cells with segmented nuclei 4 to 7-fold to up to 9% of the total cell number. With exception of 2 µg/cm² bulk V₂O₅ and 1 µg/cm² vanadate, these values were statistically highly significant. Thus, the soluble vanadium oxide species were apparently able to induce a change in nuclear morphology.

Moreover, I also remarked numerous mitotic cells which showed unusual chromosomal arrangements (see Fig. 33). Hence, the presence of vanadium oxides seems to affect mitosis and nuclear structure.

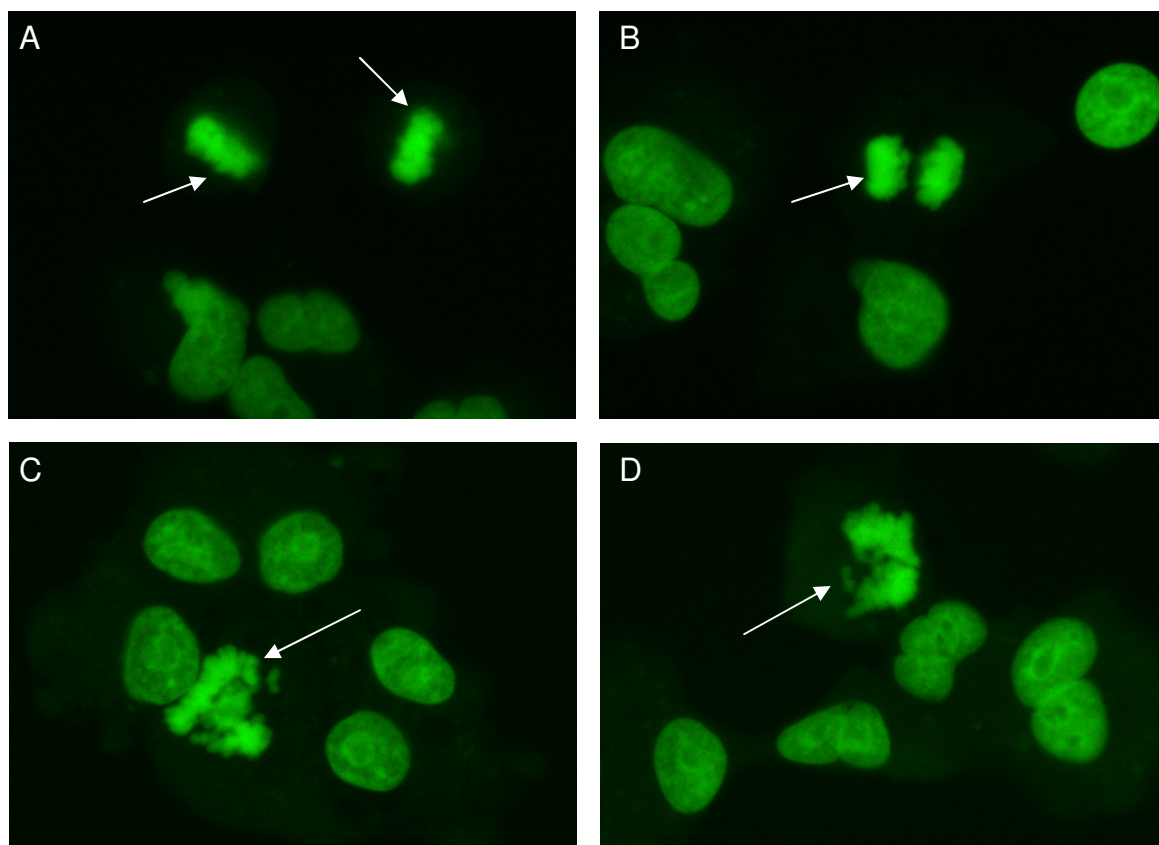


Fig. 33 Irregular mitosis in cells treated with vanadium oxides.

A549 cells were grown and treated for 24 hours in 4-well chamber slides with vanadium oxides (1 and 2 $\mu\text{g}/\text{cm}^2$) or DEG as a solvent control. Simultaneous incubation with cytochalasin B (4 $\mu\text{g}/\text{ml}$ for 24 hours) was used to induce binucleated cells. Cells were fixed with ethanol and stained with acridinorange and analyzed using fluorescence microscopy. (A) Regular metaphase in control cells. (B) Regular anaphase in control cells. (C and D) irregular mitosis in treated cells. Arrows: Cells undergoing mitosis. Magnification 630x.

3.11 Nano vanadium trioxide, bulk vanadium pentoxide and vanadate induce cell cycle arrest

Finally, I was interested in the cellular consequences of the oxidative DNA damage caused by nano V_2O_3 and bulk V_2O_5 . If 8-oxo-guanine is not excised from the DNA before replication, mutagenic G:C to T:A transversions can occur (Shibutani *et al.* 1991). Furthermore, strand breaks also have to be repaired before a cell is allowed to progress in cell cycle. Arresting the cell cycle before mitosis enables the cell to repair the DNA. It has been reported that vanadate induced a G2/M arrest in A549 cells (Zhang *et al.* 2001; Zhang *et al.* 2003). To see if this was also the case for the vanadium oxides used in this study, a cell cycle analysis was performed.

Cellular DNA levels change during cell cycle: It is 1n during G0/G1 phase, increases during the DNA-synthesis in S-phase and reaches 2n before mitosis. After mitosis, it

is 1n for every daughter cell. Staining of the DNA with a fluorescent dye makes it possible to analyze the cellular DNA content and thus the distribution of cell cycle phases in a cell population.

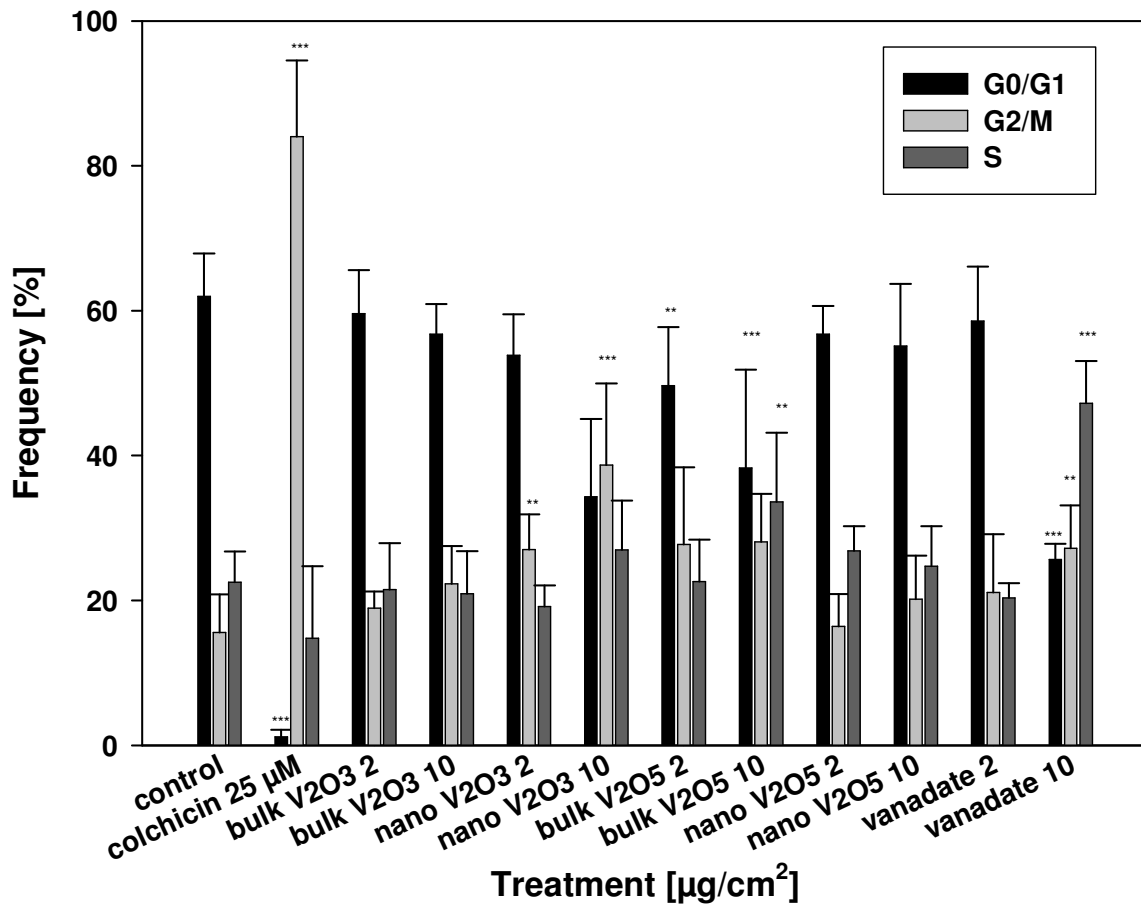


Fig. 34 Nano V_2O_3 , bulk V_2O_5 and vanadate induce cell cycle arrest.

A549 cells were exposed to 2 and 10 $\mu\text{g}/\text{cm}^2$ of vanadium oxides for 24 hours. Cells were fixed and stained with DAPI. DAPI fluorescence is proportional to DNA content and was analyzed by flow cytometry. Different cell cycle phases are characterized by different DNA content: 1 n in G0/G1 phase, 2 n in G2/M phase and 1-2n in S-Phase. Colchicin (25 μM) was used as a positive control for G2/M arrest. Values are means of at least three independent experiments with standard deviations. Significant differences to the control were determined by Student's *t*-Test: (**) $p < 0.01$; (***) $p < 0.001$.

Fig. 34 shows the distribution of cells in G0/G1 phase, G2/M phase and S-phase after different treatments. In control cells, 60% of the cells are in G0/G1 phase, and each approximately 20% in G2/M and S-phase. This distribution is unchanged in cells treated with bulk V_2O_3 . After exposure to nano V_2O_3 and bulk V_2O_5 , the fraction of cells in G2/M is markedly increased at the expense of cells in G0/G1. These changes were statistically significant for both concentrations of nano V_2O_3 and bulk V_2O_5 . For 10 $\mu\text{g}/\text{cm}^2$ vanadate, there were also significant alterations in the cell cycle, but the amount of cells in G2/M was only slightly elevated, whereas the ratio of cells in S-

phase was particularly increased. Thus, after exposure to certain vanadium oxides, a G2/M arrest occurs.

3.12 No induction of DNA strand breaks by TiO₂, CB and ZnO nanoparticles

To compare the effects of the different vanadium oxides with particles made from other materials, the genotoxic potential of Carbon Black, TiO₂ and ZnO nanoparticles was examined. In contrast to vanadium oxide nanomaterials which find only limited application these particles are produced and used at large scale in more and more products of everyday-life (e.g. cosmetics, printer toners, paint). Thus, knowledge of a possible genotoxicity is required to prevent threats to human health.

The comet assay was performed for the three nanomaterials. Tail intensities after 24 and 48 hours were examined. Fig. 35 shows no statistically significant increase in tail intensities for any of the nanoparticles. Thus, Carbon Black, TiO₂ and ZnO do not induce strand breaks in lung epithelial cells.

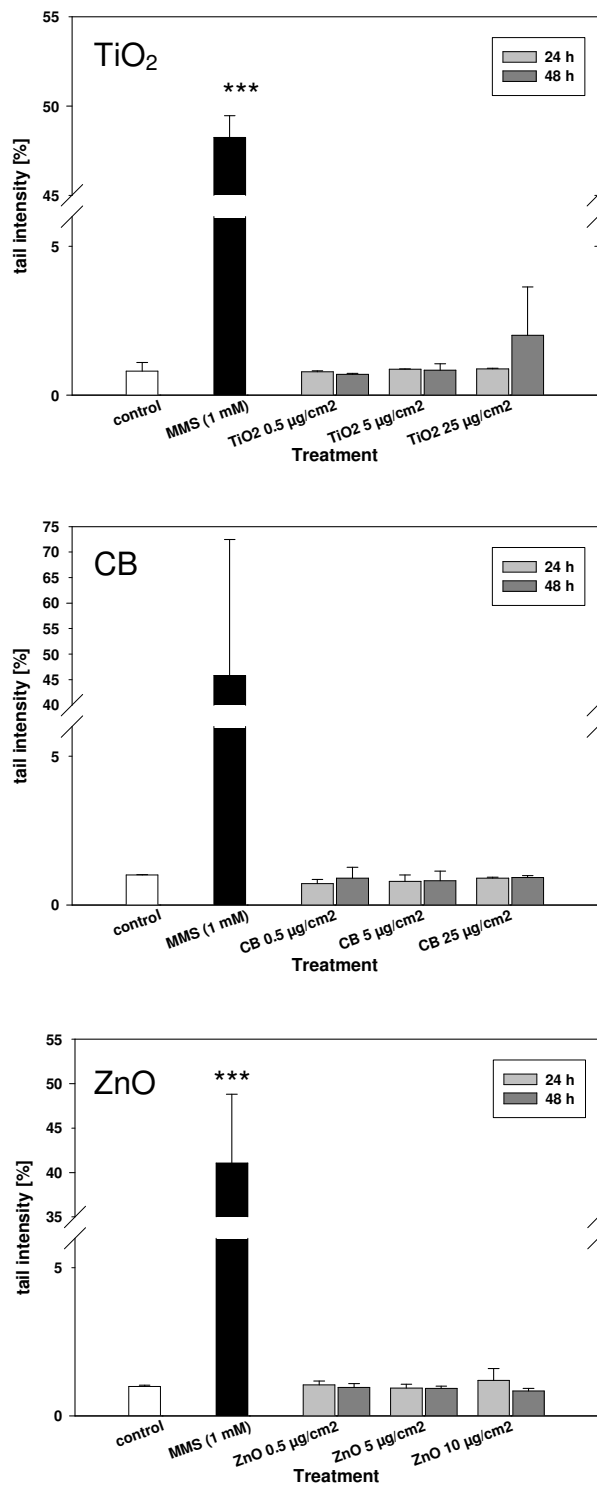


Fig. 35 No induction of DNA strand breaks by TiO₂, CB and ZnO nanoparticles.

A549 cells were treated for 24 and 48 hours with TiO₂, CB (concentrations were 0.5, 5 and 25 µg/cm²) or ZnO (0.5, 5 and 10 µg/cm²) or left untreated. Methyl methanesulfonate (MMS, 1 mM) was used as a positive control. An alkaline comet assay was performed to measure the amount of DNA strand breaks (tail intensity indicates percentage of DNA in the tail of the comet). Samples were run in duplicates; per slide, 50 cells were analyzed blinded. Values are means of three independent experiments with standard deviations. Significant differences to the control were determined by Student's *t*-Test: (***) $p < 0.001$.

3.13 No induction of micronuclei by TiO₂

The micronucleus test was performed with TiO₂ nanoparticles. TiO₂ nanoparticles are used for example in sunscreens.

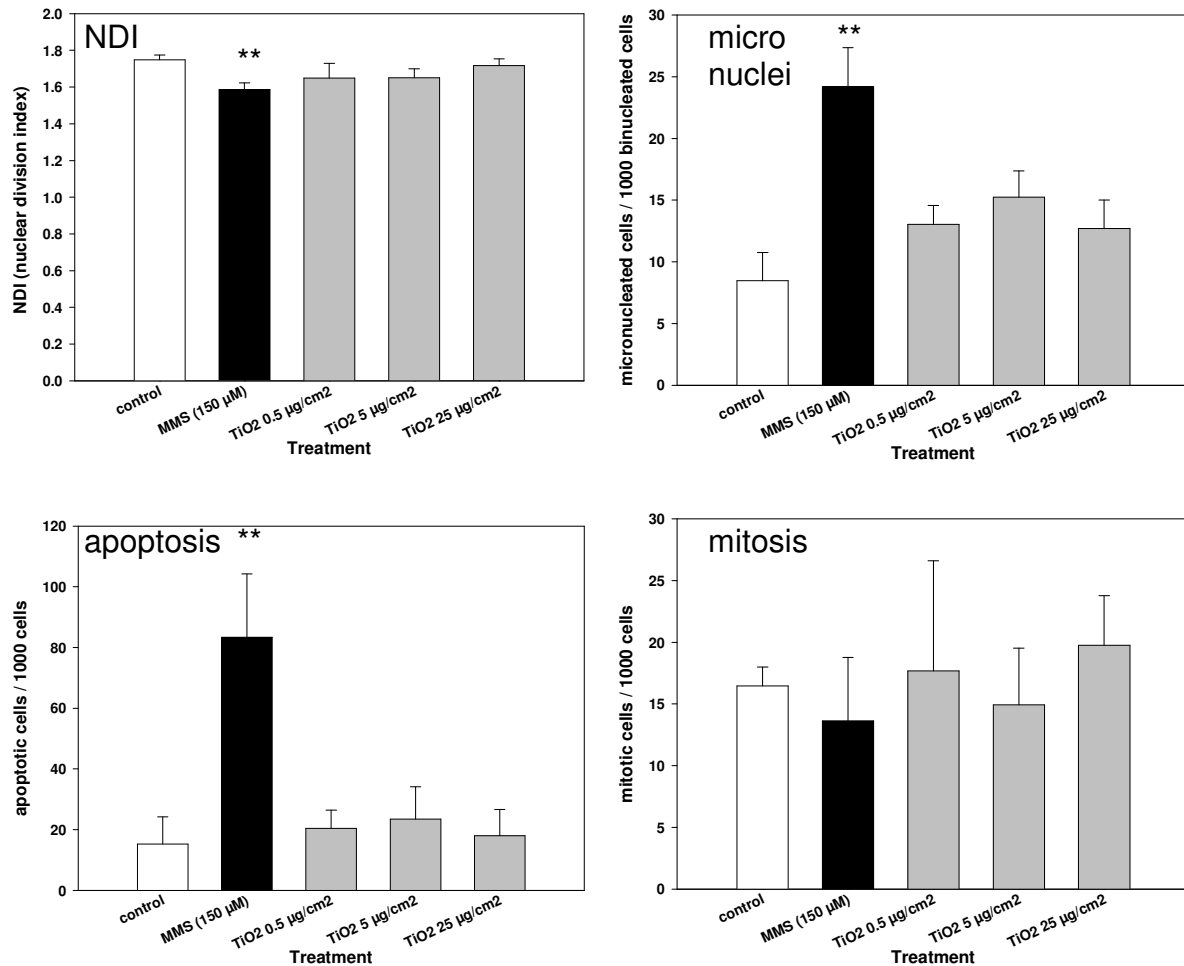


Fig. 36 Treatment with TiO₂ induces no changes in micronucleus test parameters.

A549 cells were exposed to TiO₂ (0.5, 5 and 25 μg/cm²) for 24 hours or left untreated. Methyl methanesulfonate (MMS, 150 μM) was used as a positive control. Simultaneous incubation with cytochalasin B (4 μg/ml for 24 hours) was used to induce binucleated cells. Cells were fixed with ethanol and stained with acridinorange. Scoring was performed blinded. Values are means of three independent experiments with standard deviations. Student's *t*-Test was performed to determine significant differences from the control. (**) *p*<0.01.

Fig. 36 shows that TiO₂ slightly reduced the nuclear division index (NDI) in comparison to control cells, which had a NDI of 1.75. It was 1.65 for 0.5 and 5 μg/cm² TiO₂ and 1.72 for 25 μg/cm² TiO₂. The frequency of micronuclei in all concentrations tested was slightly increased (control: 0.8%; 0.5 μg/cm²: 1.3%; 5 μg/cm²: 1.5%; 25 μg/cm²: 1.2%), but without reaching statistical significance. The number of apoptotic and mitotic cells were comparable to control levels. Thus, TiO₂ is not genotoxic in the micronucleus test.

3.14 Carbon black nanoparticles induce micronuclei at high concentrations

The micronucleus test was performed with CB nanoparticles. Carbon black finds application in printer toners or as additive for tires.

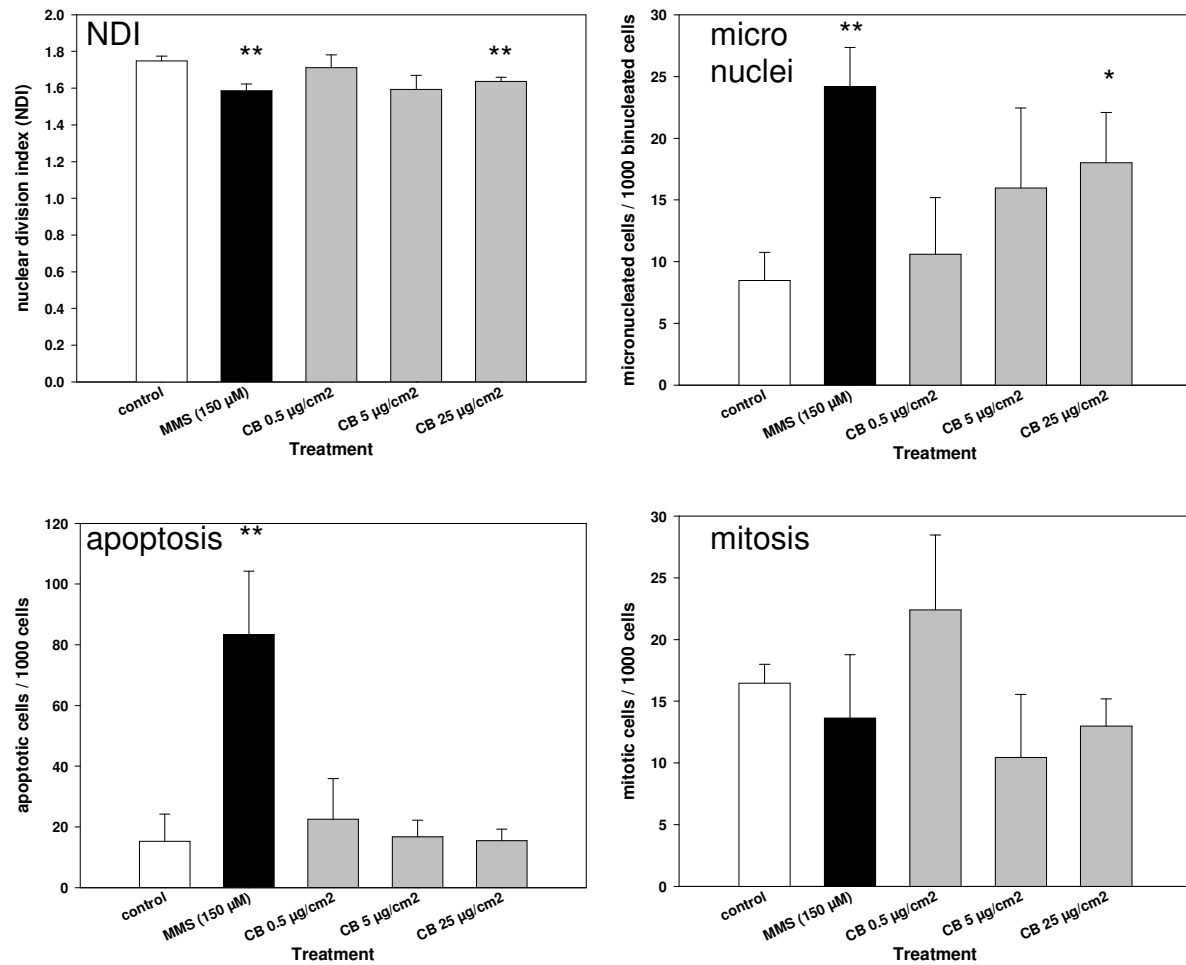


Fig. 37 Carbon black induces micronuclei.

A549 cells were exposed to carbon black (CB) (0.5, 5 and 25 µg/cm²) for 24 hours or left untreated. Methyl methanesulfonate (MMS, 150 µM) was used as a positive control. Simultaneous incubation with cytochalasin B (4 µg/ml for 24 hours) was used to induce binucleated cells. Cells were fixed with ethanol and stained with acridinorange. Scoring was performed blinded. Values are means of three independent experiments with standard deviations. Student's *t*-Test was performed to determine significant differences from the control. (*) $p < 0.05$; (**) $p < 0.01$.

Fig. 37 shows that the highest concentration of CB (25 µg/cm²) significantly reduced the NDI (control: 1.75, 25 µg/cm² CB: 1.64). Moreover, the number of micronucleated cells increased in a dose-dependent manner. At the highest concentration, the micronucleus frequency was more than 2-fold higher than in control cells (control: 0.8%; CB 25 µg/cm²: 1.8%); this was statistically significant. The number of apoptotic

and mitotic cells did not deviate significantly from control levels. Thus, carbon black apparently holds a genotoxic potential at high concentrations.

3.15 No induction of micronuclei by ZnO nanoparticles

Like TiO₂, ZnO nanoparticles are used in sunscreens. The micronucleus test was performed for these particles as well.

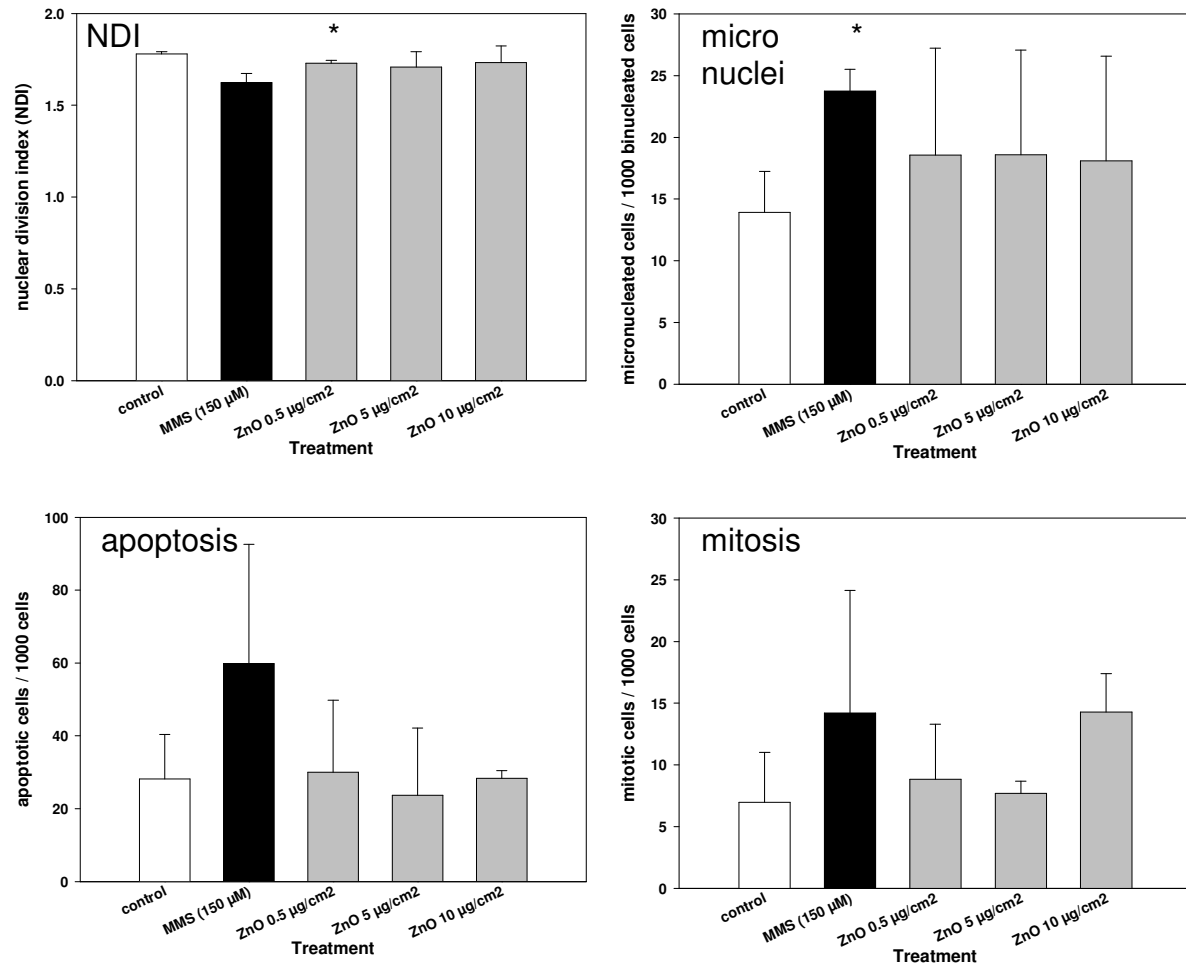


Fig. 38 Treatment with ZnO induces no changes in micronucleus test parameters.

A549 cells were exposed to ZnO (0.5, 5 and 10 µg/cm²) for 24 hours or left untreated. Methyl methanesulfonate (MMS, 150 µM) was used as a positive control. Simultaneous incubation with cytochalasin B (4 µg/ml for 24 hours) was used to induce binucleated cells. Cells were fixed with ethanol and stained with acridinorange. Scoring was performed blinded. Values are means of three independent experiments with standard deviations. Student's *t*-Test was performed to determine significant differences from the control. (*) $p < 0.05$; (**) $p < 0.01$.

Fig. 38 shows that the NDI was slightly decreased for treatment with 0.5 µg/cm² ZnO. The number of micronucleated cells was slightly increased in all concentrations tested, but this was never statistically significant due to high standard deviations. The

number of apoptotic and mitotic cells were comparable to control levels. Thus, ZnO apparently holds no clear genotoxic potential.

4 Discussion

Exposure of humans to novel nanomaterials is growing faster than the knowledge about possible adverse health effects. However, studies about the effects of airborne particulate matter suggest negative consequences for human health. An increase of $30 \mu\text{g}/\text{m}^3$ particulate matter of a size of $2.5 \mu\text{m}$ ($\text{PM}_{2.5}$) resulted in 0.9% higher general mortality of respiratory causes; death from specific respiratory diseases showed even an increase of 2.7% (Borm *et al.* 2004). But even besides death as the “worst case”, numerous adverse health effects have been observed. Inflammatory reactions are common. Moreover, alterations of blood coagulation and impairment of heart function have been reported (Peters *et al.* 1997a; Peters *et al.* 1997b; Gold *et al.* 2000; Peters *et al.* 2000; Donaldson *et al.* 2001; Ghio *et al.* 2001; Peters *et al.* 2001a; Peters *et al.* 2001b; Duggen 2004). Susceptible individuals, such as arteriosclerosis patients, asthmatics or persons suffering from chronic obstructive pulmonary disease (COPD) are particularly affected by exacerbation of their symptoms and mortality of respiratory and cardiovascular causes (Donaldson *et al.* 2001).

Furthermore, lung cancer incidence increased by 8% per $10 \mu\text{g}/\text{m}^3$ PM_{10} (Pope *et al.* 2002). The molecular mechanisms of tumorigenesis induced by particulate matter have been studied. It was concluded that the inhalation of particles induced inflammatory reactions associated with oxidative stress that lead to DNA damage and cancer formation (Borm *et al.* 2004). Comparison of the effects of particles (Al_2O_3 , CoCr, TiO_2 , Ga_2O_3) of a larger size (“fine” or micronized material) with nanomaterials of the same chemical composition suggests that the elevated DNA damage is size-related and stronger for nanosized material (Webb *et al.* 1986; Wolff *et al.* 1988; Gurr *et al.* 2005; Oberdorster *et al.* 2005; Papageorgiou *et al.* 2007; Balasubramanyam *et al.* 2009). Oberdörster showed that inhalation of aggregated ultrafine TiO_2 and carbon black induced lung tumors in rats at considerably lower gravimetric lung burdens than larger sized TiO_2 (Oberdorster *et al.* 1994; Oberdorster 1996). Here again, the reason is supposed to be the higher inflammogenic potential of ultrafine particles (Oberdorster *et al.* 1994; Oberdorster 1996; Monteiller *et al.* 2007).

However, other mechanisms could furthermore be responsible for an increased genotoxic potential of nanomaterials: The higher surface reactivity of nanomaterials

leads to the production of reactive oxygen species that can oxidatively damage the DNA (Nel *et al.* 2006). Moreover, nanoparticles might access cellular organelles and directly bind to proteins or the DNA, hence inhibiting and impairing their function (Borm *et al.* 2004; Donaldson *et al.* 2004; Kreyling *et al.* 2004). Leaching of toxic metal ions from nanomaterials (Borm *et al.* 2006; Pickrell *et al.* 2006; Franklin *et al.* 2007) or the introduction of volatile genotoxic compounds into the alveolar region as “blind passengers” adsorbed to the inhaled nanomaterial (Schins 2002; Balbus *et al.* 2007) might also expose lung cells to genotoxic attacks.

In the past years, genotoxicity testing of nanomaterials attracted more and more notice. Studies were mainly focusing on nanomaterials produced at large scale such as TiO₂ or carbon black. Results were often ambiguous. For example, TiO₂ was found to induce DNA damage in studies by Gurr *et al.* and Wang *et al.* (Gurr *et al.* 2005; Wang *et al.* 2007a). Dunford *et al.* and Nakagawa *et al.* reported genotoxicity only after illumination (“photogenotoxicity”) (Dunford *et al.* 1997; Nakagawa *et al.* 1997). Other authors observed no genotoxic effects at all (Theogaraj *et al.* 2007; Warheit *et al.* 2007). Genotoxicity data for more “exotic” nanomaterials are scarce. In general, the underlying mechanisms for toxicity and genotoxicity of nanomaterials are still poorly understood. However, tumorigenesis is a long-term process which occurs often decades after exposure to a carcinogen. Thus, knowledge about the genotoxic potential of the many novel nanomaterials is urgently required to prevent future threats to the health of producers and consumers of nanomaterials, as well as unwillingly and incidentally exposed individuals, including animals and plants.

This work aims at increasing the current knowledge about the genotoxic potential of nanomaterials. I compared the DNA damaging capacities of different nanomaterials (vanadium oxides, carbon black, TiO₂, ZnO) and of different sizes (bulk and nanomaterial of vanadium oxides) in the comet assay and the micronucleus test. As oxidative stress is supposed to be an important mediator of genotoxicity, ROS production and oxidative modification of DNA bases have been analyzed as well.

Moreover, to get insight into toxicological mechanisms, I determined the physico-chemical properties and examined the different vanadium oxides for acute toxicity and effects on cell proliferation.

Inhalation is the most important way of exposure to nanomaterials; hence, a human alveolar epithelial cell line (A549) was chosen as a model system. The advantage of an *in vitro* study in contrast to *in vivo* studies is – besides financial and ethical

reasons - the reduced complexity and enhanced reproducibility of a cell system, which is favorable when looking for basic working principles and mechanisms. In case of positive results, an *in vivo* follow-up is certainly required to correctly assess the risk for humans. But this was beyond the aim of this work, which was to examine the genotoxic potential of nanomaterials with standard genotoxicity tests and to derive mechanistic conclusions which could serve as a hypothesis for further *in vivo* experiments.

4.1 Solubility for different vanadium oxides differs: higher solubility for nanomaterials

When working with novel nanomaterials, characterization of their physico-chemical properties is required to be able to compare the results to other studies, and in particular, to be able to find possible correlations between physico-chemical characteristics and biological effects. Such correlations can be helpful to predict the toxicological behavior of unknown novel substances with similar properties.

Thus, the novel vanadium oxide nanomaterials used in this study were characterized with regard to metrics and specific surface (for results, see Tab. 1). The specific surfaces of nanomaterials were considerably (15 to 38-fold) higher than the specific surfaces of bulk materials. Another property which also changes due to reduction in size, but which until now is rarely considered in toxicological studies, is solubility (compare Report of the Nanokommission 2008). As a consequence of their increased specific surface and the elevated surface reactivity, nanomaterials are supposed to dissolve faster and to a higher extent than the corresponding bulk material (Borm *et al.* 2006). Moreover, the two bulk vanadium oxide species used in this work (vanadium trioxide and vanadium pentoxide) are known to have a different water solubility: Vanadium trioxide is poorly soluble, ca. 0.1 g/l in water (BGIA GESTIS database), whereas vanadium pentoxide displays a solubility of 1-8 g/l in water (IARC 2006). Hence, bulk vanadium pentoxide is approximately 10 to 80-fold more soluble than bulk vanadium trioxide. Thus, probing the solubility of the four different vanadium oxides (bulk and nano V_2O_3 and V_2O_5 respectively) seemed interesting and important, as different solubilities were expected. Fig 16 shows that the water solubility at 37 °C over time was indeed different for the four vanadium oxide species: As expected, the solubility of the pentoxide was approximately 10 times higher than

for vanadium trioxide, and the nanomaterials displayed an increased solubility in comparison with the bulk material.

Higher solubility for nano versus bulk materials has also been reported for MgO (Pickrell *et al.* 2006) and for ZnO (Franklin *et al.* 2007).

After 24 hours of incubation (which was the most frequently used time point in the biological experiments), 1% (bulk V₂O₃), 5% (nano V₂O₃), 6% (bulk V₂O₅) and 14% (nano V₂O₅) of the total vanadium oxide had dissolved. In the biological experiments, these percentages are most likely somewhat higher. This is because of two reasons. Firstly, for the solubility analysis, 1 mg vanadium oxide in 1 ml water has been used, i.e. a concentration of 1 mg/ml, which is approximately 1.000-fold higher than the concentrations used in biological experiments (concentrations were in the µg/ml range: 1 µg/cm² in a 6-well of a surface of 9.6 cm² with 2 ml medium corresponds to 5 µg/ml). A lower concentration of a substance facilitates dissolution: The concentration of the substance in the solvent is and remains low; thus, the diffusion gradient is very steep. Dissolved molecules hence diffuse very rapidly from the diffusion layer surrounding the dissolving substance into the solvent, and subsequently, new molecules have the possibility to dissolve (Borm *et al.* 2006). For higher concentrations, the driving force of the diffusion gradient decreases gradually when approaching the equilibrium concentration in the solvent; the dissolution process slows down.

Secondly, it has to be considered that vanadium oxides are up to 8 times better soluble in “artificial biological fluids”, e.g. in cell culture medium than in water (Toya *et al.* 2001). Hence, when using cell culture medium to dissolve vanadium oxides, the amount of soluble species might be even higher. However, the order of solubility (bulk V₂O₃ < nano V₂O₃ < bulk V₂O₅ < nano V₂O₅) and the relative amount of dissolved vanadium oxides should stay the same.

To account for the fact that vanadium oxides dissolve, a solution of vanadium oxide ions, referred to as “vanadate” in this work, has been included into the biological experiments to be able to assess the effect of soluble species separately and to compare it to the samples where vanadium oxides were present both undissolved and as ions.

The usage of the term “vanadate” may be misleading insofar as it suggests the presence of a single ionic species. However, solution chemistry of vanadium oxides

is complex. Depending on the pH and the concentration, numerous species of vanadium oxide ions occur: Tetravalent vanadyl (VO^{2+}) and pentavalent vanadate (HVO_4^- , VO_3^- and / or H_2VO_4^-) are the most common monomeric species. At higher concentrations (above 0.1 mM at pH 7), polymerization occurs up to hexamers. Acidic solutions harbor even decamers (Gordon 1991; Crans 1994; Djordjevic *et al.* 1995; Morinville *et al.* 1998; Evangelou 2002). The vanadate solution which I prepared from dissolution of bulk V_2O_5 had a concentration of 306 $\mu\text{g}/\text{ml}$ (corresponding to 2.6 mM H_2VO_4^-), was acidic and of yellow color. This suggests the presence of decameric vanadate. For biological experiments, the vanadate solution was diluted in cell culture medium. These dilutions did not exceed neutral pH. The return to neutral pH induces the depolymerization of vanadate decamers, even though, this is a rather slow process (Evangelou 2002). Thus, the effects observed after treatment with “vanadate” cannot easily be attributed to a specific vanadium oxide species. But I decided to use this slightly elusive mixture instead of e.g. a sodium orthovanadate solution, as the variation of species is probably also occurring in the dissolution process during incubation of cells with undissolved vanadium oxides. This seems to be appropriate, as Crans suggested likewise for enzyme inhibition studies that “measuring the effects must be carried out in an equilibrium mixture containing the other vanadate oligomers” (Crans 1994).

4.2 Uptake of vanadium into A549 cells is correlated to solubility

A substance which is unable to pass the cell membrane has only limited possibilities to disturb cellular integrity (e.g. via external production of reactive oxygen species or binding to membrane receptors). In contrast, if a substance gains access to the cytoplasm and / or the cellular organelles, it can affect cellular structures or inhibit enzymes and important metabolic processes. I was thus interested in knowing if vanadium oxides enter A549 cells. Incubation of cells with 10 $\mu\text{g}/\text{cm}^2$ vanadium oxides for 24 hours and subsequent analysis of the soluble fraction of a cell lysate by ICP-OES showed an uptake of 0.1 μg V/mg protein for bulk V_2O_3 ; ca. 0.25 μg V/mg protein for nano V_2O_3 and bulk V_2O_5 , 0.34 μg V/mg protein for nano V_2O_5 and 0.57 μg V/mg protein for vanadate. Thus, vanadium oxide species were obviously able to enter the cells. For vanadate, which is a structural analogue of phosphate, transmembrane transport has been shown via phosphate transport system II in fungal cells (Bowman 1983) and the anion transporter in erythrocytes (Cantley *et al.*

1978b; Heinz *et al.* 1982; Yang *et al.* 2003). For A549 cells, the possible uptake mechanism is unknown. But phosphate is essential to all cells and every cell type requires phosphate transporting systems which might also transport vanadate. Hence, uptake via anion transporters is plausible, a fortiori as diffusion through the membrane is hardly possible for charged vanadate ions (Yang *et al.* 2003).

Moreover, it is conceivable that the dissolved vanadium oxide species not only enter lung epithelial cells, but also other cell types in the lung, such as macrophages, and consequently gain access to further compartments of the body. Thus, inhalative exposure to soluble nanomaterials may result in distribution of toxic ions all over the body.

It was striking that the vanadium content was the lowest in cells treated with the poorly soluble bulk V_2O_3 , intermediate for substances with intermediate solubility and the highest for the vanadate solution. Plotting of the percentage of soluble vanadium oxides at 24 hours against the log of the percentage of vanadium uptake showed a strong correlation ($r^2 = 0.99$) of the two parameters. It is therefore well conceivable that dissolution precedes uptake – i.e. only dissolved vanadate is able to enter the cells. Nevertheless, another possible explanation could be that vanadium oxides are taken up and dissolved intracellularly. Undissolved vanadium oxide should in this case be found in the pellet of cell debris that forms after centrifugation of the lysate. Analysis of these pellets (data not shown) did not contain vanadium, thus, this mechanism appears rather unlikely.

Interestingly, correlation analysis revealed a linear behavior (linear scale) for vanadium uptake, and an exponential behavior for dissolution (log scale). This may point to the fact that the concentration in a solvent caused by dissolution is described by an exponential function: The concentration of solute molecule is proportional to e^{kt} (with t = time and k = rate constant of dissolution) (Borm *et al.* 2006). On the other hand, uptake via transporters is mostly limited by the number of transporters and thus only increases linearly. In contrast, Bracken *et al.* observed accumulation of vanadium within bovine kidney cells which was linearly proportional to the concentration in medium. However, they exposed cells to already dissolved orthovanadate, thus, no dissolution had to occur (Bracken *et al.* 1985a).

For many nanoparticles, uptake via vesicular mechanisms has been demonstrated (Rejman *et al.* 2004; Singh *et al.* 2007). A Trojan-horse type mechanism has been described for metal oxide nanoparticles. The particles could enter the cells and once

internalized, dissolve and produce ROS intracellularly. In contrast, aqueous solutions of the metal ions were innocuous as they did not gain access to the cells (Limbach *et al.* 2007). A reason why this mechanism does not apply to vanadium oxide nanomaterial might be the shape – both nano V_2O_3 and V_2O_5 are needle- and rod-shaped respectively with a very high length to width ratio. Chitrani *et al.* showed that the uptake of gold nanorods was much lower than for spherical gold particles (Chitrani *et al.* 2007). They speculated that the protein coating facilitating the endocytosis is less pronounced in nanorods. Similar effects might prevent the effective uptake of vanadium oxide nanomaterials into A549 cells.

4.3 Two-sided effect of vanadium oxides: Low concentrations stimulate proliferation, high concentrations induce cytotoxicity

Vanadium oxides enter cells in a solubility-dependent manner. What is the effect of intracellular vanadium oxides on cell viability? Several authors reported a two-sided effect on cell proliferation: Low concentrations stimulate cell proliferation (“insulin-like effect”), higher concentrations inhibit cell progression or are even cytotoxic (Hanuske *et al.* 1987; Cortizo *et al.* 1995; Cruz *et al.* 1995; Rehder *et al.* 2002).

I performed three different kinds of cell proliferation assays (cell count, AlamarBlue™ assay, BrdU incorporation). The results of these experiments were similar and in accordance with former studies: At very low concentrations ($1 \mu\text{g}/\text{cm}^2$ bulk V_2O_3), a pro-proliferative effect was observed which was comparable to that of $10 \mu\text{g}/\text{ml}$ insulin (2 to 3-fold increased proliferation in comparison to untreated control cells). The reported concentrations at which this “insulin-like effect” occurs differ: “0.01 mM and below” (Rehder *et al.* 2002), “below 10^{-10} M” (Hanuske *et al.* 1987). This is most likely due to the use of different cell types with different sensitivities (transformed mouse fibroblasts and non-transformed human fibroblasts in Rehder’s study; human tumor specimens in Hanuske *et al.*) and different vanadium compounds (ammonium metavanadate, vanadyl sulfate trihydrate and ortho sodium vanadate in Hanuske’s study, vanadate, $[\text{VO}(\text{acetylacetonate})_2]$, $[\text{VO}_{(2)}(\text{dipicolinate})]^{(-)}$ and $[\text{VO}(\text{maltolate})_2]$ in Rehder’s work). A fact that further complicates direct comparison of the concentrations reported in these studies with the values in my experiments is the use of dissolved vanadium species versus undissolved vanadium oxides which were undergoing dissolution. Moreover, I applied a dose metric based on the surface of the reaction container ($\mu\text{g}/\text{cm}^2$) and not on the

volume ($\mu\text{g/ml}$ or M which is mol/l , respectively). The surface-based dose metric is supposed to be more appropriate for particulate substances as they tend to sediment onto the cells. In my case, I must admit that both metrics may be questionable, as both particulate vanadium oxides and dissolved ionic species are present to different extents at different time points. Hence, to be able to convert $\mu\text{g/cm}^2$ concentrations into correct molar values for dissolving substances, knowledge of the exact content and the type of soluble species at a certain time point would be required. This would be a rather complex task. A way to handle dosimetry of partly soluble (nano)materials is thus still lacking.

However, the results of the experiments shown here were in accordance with the finding that low concentrations of vanadium oxides stimulate cell proliferation.

The results of the proliferation assays already revealed the other side of vanadium effects: Cytotoxicity at high concentrations, observed as a decrease in cell proliferation. To further assay this observation, three different types of viability assays have been performed. The need to use several viability assays has been found in former studies in our group, because many nanomaterials, e.g. carbon nanotubes, are able to interfere with these tests by e.g. binding the dye (Worle-Knirsch *et al.* 2006). Hence, to exclude false positives or negatives, the results of viability tests should always be confirmed with viability tests using different end points or working principles.

However, for the vanadium oxides, the results of the three different viability assays were in agreement with each other. Thus, there was no apparent interference of vanadium oxides with standard viability tests.

The MTT and the XTT assay revealed significant dose-dependent cytotoxicity after 24 hours of incubation, whereas the LDH assay showed a - much weaker - cytotoxicity response only after 48 hours. This may reflect the different end points: metabolic activity for the MTT and XTT assays, and membrane damage in the LDH assay. Apparently, the vanadium oxide species that gained access to the cell impair metabolic activity first, by binding to enzymes and non-enzymatic proteins, inhibiting their activity and in consequence altering the cellular metabolism (Nechay *et al.* 1986; Tasiopoulos *et al.* 2000; Evangelou 2002). It seems to take some more time until this metabolic disturbance leads to membrane leakage or until lipid peroxidation damages the membrane sufficiently to provoke LDH release. Thus, the LDH assay was less sensitive for probing vanadium oxide toxicity.

Anyway, all viability assays suggested a correlation of cytotoxicity to solubility: Viability was the highest for low-soluble vanadium oxide species and the lowest for highly soluble vanadium oxides. Taken into consideration the solubility-dependent uptake of vanadium into the cells, this is in accordance with the fact that “cytotoxicity of vanadium compounds was associated with their capacity of cellular accumulation”, as Yang *et al.* already reported (Yang *et al.* 2004).

Bhattacharya *et al.* studied the cytotoxicity of TiO₂ particles coated with V₂O₅. They found a higher decrease in viability for the coated particles (20 to 40% viability at a concentration of 25 µg/cm²) than for the uncoated particles (70% viability) at the same concentration (Bhattacharya *et al.* 2008). Moreover, they compared the effects of pure V₂O₅ at concentrations equal to the amount of V₂O₅ contained in the coating (60 – 300 ng). They did not find cytotoxicity at these concentrations, which might have been too low to induce a decrease in cell viability. Thus, for this kind of particle, a Trojan-horse effect might be causing the cytotoxicity of the coated particles, i.e. uptake into the cells and subsequent intracellular dissolution, which is the opposite of the mechanism of toxicity observed with the vanadium oxides in this work.

Moreover, for all substances, a dose-dependent increase in cytotoxicity was observed. The concentration of a substance exerting 50% decrease in viability is an important value to compare the toxicity of different substances. For vanadium compounds, 50% toxicity values ranging from 100 µM (Bracken *et al.* 1985b) to 1.27 ± 0.28 mM (Yang *et al.* 2004) and “the 1 mM concentration level” (Rehder *et al.* 2002) have been reported. For the reasons explained above, it is difficult to directly compare these values to the values resulting from my experiments. However, as I used a set of different vanadium oxides, I was able to compare the values for the different vanadium oxides within the same experimental setup. The concentrations at which 50% viability (LC₅₀) was retained, was > 62.5 µg/cm² for bulk V₂O₃, nano V₂O₃ and bulk V₂O₅, 31.25 µg/cm² for nano V₂O₅ and 20 µg/cm² for vanadate. Thus, cytotoxicity was the lowest for bulk V₂O₃, nano V₂O₃ and bulk V₂O₅, higher for nano V₂O₅ and highest for vanadate. This again reflects the solubility-dependence of cytotoxicity and the fact that nanomaterials are more cytotoxic than bulk material due to their increased solubility.

Many authors reported increased cytotoxicity of nanomaterial versus bulk material, e.g. for cobalt-chromium alloy particles (Papageorgiou *et al.* 2007), coated TiO₂ particles (Sayes *et al.* 2008) Ga₂O₃ (Webb *et al.* 1986; Wolff *et al.* 1988) ZnO (Reddy

et al. 2007) and NiO (Veranth *et al.* 2007). However, with the exception of ZnO, the increased cytotoxicity is most likely not due to elevated solubility. For other nanomaterials (Al₂O₃, CeO₂, Fe₂O₃, SiO₂ and TiO₂), no higher cytotoxicity for nano versus bulk material was reported (Veranth *et al.* 2007).

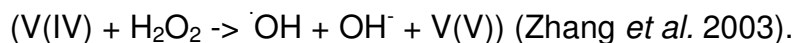
Concerning the importance of solubility and thus the release of ions as a mediator of cytotoxicity, increased cytotoxicity was also observed for quantum dots releasing toxic Cd²⁺ ions in contrast to “stable” quantum dots (Derfus *et al.* 2004). Contrarily, ZnO nanoparticles which were better soluble than ZnO bulk material, showed no increased cytotoxicity in the study published by Franklin *et al.* (Franklin *et al.* 2007). Anyway, one has to consider that the test conditions and the particle characteristics were very different in all of these studies. Cytotoxicity data found in exposure of bacteria, plants or human cells are most likely hardly comparable. Moreover, the physico-chemical properties are supposed to play an important role. For example, TiO₂ comes in different crystal structures, anatase and rutile, and both may have different cytotoxicities. Veranth *et al.* (Veranth *et al.* 2007) used anatase TiO₂ nanoparticles and compared their cytotoxicity to micron-sized rutile TiO₂— they did not find a difference, but this might have been different if they had used the same crystal structure for both sizes (Zhao *et al.* 2005). This underlines the need to choose the right material and to thoroughly characterize materials in order to be able to compare the results of different studies.

4.4 ROS generation by soluble vanadium oxides

Reactive oxygen species are generated endogenously by various cellular processes (e.g. electron transport in the mitochondria). Cells have diverse mechanisms to cope with these reactive species. However, if additional ROS are produced due to toxic substances or irradiation, cells may be unable to eliminate the reactive species effectively. The consequence is oxidative stress which is characterized by oxidative modification of cellular structures such as membrane lipid peroxidation, oxidation of DNA bases, proteins and enzymes. The affected cell may be strongly impaired, and finally be condemned to cell death.

The production of ROS is supposed to be the main mechanism of vanadium oxide toxicity (Evangelou 2002). Vanadium(V) enters the cell and is reduced intracellularly to V(IV) whereby superoxide radical (O₂^{•-}) and hydrogen peroxide (H₂O₂) are

generated. Fenton-like reactions using V(IV) as a catalyst can further lead to the production of hydroxyl radical:



Regenerated V(V) can enter another redox-cycle generating even more ROS (Zychlinski *et al.* 1991).

It has been reported that vanadium oxides produce ROS, both in cell-free systems (Shi *et al.* 1990) and in combination with cells (Shi *et al.* 1991). The results shown in this work are in accordance with these observations: I found a concentration-dependent increase in ROS production for vanadium oxides both in medium only and intracellularly in incubations of A549 cells. The well-soluble vanadium oxides (nano V_2O_3 , bulk V_2O_5 , nano V_2O_5 and vanadate) increased the amount of ROS significantly in both systems. Bulk V_2O_3 did not produce ROS in medium only; this suggests that solubilization is required for ROS production. However, a weak ROS generation was observed in incubations with cells. Cells excrete acidic “waste” which may help to dissolve bulk V_2O_3 and thus, ROS production could be observed in incubations with cells, but not without.

A study which compared the oxidative stress induced by four different nanomaterials (carbon black, single wall carbon nanotubes, SiO_2 and ZnO) found the highest ROS production for ZnO (Yang *et al.* 2009) – which is supposed to be the one of the four with the highest tendency to dissolve, thus, another hint that solubility may be a prerequisite for ROS generation for certain types of nanomaterials.

The DHR assay which I used for detection of ROS is supposed to react preferentially with superoxide anion and hydrogen peroxide (Emmendorffer *et al.* 1990; Henderson *et al.* 1993; Royall *et al.* 1993). Superoxide anions and hydrogen peroxide are together with hydroxyl radicals the main ROS species generated by vanadium oxides in microsomes, via NADH-dependent flavoenzymes or Fenton-like mechanisms (Shi *et al.* 1991; Shi *et al.* 1992; Zhang *et al.* 2003). Thus, concerning the ROS species, the ROS generation I detected is in accordance with earlier reports.

ROS generation was found to be the highest for nano V_2O_3 , followed by nano V_2O_5 , bulk V_2O_5 and finally by bulk V_2O_3 . Higher ROS generation of nanosized, in comparison to micron-sized material might reflect the increased surface reactivity of nanomaterials (Nel *et al.* 2006). Similar observations have been reported e.g. for

ultrafine TiO₂ in contrast to fine TiO₂ (Singh *et al.* 2007) and for particulate matter of different sizes (Li *et al.* 2003). Moreover, TiO₂ particles coated with V₂O₅ produced more ROS (approximately twice as much) than pure TiO₂ particles (Bhattacharya *et al.* 2008) which highlights the fact that the chemical composition is also very important. That nano V₂O₃ yielded the highest ROS generation may be due to the fact that it has to be oxidized to become soluble (Worle-Knirsch *et al.* 2007). These further oxidation steps might lead to more reactive oxygen species than for the pentoxide.

Worle-Knirsch *et al.* reported lipid peroxidation in murine macrophage-like cells (RAW-264) after treatment with vanadium oxides. Lipid peroxidation was the strongest after treatment with nano V₂O₃, followed by bulk V₂O₅ and at last bulk V₂O₃. Thus, the order of ROS generation I found is in agreement with the order of the extent of oxidative stress effects observed in this study (Worle-Knirsch *et al.* 2007). Contrary to my results, they found approximately equal amounts of ROS production for bulk V₂O₃, nano V₂O₃ and bulk V₂O₅ up to concentrations of 50 µg/ml. At higher concentrations, bulk V₂O₅ was the substance generating the most ROS, followed by bulk V₂O₃ and nano V₂O₃ (Worle-Knirsch *et al.* 2007). However, they used a different cell line (the endothel cell line ECV304), which revealed a different reaction than A549 cells to oxidative stress: Induction of hemoxygenase (HO-1), an antioxidative enzyme, was found in ECV cells exposed to nano V₂O₃, whereas the same treatment lead to a decrease of HO-1 in A549 cells. This apparently reflects cell-type specific differences in oxidative stress management, or differences in generation of and susceptibility to ROS.

Interestingly, the combination of vanadate and H₂O₂ yields different peroxovanadium species, dependent upon the respective concentrations and the pH. Mono and diperoxo products occur preferentially at low concentrations, whereas higher concentrations result in triperoxo- and tetraperoxovanadates (Shaver *et al.* 1995). Their effects have been reported to be different from vanadate. For example, peroxovanadium compounds are very potent in increasing protein tyrosine phosphorylation at the insulin receptor (Crans 2005). Moreover, they are 100-1.000 times more effective protein tyrosine phosphatases inhibitors than vanadate (Bevan *et al.* 1995), because peroxovanadates induce irreversible inhibition, in contrast to

vanadate, which is a competitive phosphatase inhibitor (Huyer *et al.* 1997). As I observed vanadate uptake and ROS production, these peroxovanadates may also occur in my experiments and be responsible for some of the observed effects.

4.5 Genotoxicity of nano V_2O_3 and bulk V_2O_5 : DNA oxidation, strand breaks and cell cycle arrest

For (bulk) V_2O_5 and vanadate the induction of guanine hydroxylation, DNA strand breaks and cell cycle arrest have been described in numerous studies (Owusu-Yaw *et al.* 1990; Migliore *et al.* 1993; Zhong *et al.* 1994; Altamirano-Lozano *et al.* 1996; Rojas *et al.* 1996; Shi *et al.* 1996; Lloyd *et al.* 1998; Altamirano-Lozano *et al.* 1999; Ivancsits *et al.* 2002; Rodriguez-Mercado *et al.* 2003; Zhang *et al.* 2003). Accordingly, I found an increase in the content of 8-oxo-guanine, DNA strand breaks and an arrest in G2/M phase after treatment with bulk V_2O_5 , confirming the reported genotoxic potential of this substance. Moreover, I observed the same effects for the novel nano V_2O_3 . Thus, out of the four vanadium oxide species in this study, two (nano V_2O_3 and bulk V_2O_5) showed a clear genotoxic potential including oxidation of bases, strand breaks and cell cycle arrest. The vanadate solution induced 8-oxo-guanine and cell cycle arrest as well, but no DNA strand breaks, which suggests a moderate genotoxic potential. The two remaining vanadium oxides, bulk V_2O_3 and nano V_2O_5 , apparently did not affect the DNA. A summary of these results is found in Tab. 6.

Tab. 6 Genotoxicity of vanadium oxides.

The outcome of the analysis of the 8-oxo-guanine content (8-oxo-G), the comet assay (strand breaks), the micronucleus test (micronuclei) and cell cycle analysis (G2/M arrest) have been summarized for bulk vanadium trioxide (bV_2O_3), nano vanadium trioxide (nV_2O_3), bulk vanadium pentoxide (bV_2O_5), nano vanadium pentoxide (nV_2O_5) and a solution of vanadium oxides (vanadate). (-): no induction; (+): 2-fold increase relative to the control; (++) : 5-fold increase relative to the control; (+++) : 10-fold increase relative to the control. (For 8-oxo-G, no values relative to the control are shown; (++) means a D/s(n) value above 30) (n): no genotoxicity; (y): weak genotoxicity (yy): strong genotoxicity. The shading represents the strength of the effects; the darker the color, the stronger the effect.

material	8-oxo-G	strand breaks	micro-nuclei	G2/M arrest	genotoxic
bV_2O_3	-	-	-	-	n
nV_2O_3	++	+++	-	+	yy
bV_2O_5	++	++	-	+	yy
nV_2O_5	-	-	-	-	n
vanadate	++	-	-	+	y

Interestingly, for genotoxicity, no direct correlation to the solubility of the substance seems to exist. The most genotoxic are the substances of intermediate solubility. That the poorly soluble bulk V_2O_3 , which is found at low concentrations inside the cell and which generated hardly any ROS, does not induce DNA damage was not surprising. In contrast, the absence of DNA damage after treatment with nano V_2O_5 was unexpected. Nano V_2O_5 is taken up readily into the cells due to its high solubility and generates considerable ROS. But this does not lead to guanine oxidation, DNA strand breaks or cell cycle arrest. As to the reason for this observation, it is hard to say. A possible explanation might be the generation of different mixtures of different ionic vanadium oxide species during dissolution of different vanadium oxides. Different oligomers of vanadate have been found to have different toxicity (Wei *et al.* 1982). Moreover, vanadium oxides are taken up into the cells to a different amount and generate different amounts of ROS intracellularly. The combination of vanadate and ROS yields peroxovanadium compounds depending on the concentration (Shaver *et al.* 1995). The intracellular concentration of vanadium after treatment with nano V_2O_5 might be appropriate to induce formation of peroxovanadium compounds. The effects of peroxovanadium compounds are different to those of vanadate. For example, they inhibit protein tyrosine phosphatases 100 to 1.000 times more effectively than vanadate (Bevan *et al.* 1995) by irreversibly binding to the enzyme. Thus, it might be conceivable that, in case such peroxovanadium species are produced, vanadate and ROS combined in a peroxovanadium compound are sequestered to the enzymes and are not able to come close to the DNA, oxidize bases and consequently induce DNA damage.

A summary of the hypothetical mechanisms leading to DNA damage (or not) after treatment with vanadium oxides is shown in Fig. 39.

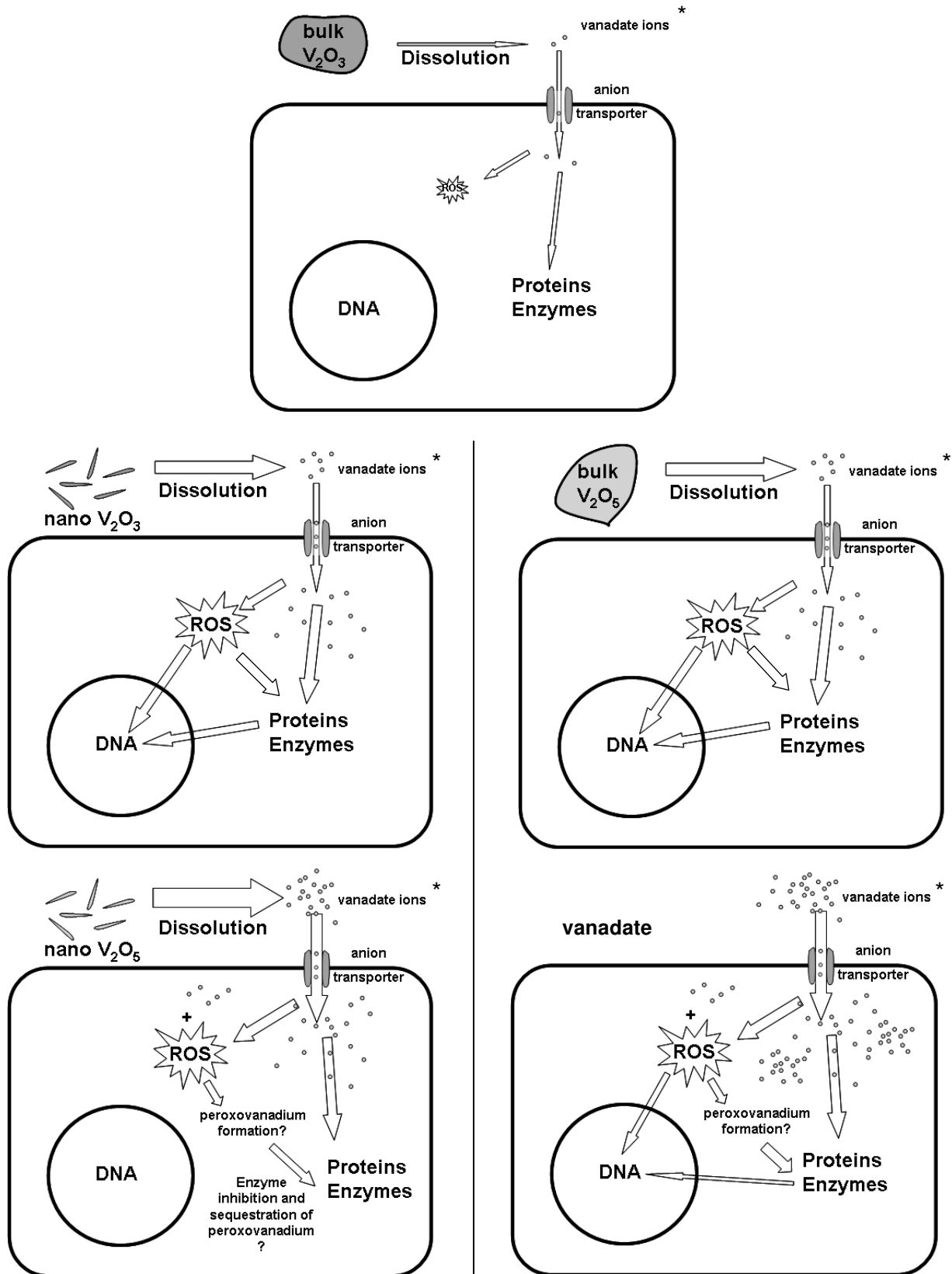


Fig. 39 Summary of the toxic effects and (hypothetical) mechanisms of different vanadium oxide species.

Vanadium oxides undergo dissolution to different extents. The resulting vanadate ions may enter the cell via anion transporters. Bulk V_2O_3 is poorly soluble and the low amounts that are found in the cell exert no toxicity. The more soluble vanadium oxide species yield higher intracellular vanadate amounts and generate ROS. ROS can impact on proteins and enzymes by oxidizing amino acid

residues. Moreover, ROS seem to directly affect and damage the DNA in the case of nano V_2O_3 and bulk V_2O_5 and to a lower degree in the case of vanadate. For nano V_2O_5 , additional mechanisms seem to be involved, maybe the formation of peroxovanadium compounds that irreversibly bind to proteins and enzymes, but do not damage the DNA. Vanadate toxicity may involve both direct oxidative DNA modifications and additional mechanisms; such as the formation of oxidized guanine, but no DNA strand breaks have been observed.

* vanadate ions may include different vanadate mono- and oligomers, depending on the dissolving vanadium oxide species and the concentration of dissolved vanadium oxides.

On the other hand, the vanadate solution was able to induce oxidative DNA damage. This might be due to the fact that the intracellular concentration is even higher than for nano V_2O_5 ; thus there might be some vanadate “left over” after formation of peroxovanadium compounds which can induce DNA oxidation and cell cycle arrest, but not as much as bulk V_2O_5 and nano V_2O_3 which might not generate peroxovanadium compounds.

In summary, when comparing the genotoxic potential of bulk and corresponding nanomaterial, I found a considerably elevated genotoxic potential in the V_2O_3 nanomaterial, but not in the bulk material. Several studies reported similar findings for other nanomaterials: Gurr examined anatase TiO_2 at to different sizes (10 nm, 20 nm, 200 nm, > 200 nm) and found oxidative DNA damage for the 10 and 20 nm particles, but not for the larger ones (Gurr *et al.* 2005). Mroz observed DNA strand breaks for nano, but not for micron carbon black in A549 cells (Mroz *et al.* 2007). Papageorgiu tested CoCr and reported a higher strand breaking capacity for nano versus micron-sized particles in human fibroblasts (Papageorgiou *et al.* 2007). Balasubramanyam showed an increase in DNA strand breaks and a dose-dependent micronuclei induction for nano Al_2O_3 , but not for bulk Al_2O_3 in mice (Balasubramanyam *et al.* 2009).

Surprisingly, I found no DNA-damaging capacity for the known genotoxic substance V_2O_5 as a nanomaterial. To the best of my knowledge, similar results have not yet been reported before. In contrast, Bhattacharya *et al.* reported the genotoxicity of TiO_2 nanoparticles coated with V_2O_5 (Bhattacharya *et al.* 2008). But in this study, the nanomaterial was spherical and the vanadium pentoxide might have acquired characteristics in the coating process that differ considerably from the rod-shape nanomaterial prepared by polyol-mediated synthesis used in this work.

The importance of oxidative DNA damage for carcinogenesis is well known. Elevated levels of 8-oxo-G have been found in numerous tumors (Mates *et al.* 2008).

Mutagenesis as a consequence of 8-oxo-G formation has been described for the carcinogenic asbestos fibers (Xu *et al.* 1999; Unfried *et al.* 2002). Moreover, Ichinose *et al.* reported a dose-dependent increase in 8-oxo-G in DNA of mice treated for 10 weeks with diesel exhaust particles. The tumor incidence in the animals was significantly correlated to the 8-oxo-G content (Ichinose *et al.* 1997). Thus, as I found an elevated amount of 8-oxo-G for bulk V_2O_5 and the novel nano V_2O_3 , a similar mechanism of carcinogenesis including oxidative DNA damage may be conceivable for these substances as well. However, nano V_2O_3 and bulk V_2O_5 also induced a cell cycle arrest at G2/M phase. It is possible that this arrest enables the cells to repair the acquired DNA damage which could prevent development of tumor cells. Thus, to correctly assess the *in vivo* carcinogenic potential, long-term *in vivo* animal studies would be required.

4.6 No increase in micronucleated cells – but morphological changes in cell nuclei

The induction of micronuclei has been reported for various nanomaterials including SiO_2 (Wang *et al.* 2007b), TiO_2 (Wang *et al.* 2007a), anatase TiO_2 (Gurr *et al.* 2005), multi-walled carbon nanotubes (Muller *et al.* 2008), CoCr (Papageorgiou *et al.* 2007) and Al_2O_3 (Balasubramanyam *et al.* 2009). For vanadium oxides, an increase in micronucleus frequency in murine bone marrow cells, human lymphocytes, polychromatic erythrocytes and V79 cells has been shown (Migliore *et al.* 1993; Zhong *et al.* 1994; Ciranni *et al.* 1995; Migliore *et al.* 1995; Leopardi *et al.* 2005; Villani *et al.* 2007; Bhattacharya *et al.* 2008; Ehrlich *et al.* 2008). Most authors reported the occurrence of kinetochore-positive micronuclei. Thus, an aneugenic effect (e.g. disturbance of the mitotic spindle) was suggested for vanadium oxides (Migliore *et al.* 1993; Zhong *et al.* 1994; Ciranni *et al.* 1995; Migliore *et al.* 1995; Ehrlich *et al.* 2008). It was therefore interesting to test the novel vanadium oxide nanomaterials in the micronucleus test. I could not detect a statistically significant increase in the number of micronucleated cells. Only $2 \mu\text{g}/\text{cm}^2$ bulk V_2O_5 led to an elevated micronucleus frequency, but the difference to the control cells was not statistically significant. What is the reason that I did not observe micronucleus formation after treatment with vanadium oxides, in particular with bulk V_2O_5 and vanadate, which induced micronuclei in many other studies? Firstly, due to the occurrence of cells with strange nuclear morphology, which I excluded from

micronucleus scoring, I might have missed some micronucleated cells (see also below). Moreover, the vanadium oxide species contained in the vanadate solution prepared from bulk V_2O_5 might be different from the vanadate solutions other authors used. The mainly applied sodium orthovanadate, ammonium metavanadate or vanadyl sulphate (V_2O_5 was only used by Zhong *et al.* and Bhattacharya *et al.*; in the latter as V_2O_5 coated TiO_2 nanoparticles). Moreover, the target cells and exposure conditions varied considerably: Ciranni *et al.*, Leopardi *et al.* and Villani *et al.* used the bone marrow or reticulocytes of orally exposed mice, Migliore *et al.* human lymphocyte cultures, Zhong *et al.* and Bhattacharya *et al.* V79 (Chinese hamster fibroblast) cells. Maybe A549 cells are less sensitive to vanadium oxides than the primary blood / bone marrow cells that were used in many of the studies with positive outcome.

However, there was a significant decrease in the nuclear division index, a result which was also observed in the study of Zhong *et al.* (Zhong *et al.* 1994), pointing to a cytostatic property of bulk V_2O_5 .

However, the appearance of the mitotic cells in samples treated with vanadium oxides often looked bizarre (see Fig. 33): Chromosomes were kind of clustered irregularly; no formation of a metaphase plate at the equator of the cell was apparent, and sometimes several chromosomes seemed scattered and not included into the apparatus that was holding together most of the chromosomes. This may be a hint to an impaired function of the mitotic spindle, pointing to the aneugenic potential of vanadium oxides described by the authors cited above. A reason for disturbed spindles may be the interaction of vanadate oligomers with microtubule-associated proteins (MAP) which are regulated by phosphorylation. Whereas monomeric vanadate does not interact with microtubule formation, the binding of decavanadate to MAPs inhibits the assembly of microtubule proteins (Lobert *et al.* 1994).

Moreover, during scoring I repeatedly noticed cells displaying a strange nuclear morphology (see Fig. 31). Nuclei were segmented; the segments were often distributed like the petals of a flower and connected by structures resembling nucleoplasmatic bridges. I started scoring these cells as an additional parameter to see if there was a correlation to a specific treatment. Indeed, the frequency of these “cells with segmented nuclei” was significantly increased in cells treated with nano V_2O_3 , bulk V_2O_5 , nano V_2O_5 and vanadate, thus, the water-soluble vanadium oxide

species. The numbers of cells with altered nuclear morphology were 2- to 6-fold higher in these samples; at the most, 10% of nuclei looked like that. Considering this high amount of “strange” cells and the fact that I excluded these cells from micronucleus scoring (even though they sometimes contained small fragments which could have been micronuclei), it is possible that I have missed a fraction of micronucleated cells, and therefore not found an increase in micronucleus frequency. But what caused this strange morphology? Considering the irregular appearance of mitotic cells and the fact that vanadate is a potent phosphatase inhibitor, I looked for protein kinases and phosphatases involved in mitosis whose activation or inhibition could be responsible for the observed altered nuclear morphology. Literature studies suggested polo-like kinase 1 (Plk1) and Cdc14 phosphatase as possible candidates. During mitosis, the activity of Plk1 is enhanced by phosphorylation (Mundt *et al.* 1997). An overexpression of Plk1 was found to lead to a “significant increase in large cells with multiple, often fragmented nuclei” (Mundt *et al.* 1997). Vanadium oxide mediated inhibition of the phosphatase which dephosphorylates Plk1 would result in persistent activation of Plk1 and could have the same effect as the one described for overexpression, namely the fragmented appearance of nuclei.

Nalepa *et al.* reported the Cdc14B phosphatase to be, together with Plk1, “critical for the maintenance of proper nuclear structure” (Nalepa *et al.* 2004). They discovered an “intranuclear filamentous framework” that is impaired if Cdc14B lacks or is catalytically inactive. Knock-down of Cdc14B by shRNA resulted in “defects in mitotic progression, including multipolar spindles, inhibition of cytokinesis to produce cells with multiple nuclei, and incomplete chromosome segregation”. Moreover, if cells ectopically expressing Plk1 were transfected with catalytically inactive Cdc14B mutants or Cdc14B siRNA, Nalepa *et al.* observed “strikingly grotesque morphology: Multinucleated cells with numerous macro- and micronuclei as well as cells with deformed nuclei” (Nalepa *et al.* 2004).

Thus, the inhibition of Cdc14B phosphatase by vanadium oxides might induce an increased activity of Plk1 which results in the altered nuclear morphology with segmented nuclei that I observed in the micronucleus test.

A hint that these changes in nuclear morphology might not only occur *in vitro* is a Mexican study by Sanchez *et al.* cited in the IARC report. In mice exposed to inhalation of 0.01 to 0.02 M vanadium pentoxide, they observed “distorted nuclear morphology in non-ciliated bronchiolar Clara cells” (IARC 2006).

The cellular consequence of such fragmented, segmented nuclei is totally unclear. Nevertheless, it is hard to imagine that such a cell is able to undergo further regular cell divisions.

4.7 Genotoxic potential of TiO₂, CB and ZnO

TiO₂, CB and ZnO are among the commercially most important nanoparticles. They are produced at large scale and used in products such as sunscreens (TiO₂ and ZnO), paint (TiO₂) or printer toners (CB). Thus, exposure of consumers to these nanomaterials is highly probable. It is therefore important to know if these materials hold a genotoxic potential.

Examination of these nanoparticles in the comet assay revealed no DNA strand breaking capacity for any of the three materials.

Similar results were reported in several studies for TiO₂ (Dunford *et al.* 1997; Nakagawa *et al.* 1997; Vevers *et al.* 2008): None of the studies found an increase of DNA damage in the comet assay if no additional irradiation with UV light occurred.

For CB, Karlsson *et al.* detected no increase in tail intensity in A549 cells at concentrations up to 40 µg/cm² (Karlsson *et al.* 2008). Zhong *et al.* did not detect DNA strand breaks after treatment of V79 or He1 299 cells with CB (Zhong *et al.* 1997).

Karlsson *et al.* (Karlsson *et al.* 2008) showed that DNA damage induced by ZnO occurred only after incubation with 40 µg/cm², but not with 20 µg/cm². The highest concentration I used was 10 µg/cm², thus the absence of DNA strand breaks I saw is in accordance with Karlsson's results. However, incubation with nanoparticles was much shorter in these studies than in my work. It was 3 hours in Zhong *et al.* and 4 hours in Karlsson *et al.* (in contrast to 24 and 48 hours in my work).

In contrast, several studies found DNA damage in the comet assay for these nanomaterials. TiO₂: Gurr *et al.* 2005; Wang *et al.* 2007a; Karlsson *et al.* 2008. CB: Don Porto Carero *et al.* 2001; Jacobsen *et al.* 2007; Mroz *et al.* 2008; Yang *et al.* 2009. ZnO: Sharma *et al.* 2009; Yang *et al.* 2009. However, in some of the studies, DNA damage was observed in cell types other than A549, which might be more susceptible to DNA damage (Wang *et al.* used B-cell lymphoblastoid cells; Gurr *et al.* BEAS-2B, Jacobsen *et al.* mouse epithelial cells, Sharma *et al.* A431 cells, a human epidermal cell line).

Moreover, even if Mroz *et al.* also used A549 cells, they detected DNA damage at concentrations that were higher than the ones I used. The highest concentration of CB in my work was $25 \mu\text{g}/\text{cm}^2$ (corresponding to $83 \mu\text{g}/\text{ml}$). Mroz *et al.* applied $100 \mu\text{g}/\text{ml}$. Very high concentrations were also used in the study by Sharma *et al.* They observed increased DNA damage after 6 hours of incubation with $0.8 \text{ g}/\text{ml}$ ZnO (Sharma *et al.* 2009).

The application of such high concentrations may not be suitable, as the particle “overload” can cause unspecific cytotoxicity. The use of cytotoxic concentrations is not recommended for genotoxicity testing as e.g. the induction of apoptosis can lead to false positive results. DNA fragmentation is a characteristic of apoptosis and produces comets as well. Thus, comparability of different studies is somewhat difficult because of the use of different cell lines, dose metrics, experimental set-up etc. Hence, standardization of genotoxicity testing for nanomaterials is required to yield conclusive and reliable results for risk assessment.

In the micronucleus test I performed, TiO_2 and ZnO increased the micronucleus frequency slightly, but not to a statistically significant extent. In contrast, the highest concentration of CB ($25 \mu\text{g}/\text{cm}^2$) yielded a statistically significant, 2-fold increase in micronucleated cells.

No induction of micronuclei after treatment with TiO_2 was reported as well by a study in rat liver epithelial cells at concentrations of 5, 10 and $20 \text{ pg}/\text{cm}^2$ (Linnainmaa *et al.*, 1997, cited in (Landsiedel *et al.* 2009)) and in a fish cell line (RTG-2 cells) at concentrations up to $50 \mu\text{g}/\text{ml}$ (Vevers *et al.* 2008). Contrarily, a 2.5-fold increase in micronucleus frequency has been found in human B-cell lymphoblastoid WIL2-NS cells at $130 \mu\text{g}/\text{ml}$ after 6 hours (Wang *et al.* 2007a) and in BEAS-2B cells after incubation with $10 \mu\text{g}/\text{ml}$ for 24 hours (Gurr *et al.* 2005). Here again, experimental conditions in the different studies vary considerably, which complicates the comparison and the conclusion as to what results are the most relevant, and if there is a threat to DNA integrity following exposure to TiO_2 .

Poma *et al.* reported a 1.5 to 3.5-fold increase in micronucleus frequencies after treatment with carbon black in the murine macrophage cell line RAW 264. The induction of micronuclei frequency was dose-dependent and statistically significant for all concentrations ($1 \mu\text{g}/\text{cm}^2$, $3 \mu\text{g}/\text{cm}^2$ and $10 \mu\text{g}/\text{cm}^2$) (Poma *et al.* 2006). In

contrast to my experiments which applied 24 hours of incubation, they treated cells for 48 hours. This longer incubation might be – besides a possibly increased sensitivity of mouse macrophages – a reason for the statistically significant increases in micronucleus formation already at lower doses.

Moreover, studies with particulate matter which consists mainly of carbon, found increases in micronucleus formation as well. Poma *et al.* directly compared micronucleus induction by carbon black and particulate matter and reported even higher micronucleus frequencies for airborne particulate matter (Poma *et al.* 2006). This was suggested to be due mainly to organic contaminants. Similar results were also published by other scientists (Gu *et al.* 2005; Roubicek *et al.* 2007).

Studies examining the genotoxicity of zinc compounds reported ambiguous results. Zenzen *et al.* did not find genotoxic effects in human lymphocytes exposed to zinc dithiocarbamates at concentrations of 0.1, 1 and 10 µg/ml (Zenzen *et al.* 2001). However, the others did not state if this effect was mediated mainly by the zinc or the dithiocarbamate.

Other authors used zinc salts which might be more suitable to compare to ZnO nanoparticles. An 8 to 9-fold increase in micronucleated cells was observed in human leukocytes after treatment with 0.15 and 0.3 mM zinc chloride (ZnCl₂) (Santra *et al.* 2002). Zinc sulphate (ZnSO₄) induced micronucleus frequencies in *Vicia faba* root tips at concentrations of 100 µM that were 10 times higher than in control treatments (Marcato-Romain *et al.* 2009). Moreover, another study examined chromosome aberrations induced by ZnO in CHO cells. The authors reported a positive outcome at a concentration of 105 µg/ml (Dufour *et al.* 2006).

However, the concentrations used in the studies that showed genotoxicity of zinc compounds were much higher than the ones in this work. This is particularly true when taking into account that the water solubility of zinc salts is much higher than the solubility of ZnO nanoparticles (BGIA GESTIS database); thus the concentrations of zinc ions released by the nanoparticles into the medium are certainly much lower than in solutions of ZnCl₂ or ZnSO₄.

Interestingly, treatment with ZnO nanoparticles did not elevate the number of apoptotic cells in the micronucleus test. In various types of immune cells (murine thymocytes, murine splenic lymphocytes, human Ramos B and human Jurkat T cells,

human B-cell lymphomas and human peripheral blood monocytes), exposure to Zn²⁺ resulted in induction of apoptosis (Provinciali *et al.* 1995; Ibs *et al.* 2003; Lecane *et al.* 2005; Mann *et al.* 2005; Chang *et al.* 2006). This discrepancy might be explained by the comparably low doses of zinc ions that are present in incubations with ZnO nanoparticles. Apoptosis was found to be induced mostly by high zinc concentrations (above 75 µM and 100 µM respectively) (Provinciali *et al.* 1995; Chang *et al.* 2006). Nevertheless, low concentrations can also trigger apoptosis. However, Provinciali *et al.* reported that the length of the incubation is important: Apoptosis is induced by zinc after 8 hours, but blocked after 20 hours (Provinciali *et al.* 1995). The micronucleus test takes 24 hours, thus the early induction of apoptosis might be missed.

Moreover, the A549 cell line might respond to zinc differently than immune cells. For example, apoptosis of A549 cells induced by primary lung fibroblasts from patients with idiopathic pulmonary fibrosis was inhibited by 50 µM zinc (Uhal *et al.* 1995).

In conclusion, the limited number of studies on genotoxicity of nanomaterials, which are moreover hardly comparable, suggest the urgent need to standardize protocols and to increase the knowledge about the genotoxic potential of novel nanomaterials in order to be able to assess possible health effects and to prevent adverse effects.

My results suggest that the genotoxic potential of TiO₂ and ZnO is very low. Thus, the use of these nanoparticles e.g. in sunscreens seems to be safe, in particular as healthy skin does not allow penetration of nanoparticles (Kiss *et al.* 2008). In contrast, carbon black is apparently genotoxic at higher concentrations. Considering this genotoxicity, occupationally exposed persons should be protected against inhalation of carbon black particles. Consumer products containing carbon black (e.g. printer toners) should apply formulations that minimize or prevent aerosol formation. Moreover, the disposal or recycling of products with carbon black has to be done carefully in order to prevent emission of carbon black particles into the environment.

4.8 Conclusions

4.8.1 Biological effects and genotoxicity differ for bulk and nano vanadium oxides

An important question of this work was to figure out if corresponding bulk and nano materials have different effects and to find (mechanistic) explanations for such differences. Indeed, the majority of experiments performed revealed different outcomes for bulk and nanomaterial of the same chemical composition. Solubility, uptake and cytotoxicity were higher for nano than for bulk materials. Even though ROS generation was observed for all soluble vanadium oxides, it was somewhat higher for nanosized than for bulk vanadium oxides. Regarding genotoxicity, the difference between the corresponding nano and bulk substances was even more striking: For V_2O_3 , the bulk material was not genotoxic, whereas the nanomaterial was highly genotoxic. For V_2O_5 , it was the other way round: Genotoxic bulk substance, non-genotoxic nanomaterial.

Thus, this study clearly showed that bulk and nanomaterial of the same chemical composition have distinct effects on cells. In most cases, the (mostly negative) effects were stronger for the nanomaterial. This confirms one of the main concerns that nanotoxicology addresses: The toxic potential of nanomaterials differs from the toxic potential of bulk substances and toxicity is higher for nanomaterials. Similar observations for various substances have been published by several groups (Webb *et al.* 1986; Wolff *et al.* 1988; Oberdorster *et al.* 1992; Oberdorster *et al.* 2000; Gurr *et al.* 2005; Monteiller *et al.* 2007; Papageorgiou *et al.* 2007; Reddy *et al.* 2007; Mroz *et al.* 2008; Balasubramanyam *et al.* 2009).

Anyway, this study showed that a decreased genotoxicity of a nanomaterial is possible as well. Bulk V_2O_5 is a known genotoxic compound; at any rate, the outcome of my experiments suggests no genotoxicity of the nanosized V_2O_5 . To the best of my knowledge, such a toxicological behavior has not been reported before for any other material. However, these *in vitro* results would have to be confirmed by *in vivo* studies to exclude that there is really no genotoxicity, and that a DNA damaging capacity is not only masked by secondary effects.

In any case, it must be concluded that one cannot easily derive the toxic potential of a nanomaterial from the toxicity data of the bulk material. Thus, toxicity testing of novel nanomaterials is still indispensable.

4.8.2 Mechanisms of bulk versus nanotoxicity of vanadium oxides

Nanotoxicology aims not only at testing nanomaterials in the lab one by one. An essential objective is also to elucidate specific mechanisms of nanotoxicity and to establish correlations between physico-chemical properties and toxicological data. Such knowledge could help to predict the toxicity of other materials with similar characteristics. This would enable toxicologists that are faced with an ever rising number of novel nanomaterials to determine from physico-chemical data which nanomaterials might be the most harmful and consequently should be tested at first.

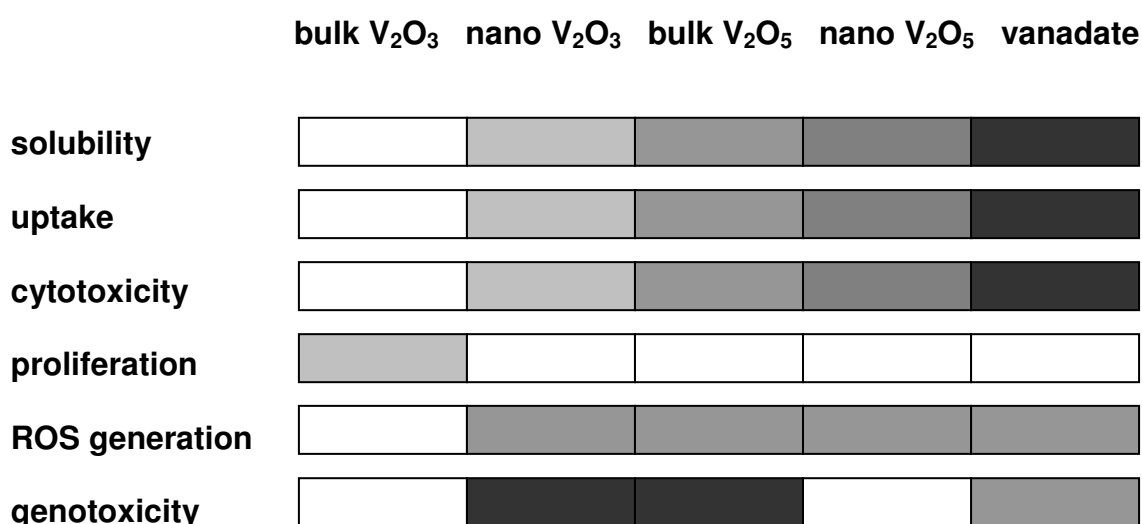


Fig. 40 Summary of the biological effects of vanadium oxides.

The results of different experiments (solubility, uptake, cytotoxicity, proliferation, ROS generation, genotoxicity) are shown for the five vanadium oxides used. The shading represents the observed strength; the darker the color, the stronger was the effect.

Fig. 40 shows a summary of the results of different vanadium oxides species presented in this work. From the figure, it becomes evident that uptake and cytotoxicity are positively and the stimulation of proliferation is negatively correlated to the solubility of the substance. The generation of ROS is not increasing with increasing solubility, thus, there is no direct correlation, but as the generation of ROS was found for all soluble vanadium oxides, but hardly for the insoluble bulk V_2O_3 , solubility seems to be at least a prerequisite for this parameter as well. Thus, the

solubility of a substance is apparently critical for the toxicological behavior. Determination of the solubility of nanomaterials could therefore serve to estimate cytotoxicity, in particular if the soluble species that are released are toxic. Borm *et al.* (Borm *et al.* 2006) already pointed out the importance of dissolution for toxicity of nanomaterials; however, data about the solubility are unfortunately rarely found in studies about nanotoxicity.

When it comes to genotoxicity, I could not find a direct correlation to solubility. The most genotoxic were the two substances of intermediate solubility (nano V_2O_3 and bulk V_2O_5), followed by dissolved vanadate ions. Hence, the mere concentration of dissolved ions may not serve to predict the genotoxic potential. A secondary mechanism seems to be involved in genotoxicity of vanadium oxides; possibly the sequestration of the dissolved molecules to different cellular compartments, maybe as a result of the formation of peroxovanadium compounds. Anyway, the exact mechanism is still unclear and awaits further examination.

4.8.3 Genotoxicity of different nanomaterials is different

Does the comparison of the genotoxic potential of nanomaterials of different chemical composition help to find a parameter which is responsible or correlated to genotoxicity? I examined the genotoxicity of different nanomaterials, TiO_2 , ZnO and carbon black, and compared it to the genotoxicity data acquired in the experiments with vanadium oxides. A summary of these results is shown in Tab. 7. No genotoxic potential was found for nano V_2O_5 , TiO_2 and ZnO. Carbon black was weakly genotoxic. Genotoxicity was considerable for nano V_2O_3 . Thus, some of the nanomaterials tested were genotoxic (nano V_2O_3 , CB), the others not. But what determines genotoxicity? Is the DNA damaging capacity correlated to specific nano-characteristics, like increased specific surface or elevated surface reactivity? Or is the toxicity mainly dependent on the material and therefore different for chemically different nanomaterials, even if they are of the same size or specific surface?

From Tab. 7, it becomes evident that a correlation to the size of the nanomaterials was not apparent. It has been suggested that the specific surface is more suitable to find correlations (Oberdorster *et al.* 1994; Oberdorster 1996). Unfortunately, this parameter was not available for all materials.

Physico-chemical characteristics like solubility might play a role, too, if one thinks about the fact that water-soluble nano V_2O_3 was much more genotoxic than the hardly water soluble bulk V_2O_3 . However, this did not hold true when comparing nano V_2O_3 (good solubility, high genotoxic potential) and nano V_2O_5 (higher solubility than nano V_2O_3 , but no apparent genotoxicity). ZnO is also supposed to be more genotoxic than TiO_2 because of its solubility leading to release of toxic ions (Franklin *et al.* 2007); however, genotoxicity for ZnO could not be observed in this study.

Oxidative stress is supposed to play an essential role in the induction of DNA damage by nanomaterials. Could the amount of ROS generation give a hint to the genotoxic potential? All nanomaterials generated ROS to different extents. Low ROS generation (as seen for TiO_2 and ZnO) correlates to a low genotoxic potential. The high ROS production by CB and nano V_2O_3 comes along with a genotoxic potential, but this does not hold true for nano V_2O_5 : ROS is generated, but does not result in DNA damage. Thus, the production of ROS might work as a predictive parameter, but there are obviously exceptions to the rule.

In conclusion, the chemical composition of a nanomaterial is most likely the most important factor in determining genotoxicity (Gojova *et al.* 2007). Nano-characteristics as increased specific surface, solubility and ROS generation may play a role as well in modulating the characteristics of the substance, mostly towards a higher genotoxic potential. However, as long as no factor is found that is clearly correlated to genotoxicity, the genotoxic potential of a novel nanomaterial cannot be predicted. Hence, the question if nanomaterials are genotoxic has to be answered case by case. Genotoxicity testing, preferentially under standardized conditions, is thus further urgently required to be able to assess the risk of nanomaterials for human health.

Tab. 7 Comparison of the genotoxic potential of different nanomaterials

Metric parameters, solubility and ROS generation as well as the outcome of the comet assay and the micronucleus test are given for nano vanadium trioxide (nV₂O₃), nano vanadium pentoxide (nV₂O₅), nano titanium dioxide (TiO₂), nano carbon black (CB) and nano zinc oxide (ZnO). (-): no difference to control; (+): 2-fold increase relative to control; (+++): 10-fold increase relative to control; (yy): strong genotoxicity; (y): weak genotoxicity; (n): no genotoxicity. (n.d.): not determined. The shading indicates the strength (or the size, respectively): the darker the color, the stronger the effect / the smaller the size of the particle.

material	size	solubility	ROS generation	DNA strand breaks	micro-nuclei	geno-toxic
nV ₂ O ₃	diameter 25 nm, length 100-1000 nm specific surface 74.9 m ² /g	++	++	+++	-	yy
nV ₂ O ₅	spherical diameter 170-180 nm	+++	++	-	-	n
TiO ₂	mean size 21 nm	n.d.	+ ²	-	-	n
CB	mean diameter 14 nm	n.d.	+++ ²	-	+	y
ZnO	mean size 40 nm	+ ¹	+ ²	-	-	n

1: (Franklin *et al.* 2007) 2: Nanocare Report 2009.

4.8.4 Are standard genotoxicity tests suitable for the testing of nanomaterials?

The genotoxicity testing of nanomaterials in this work was performed with two standard tests that are widely used. However, for viability assays, interferences of the material with components of the test system leading to erroneous results have been reported (Worle-Knirsch *et al.* 2006; Monteiro-Riviere *et al.* 2009). What about the comet assay and the micronucleus test? Are there limitations for the use with nanomaterials?

Indeed, insoluble particles may pose a problem in the comet assay. Whereas scoring was straightforward for vanadium oxides and ZnO, the analysis of samples treated with TiO₂ and CB was sometimes difficult. The particles that have been taken up into the cell may be released during cell lysis. Especially at high concentrations, particles present in the agarose gel and associated with DNA changed the fluorescence of the

comets (Fig. 41). I only scored comets without particles, but an automated analysis system or a scorer unaware of this problem might include “wrong” comets and end up with wrong results.



Fig. 41 Insoluble nanoparticles interfere with comet analysis.

Insoluble nanoparticles such as carbon black or TiO_2 are often found associated with the DNA of lysed cells in the comet assay. Scoring of such comets would yield erroneous results, as the fluorescence intensities are decreased (carbon black) or increased (TiO_2).

In the micronucleus test experiments presented in this work, no disturbance due to nanoparticles has been observed. However, it is conceivable that intracellular agglomerates of particles resembling micronuclei may wrongly be scored as micronuclei. Thus, it is very important that experienced persons perform the micronucleus scoring. Moreover, high cellular loads of nanoparticles could also hide micronuclei. Hannu Norppa's group observed this phenomenon for TiO_2 particles (personal communication). In this case, the applied doses have to be carefully chosen.

In summary, the application of standard tests with nanomaterials may not be straightforward. Scientists should always be careful and think of the possibility of interferences and validate the tests for the use with nanomaterials.

4.8.5 Nanomaterials – is there a cancer risk?

Nanomaterials are found in numerous products nowadays, and consumers may wonder if there is a cancer risk when using these products.

My results showed that the genotoxic potential of TiO_2 and ZnO , which are commonly used as sunscreens, is apparently low. Thus, there is most likely no genotoxic risk for the population, even if they are exposed to considerable amounts when applying sunscreens directly to their skin. This holds true in particular as healthy skin is not penetrated by nanoparticles (Kiss *et al.* 2008).

Carbon black was weakly genotoxic at high concentrations ($25 \mu\text{g}/\text{cm}^2$). In the general population, exposure to such concentrations is unlikely to occur. However, the results shown here are derived from short-term studies; the effect of long-term exposure to low doses might be different. Some studies reported genotoxicity of carbon black already at lower concentrations and the induction of lung tumors after (chronic) inhalative exposure to carbon black (Nikula *et al.* 1995; Schins *et al.* 2007). To be on the safe side, consumer products containing carbon black (e.g. printer toners) should apply formulations that minimize or prevent aerosol formation. Moreover, the disposal or recycling of products with carbon black has to be done carefully in order to prevent emission of carbon black particles into the environment. Individuals that are occupationally exposed to respirable carbon black should be protected and monitored to avoid the risk of cancer formation.

The applications of nano-sized vanadium oxides and thus the exposure is very limited for the general population as well. Thus, even if nano V_2O_3 possesses a considerable genotoxic potential, I do not see a general risk for human health. On the other hand, occupationally exposed individuals (e.g. during production or use of nanomaterials in catalytical processes) might face a greater risk, and should thus be monitored and protected by protective equipment when handling nanomaterials.

Finally, what we can learn from this work besides the results for single nanomaterials, is that the genotoxic potential of nanomaterials can be very different from the corresponding bulk materials. The amount of DNA damage induced by bulk and nanomaterial of the same chemical composition may vary a lot, and this may hold true for other nanomaterials as well. Hence, as long as there is no parameter that can predict the genotoxic potential and the resulting cancer risk reliably, genotoxicity testing of novel nanomaterials may reveal unexpected results and is definitely required to be able to assess and prevent health risks correctly.

5 List of Tables and Figures

Tables

Tab. 1 Bulk and nanomaterials used in this work	27
Tab. 2 Content of medium for A549 cells.....	28
Tab. 3 Content of RIPA lysis buffer	32
Tab. 4 Content of buffers and solutions used in the comet assay	41
Tab. 5 Content of solutions and buffers used in the micronucleus test.....	44
Tab. 6 Genotoxicity of vanadium oxides.....	89
Tab. 7 Comparison of the genotoxic potential of different nanomaterials	104

Figures

Fig. 1 Generation and conversion of reactive oxygen/nitrogen species.....	4
Fig. 2 Oxidation of guanine to 8-oxo-7,8-dihydroguanine.....	8
Fig. 3 Base pairing of guanine and 8-oxo-guanine in the DNA.....	9
Fig. 4 Formation of micronuclei.....	13
Fig. 5 Cellular responses to DNA damage.....	15
Fig. 6 Overview over mechanisms of genotoxicity elicited by a genotoxic substance/particle.....	16
Fig. 7 Conversion of MTT to formazan in the MTT assay.....	35
Fig. 8 Conversion of XTT to formazan in the XTT assay.....	36
Fig. 9 Redox-reactions in the LDH assay.....	37
Fig. 10 Conversion of H ₂ DCF to DCF in the DCF assay.....	38
Fig. 11 Oxidative conversion of dihydrorhodamine123 to rhodamine123 by ROS....	39
Fig. 12 Analysis of comets using the “Viscomet” software.....	41
Fig. 13 Examples of parameters scored in the micronucleus test.....	43
Fig. 14 Quantification of cell cycle analysis using ModFit LT software.....	46
Fig. 15 Transmission electron micrographs of nano vanadium oxides.....	48
Fig. 16 Solubility of vanadium oxides.....	50
Fig. 17 Uptake of vanadium oxides into cells.....	51
Fig. 18 Correlation of vanadium solubility and uptake.....	52
Fig. 19 Low concentrations of vanadium oxides induce cell proliferation.....	53

Fig. 20 Metabolic activity of cells decreases with increasing vanadium oxide concentrations.	55
Fig. 21 Cytotoxicity of vanadium oxides measured by the LDH assay.	56
Fig. 22 Soluble vanadium oxides produce reactive oxygen species.....	57
Fig. 23 Vanadium oxides lead to generation of ROS in A549 cells.....	58
Fig. 24 Detection of 8-oxo-G in cells treated with vanadium oxides by a FITC-coupled probe.	59
Fig. 25 Changes in 8-oxo-G content after treatment with vanadium oxides.	60
Fig. 26 Analysis of the 8-oxo-G content in cells treated with vanadium oxides.....	61
Fig. 27 Nano V_2O_3 and bulk V_2O_5 induce strand breaks in A549 cells.	63
Fig. 28 Effect of vanadium oxides on cell division in the micronucleus test.....	65
Fig. 29 No induction of apoptosis or mitosis by vanadium oxides in the micronucleus test.....	65
Fig. 30 No induction of micronuclei by vanadium oxides.	66
Fig. 31 Altered nuclear morphology in cells treated with vanadium oxides.....	67
Fig. 32 Soluble vanadium oxides increase the number of cells with segmented nuclei.	68
Fig. 33 Irregular mitosis in cells treated with vanadium oxides.....	69
Fig. 34 Nano V_2O_3 , bulk V_2O_5 and vanadate induce cell cycle arrest.	70
Fig. 35 No induction of DNA strand breaks by TiO_2 , CB and ZnO nanoparticles.....	72
Fig. 36 Treatment with TiO_2 induces no changes in micronucleus test parameters.	73
Fig. 37 CB induces micronuclei.	74
Fig. 38 Treatment with ZnO induces no changes in micronucleus test parameters..	75
Fig. 39 Summary of the toxic effects and (hypothetical) mechanisms of different vanadium oxide species.	91
Fig. 40 Summary of the biological effects of vanadium oxides.	101
Fig. 41 Insoluble nanoparticles interfere with comet analysis.....	105

6 References

- Abalea, V., J. Cillard, M. P. Dubos, J. P. Anger, P. Cillard and I. Morel (1998). "Iron-induced oxidative DNA damage and its repair in primary rat hepatocyte culture." Carcinogenesis 19(6): 1053-9.
- Ahamed, M., M. Karns, M. Goodson, J. Rowe, S. M. Hussain, J. J. Schlager and Y. Hong (2008). "DNA damage response to different surface chemistry of silver nanoparticles in mammalian cells." Toxicol Appl Pharmacol 233(3): 404-10.
- Ahmed, S. A., R. M. Gogal, Jr. and J. E. Walsh (1994). "A new rapid and simple non-radioactive assay to monitor and determine the proliferation of lymphocytes: an alternative to [3H]thymidine incorporation assay." J Immunol Methods 170(2): 211-24.
- Akasaka, S. and K. Yamamoto (1994). "Hydrogen peroxide induces G:C to T:A and G:C to C:G transversions in the supF gene of Escherichia coli." Mol Gen Genet 243(5): 500-5.
- Altamirano-Lozano, M., L. Alvarez-Barrera, F. Basurto-Alcantara, M. Valverde and E. Rojas (1996). "Reprotoxic and genotoxic studies of vanadium pentoxide in male mice." Teratog Carcinog Mutagen 16(1): 7-17.
- Altamirano-Lozano, M., M. Valverde, L. Alvarez-Barrera, B. Molina and E. Rojas (1999). "Genotoxic studies of vanadium pentoxide (V(2)O(5)) in male mice. II. Effects in several mouse tissues." Teratog Carcinog Mutagen 19(4): 243-255.
- Aragon, M. A., M. E. Ayala, T. I. Fortoul, P. Bizarro and M. Altamirano-Lozano (2005). "Vanadium induced ultrastructural changes and apoptosis in male germ cells." Reprod Toxicol 20(1): 127-134.
- Baird, W. M., L. A. Hooven and B. Mahadevan (2005). "Carcinogenic polycyclic aromatic hydrocarbon-DNA adducts and mechanism of action." Environ Mol Mutagen 45(2-3): 106-14.
- Balasubramanyam, A., N. Sailaja, M. Mahboob, M. F. Rahman, S. M. Hussain and P. Grover (2009). "In vivo genotoxicity assessment of aluminium oxide nanomaterials in rat peripheral blood cells using the comet assay and micronucleus test." Mutagenesis 24(3): 245-51.
- Balbus, J. M., A. D. Maynard, V. L. Colvin, V. Castranova, G. P. Daston, R. A. Denison, K. L. Dreher, P. L. Goering, A. M. Goldberg, K. M. Kulinowski, N. A. Monteiro-Riviere, G. Oberdorster, G. S. Omenn, K. E. Pinkerton, K. S. Ramos, K. M. Rest, J. B. Sass, E. K. Silbergeld and B. A. Wong (2007). "Meeting report: hazard assessment for nanoparticles--report from an interdisciplinary workshop." Environ Health Perspect 115(11): 1654-1659.
- Barceloux, D. G. (1999). "Vanadium." J Toxicol Clin Toxicol 37(2): 265-278.
- Barnes, C. A., A. Elsaesser, J. Arkusz, A. Smok, J. Palus, A. Lesniak, A. Salvati, J. P. Hanrahan, W. H. Jong, E. Dziubaltowska, M. Stepnik, K. Rydzynski, G.

- McKerr, I. Lynch, K. A. Dawson and C. V. Howard (2008). "Reproducible comet assay of amorphous silica nanoparticles detects no genotoxicity." Nano Lett 8(9): 3069-3074.
- Barthel, A., E. A. Ostrakhovitch, P. L. Walter, A. Kampkotter and L. O. Klotz (2007). "Stimulation of phosphoinositide 3-kinase/Akt signaling by copper and zinc ions: mechanisms and consequences." Arch Biochem Biophys 463(2): 175-82.
- Becker, D. J., L. N. Ongemba and J. C. Henquin (1994). "Comparison of the effects of various vanadium salts on glucose homeostasis in streptozotocin-diabetic rats." Eur J Pharmacol 260(2-3): 169-175.
- Bevan, A. P., P. G. Drake, J. F. Yale, A. Shaver and B. I. Posner (1995). "Peroxovanadium compounds: biological actions and mechanism of insulin-mimesis." Mol Cell Biochem 153(1-2): 49-58.
- BGIA GESTIS database, <http://www.dguv.de/bgia/de/gestis/stoffdb/index.jsp#>
- Bhattacharya, K., H. Cramer, C. Albrecht, R. Schins, Q. Rahman, U. Zimmermann and E. Dopp (2008). "Vanadium pentoxide-coated ultrafine titanium dioxide particles induce cellular damage and micronucleus formation in V79 cells." J Toxicol Environ Health A 71(13-14): 976-80.
- Boiteux, S. and M. Guillet (2004). "Abasic sites in DNA: repair and biological consequences in *Saccharomyces cerevisiae*." DNA Repair (Amst) 3(1): 1-12.
- Bonassi, S., A. Znaor, M. Ceppi, C. Lando, W. P. Chang, N. Holland, M. Kirsch-Volders, E. Zeiger, S. Ban, R. Barale, M. P. Bigatti, C. Bolognesi, A. Cebulska-Wasilewska, E. Fabianova, A. Fucic, L. Hagmar, G. Joksic, A. Martelli, L. Migliore, E. Mirkova, M. R. Scarfi, A. Zijno, H. Norppa and M. Fenech (2007). "An increased micronucleus frequency in peripheral blood lymphocytes predicts the risk of cancer in humans." Carcinogenesis 28(3): 625-31.
- Borm, P., F. C. Klaessig, T. D. Landry, B. Moudgil, J. Pauluhn, T. Karluss, R. Trottier and S. Wood (2006). "Research Strategies for Safety Evaluation of Nanomaterials, Part V: Role of Dissolution in Biological Fate and Effects of Nanoscale Particles." Toxicological Sciences 90(1): 23-32.
- Borm, P. J. and K. Driscoll (1996). "Particles, inflammation and respiratory tract carcinogenesis." Toxicol Lett 88(1-3): 109-113.
- Borm, P. J. and W. Kreyling (2004). "Toxicological hazards of inhaled nanoparticles-potential implications for drug delivery." J Nanosci Nanotechnol 4(5): 521-531.
- Bowman, B. J. (1983). "Vanadate uptake in *Neurospora crassa* occurs via phosphate transport system II." J Bacteriol 153(1): 286-291.
- Bracken, W. M. and R. P. Sharma (1985a). "Cytotoxicity-related alterations of selected cellular functions after in vitro vanadate exposure." Biochem Pharmacol 34(14): 2465-2470.

- Bracken, W. M., R. P. Sharma and Y. Y. Elsner (1985b). "Vanadium accumulation and subcellular distribution in relation to vanadate induced cytotoxicity in vitro." Cell Biol Toxicol 1(4): 259-268.
- Burney, S., J. L. Caulfield, J. C. Niles, J. S. Wishnok and S. R. Tannenbaum (1999). "The chemistry of DNA damage from nitric oxide and peroxynitrite." Mutat Res 424(1-2): 37-49.
- Cande, W. Z. and S. M. Wolniak (1978). "Chromosome movement in lysed mitotic cells is inhibited by vanadate." J Cell Biol 79(2 Pt 1): 573-580.
- Cantley, L. C., Jr., L. Josephson, R. Warner, M. Yanagisawa, C. Lechene and G. Guidotti (1977). "Vanadate is a potent (Na,K)-ATPase inhibitor found in ATP derived from muscle." J Biol Chem 252(21): 7421-7423.
- Cantley, L. C., Jr., L. G. Cantley and L. Josephson (1978a). "A characterization of vanadate interactions with the (Na,K)-ATPase. Mechanistic and regulatory implications." J Biol Chem 253(20): 7361-7368.
- Cantley, L. C., Jr., M. D. Resh and G. Guidotti (1978b). "Vanadate inhibits the red cell (Na⁺, K⁺) ATPase from the cytoplasmic side." Nature 272(5653): 552-554.
- Cazales, M., R. Boutros, M. C. Brezak, S. Chaumeron, G. Prevost and B. Ducommun (2007). "Pharmacologic inhibition of CDC25 phosphatases impairs interphase microtubule dynamics and mitotic spindle assembly." Mol Cancer Ther 6(1): 318-325.
- Chang, K. L., T. C. Hung, B. S. Hsieh, Y. H. Chen, T. F. Chen and H. L. Cheng (2006). "Zinc at pharmacologic concentrations affects cytokine expression and induces apoptosis of human peripheral blood mononuclear cells." Nutrition 22(5): 465-74.
- Chen, F., W. M. Lam, C. J. Lin, G. X. Qiu, Z. H. Wu, K. D. Luk and W. W. Lu (2007). "Biocompatibility of electrophoretical deposition of nanostructured hydroxyapatite coating on roughen titanium surface: in vitro evaluation using mesenchymal stem cells." J Biomed Mater Res B Appl Biomater 82(1): 183-191.
- Chen, G., G. Luo, X. Yang, Y. Sun and J. Wang (2004). "Anatase-TiO₂ nano-particle preparation with a micro-mixing technique and its photocatalytic performance." Materials Science and Engineering 380: 320-325.
- Chithrani, B. D. and W. C. Chan (2007). "Elucidating the mechanism of cellular uptake and removal of protein-coated gold nanoparticles of different sizes and shapes." Nano Lett 7(6): 1542-1550.
- Cho, H. P., Y. Liu, M. Gomez, J. Dunlap, M. Tyers and Y. Wang (2005). "The dual-specificity phosphatase CDC14B bundles and stabilizes microtubules." Mol Cell Biol 25(11): 4541-4551.
- Cimini, D. and F. Degrossi (2005). "Aneuploidy: a matter of bad connections." Trends Cell Biol 15(8): 442-451.

- Ciranni, R., M. Antonetti and L. Migliore (1995). "Vanadium salts induce cytogenetic effects in in vivo treated mice." Mutat Res 343(1): 53-60.
- Colognato, R., A. Bonelli, J. Ponti, M. Farina, E. Bergamaschi, E. Sabbioni and L. Migliore (2008). "Comparative genotoxicity of cobalt nanoparticles and ions on human peripheral leukocytes in vitro." Mutagenesis 23(5): 377-82.
- Cortizo, A. M. and S. B. Etcheverry (1995). "Vanadium derivatives act as growth factor--mimetic compounds upon differentiation and proliferation of osteoblast-like UMR106 cells." Mol Cell Biochem 145(2): 97-102.
- Crans, D. C. (1994). "Aqueous chemistry of labile oxovanadates: relevance to biological studies." Comments on Inorganic Chemistry 16(1): 33.
- Crans, D. C., M. Mahroof-Tahir and A. D. Keramidis (1995). "Vanadium chemistry and biochemistry of relevance for use of vanadium compounds as antidiabetic agents." Mol Cell Biochem 153(1-2): 17-24.
- Crans, D. C. (2005). "Fifteen years of dancing with vanadium." Pure Appl Chem 77(9): 1497-1527.
- Cruz, T. F., A. Morgan and W. Min (1995). "In vitro and in vivo antineoplastic effects of orthovanadate." Mol Cell Biochem 153(1-2): 161-166.
- Das, P. M. and R. Singal (2004). "DNA methylation and cancer." J Clin Oncol 22(22): 4632-42.
- de Fries, R. and M. Mitsuhashi (1995). "Quantification of mitogen induced human lymphocyte proliferation: comparison of alamarBlue assay to 3H-thymidine incorporation assay." J Clin Lab Anal 9(2): 89-95.
- Dean, R. T. and K. H. Cheeseman (1987). "Vitamin E protects proteins against free radical damage in lipid environments." Biochem Biophys Res Commun 148(3): 1277-82.
- Decordier, I., L. Dillen, E. Cundari and M. Kirsch-Volders (2002). "Elimination of micronucleated cells by apoptosis after treatment with inhibitors of microtubules." Mutagenesis 17(4): 337-44.
- Demple, B. and L. Harrison (1994). "Repair of oxidative damage to DNA: enzymology and biology." Annu Rev Biochem 63: 915-48.
- Derfus, A. M., W. C. W. Chan and S. N. Bathia (2004). "Probing the Cytotoxicity of Semiconductor Quantum Dots " Nano Lett 4(1): 11-18.
- Diabate, S., S. Mulhopt, H. R. Paur, R. Wottrich and H. F. Krug (2002). "In vitro effects of incinerator fly ash on pulmonary macrophages and epithelial cells." Int J Hyg Environ Health 204(5-6): 323-6.
- Dizdaroglu, M., P. Jaruga, M. Birincioglu and H. Rodriguez (2002). "Free radical-induced damage to DNA: mechanisms and measurement." Free Radic Biol Med 32(11): 1102-15.

- Djordjevic, C., N. Vuletic, M. L. Renslo, B. C. Puryear and R. Alimard (1995). "Peroxo heteroligand vanadates(V): synthesis, spectra-structure relationships, and stability toward decomposition." Mol Cell Biochem 153(1-2): 25-29.
- Don Porto Carero, A., P. H. Hoet, L. Verschaeve, G. Schoeters and B. Nemery (2001). "Genotoxic effects of carbon black particles, diesel exhaust particles, and urban air particulates and their extracts on a human alveolar epithelial cell line (A549) and a human monocytic cell line (THP-1)." Environ Mol Mutagen 37(2): 155-63.
- Donaldson, K., V. Stone, A. Seaton and W. MacNee (2001). "Ambient particle inhalation and the cardiovascular system: potential mechanisms." Environ Health Perspect. 109 Suppl 4: 523-527.
- Donaldson, K., V. Stone, C. L. Tran, W. Kreyling and P. J. Borm (2004). "Nanotoxicology." Occup. Environ. Med. 61(9): 727-728.
- Dufour, E. K., T. Kumaravel, G. J. Nohynek, D. Kirkland and H. Toutain (2006). "Clastogenicity, photo-clastogenicity or pseudo-photo-clastogenicity: Genotoxic effects of zinc oxide in the dark, in pre-irradiated or simultaneously irradiated Chinese hamster ovary cells." Mutat Res 607(2): 215-224.
- Duggen, S. (2004). Eine Frage der Größe - Ultrafeine Teilchen schädigen Herz und Gefäße. GSF - mensch + umwelt 1: 3-4.
- Dunford, R., A. Salinaro, L. Cai, N. Serpone, S. Horikoshi, H. Hidaka and J. Knowland (1997). "Chemical oxidation and DNA damage catalysed by inorganic sunscreen ingredients." FEBS Lett 418(1-2): 87-90.
- Eastman, A. and M. A. Barry (1992). "The origins of DNA breaks: a consequence of DNA damage, DNA repair, or apoptosis?" Cancer Invest 10(3): 229-240.
- Ehrlich, V. A., A. K. Nersesyan, K. Atefie, C. Hoelzl, F. Ferk, J. Bichler, E. Valic, A. Schaffer, R. Schulte-Hermann, M. Fenech, K. H. Wagner and S. Knasmüller (2008). "Inhalative exposure to vanadium pentoxide causes DNA damage in workers: results of a multiple end point study." Environ Health Perspect 116(12): 1689-93.
- Emmendorffer, A., M. Hecht, M. L. Lohmann-Matthes and J. Roesler (1990). "A fast and easy method to determine the production of reactive oxygen intermediates by human and murine phagocytes using dihydrorhodamine 123." J Immunol Methods 131(2): 269-275.
- Eot-Houllier, G., G. Fulcrand, L. Magnaghi-Jaulin and C. Jaulin (2009). "Histone deacetylase inhibitors and genomic instability." Cancer Lett 274(2): 169-76.
- Evangelou, A. M. (2002). "Vanadium in cancer treatment." Crit Rev Oncol Hematol 42(3): 249-265.
- Feldmann, C. (2003). "Polyol-mediated synthesis of nanoscale functional materials." Advanced Functional Materials 13(2): 101-107.
- Fenech, M. (2000). "The in vitro micronucleus technique." Mutat Res 455(1-2): 81-95.

- Fenech, M., W. P. Chang, M. Kirsch-Volders, N. Holland, S. Bonassi and E. Zeiger (2003). "HUMN project: detailed description of the scoring criteria for the cytokinesis-block micronucleus assay using isolated human lymphocyte cultures." Mutat Res 534(1-2): 65-75.
- Fenech, M. (2007). "Cytokinesis-block micronucleus cytome assay." Nat Protoc 2(5): 1084-1104.
- Ferguson, L. R. and B. C. Baguley (1994). "Topoisomerase II enzymes and mutagenicity." Environ Mol Mutagen 24(4): 245-61.
- Fortini, P. and E. Dogliotti (2007). "Base damage and single-strand break repair: mechanisms and functional significance of short- and long-patch repair subpathways." DNA Repair (Amst) 6(4): 398-409.
- Franklin, N. M., N. J. Rogers, S. C. Apte, G. E. Batley, G. E. Gadd and P. S. Casey (2007). "Comparative toxicity of nanoparticulate ZnO, bulk ZnO, and ZnCl₂ to a freshwater microalga (*Pseudokirchneriella subcapitata*): the importance of particle solubility." Environ Sci Technol 41(24): 8484-8490.
- Fritsch, S., S. Diabate and H. F. Krug (2006). "Incinerator fly ash provokes alteration of redox equilibrium and liberation of arachidonic acid in vitro." Biol Chem 387(10-11): 1421-8.
- Genova, M. L., M. M. Pich, A. Bernacchia, C. Bianchi, A. Biondi, C. Bovina, A. I. Falasca, G. Formiggini, G. P. Castelli and G. Lenaz (2004). "The mitochondrial production of reactive oxygen species in relation to aging and pathology." Ann N Y Acad Sci 1011: 86-100.
- Ghio, A. J., C. Kim and R. B. Devlin (2000). "Concentrated ambient air particles induce mild pulmonary inflammation in healthy human volunteers." Am J Respir Crit Care Med 162(3 Pt 1): 981-988.
- Ghio, A. J. and R. B. Devlin (2001). "Inflammatory lung injury after bronchial instillation of air pollution particles." Am J Respir Crit Care Med 164(4): 704-708.
- Giard, D. J., S. A. Aaronson, G. J. Todaro, P. Arnstein, J. H. Kersey, H. Dosik and W. P. Parks (1973). "In vitro cultivation of human tumors: establishment of cell lines derived from a series of solid tumors." J Natl Cancer Inst 51(5): 1417-23.
- Gojova, A., B. Guo, R. S. Kota, J. C. Rutledge, I. M. Kennedy and A. I. Barakat (2007). "Induction of inflammation in vascular endothelial cells by metal oxide nanoparticles: effect of particle composition." Environ Health Perspect 115(3): 403-409.
- Gold, D. R., A. Litonjua, J. Schwartz, E. Lovett, A. Larson, B. Nearing, G. Allen, M. Verrier, R. Cherry and R. Verrier (2000). "Ambient Pollution and Heart Rate Variability." Circulation 101: 1267-1273.
- Gordon, J. A. (1991). "Use of vanadate as protein-phosphotyrosine phosphatase inhibitor." Methods Enzymol 201: 477-482.

- Grollman, A. P. and M. Moriya (1993). "Mutagenesis by 8-oxoguanine: an enemy within." Trends Genet 9(7): 246-9.
- Gruber, M. Y., B. R. Glick and J. E. Thompson (1990). "Cloned manganese superoxide dismutase reduces oxidative stress in *Escherichia coli* and *Anacystis nidulans*." Proc Natl Acad Sci U S A 87(7): 2608-12.
- Gu, Z. W., M. J. Keane, T. M. Ong and W. E. Wallace (2005). "Diesel exhaust particulate matter dispersed in a phospholipid surfactant induces chromosomal aberrations and micronuclei but not 6-thioguanine-resistant gene mutation in V79 cells." J Toxicol Environ Health A 68(6): 431-44.
- Gurr, J. R., A. S. Wang, C. H. Chen and K. Y. Jan (2005). "Ultrafine titanium dioxide particles in the absence of photoactivation can induce oxidative damage to human bronchial epithelial cells." Toxicology 213(1-2): 66-73.
- Hanauske, U., A. R. Hanauske, M. H. Marshall, V. A. Muggia and D. D. von Hoff (1987). "Biphasic effect of vanadium salts on in vitro tumor colony growth." Int J Cell Cloning 5(2): 170-178.
- Hansen, T. V., J. Aaseth and J. Alexander (1982). "The effect of chelating agents on vanadium distribution in the rat body and on uptake by human erythrocytes." Arch Toxicol 50(3-4): 195-202.
- Hardman, R. (2006). "A toxicologic review of quantum dots: toxicity depends on physicochemical and environmental factors." Environ Health Perspect 114(2): 165-172.
- Hashimoto, S., Y. Gon, I. Takeshita, K. Matsumoto, I. Jibiki, H. Takizawa, S. Kudoh and T. Horie (2000). "Diesel exhaust particles activate p38 MAP kinase to produce interleukin 8 and RANTES by human bronchial epithelial cells and N-acetylcysteine attenuates p38 MAP kinase activation." Am J Respir Crit Care Med 161(1): 280-285.
- Heddle, J. A. (1973). "A rapid in vivo test for chromosomal damage." Mutat Res 18(2): 187-90.
- Heinz, A., K. A. Rubinson and J. J. Grantham (1982). "The transport and accumulation of oxyvanadium compounds in human erythrocytes in vitro." J Lab Clin Med 100(4): 593-612.
- Henderson, L. M. and J. B. Chappell (1993). "Dihydrorhodamine 123: a fluorescent probe for superoxide generation?" Eur J Biochem 217(3): 973-980.
- Herrlich, P. and F. D. Bohmer (2000). "Redox regulation of signal transduction in mammalian cells." Biochem Pharmacol 59(1): 35-41.
- Horton, M. A. and A. Khan (2006). "Medical nanotechnology in the UK: a perspective from the London Centre for Nanotechnology." Nanomedicine 2(1): 42-8.
- Hunt, W. H., Jr. (2004). "Nanomaterials: Nomenclature, Novelty, and Necessity." JOM 56(10): 5.

- Huyer, G., S. Liu, J. Kelly, J. Moffat, P. Payette, B. Kennedy, G. Tsaprailis, M. J. Gresser and C. Ramachandran (1997). "Mechanism of inhibition of protein-tyrosine phosphatases by vanadate and pervanadate." J Biol Chem 272(2): 843-851.
- IARC (1997). "Silica, Some Silicates, Coal Dust and Para-Aramid Fibrils." IARC Monographs (68): 1-506.
- IARC (2006). Cobalt in Hard Metals and Cobalt Sulfate, Gallium Arsenide, Indium Phosphide and Vanadium Pentoxide. IARC Monographs (86): 227-292.
- Ibs, K. H. and L. Rink (2003). "Zinc-altered immune function." J Nutr 133(5 Suppl 1): 1452S-6S.
- Ichinose, T., Y. Yajima, M. Nagashima, S. Takenoshita, Y. Nagamachi and M. Sagai (1997). "Lung carcinogenesis and formation of 8-hydroxy-deoxyguanosine in mice by diesel exhaust particles." Carcinogenesis 18(1): 185-92.
- Ide, H. and M. Kotera (2004). "Human DNA glycosylases involved in the repair of oxidatively damaged DNA." Biol Pharm Bull 27(4): 480-5.
- Ivancsits, S., A. Pilger, E. Diem, A. Schaffer and H. W. Rudiger (2002). "Vanadate induces DNA strand breaks in cultured human fibroblasts at doses relevant to occupational exposure." Mutat Res 519(1-2): 25-35.
- Jacobsen, N. R., A. T. Saber, P. White, P. Moller, G. Pojana, U. Vogel, S. Loft, J. Gingerich, L. Soper, G. R. Douglas and H. Wallin (2007). "Increased mutant frequency by carbon black, but not quartz, in the lacZ and cII transgenes of muta mouse lung epithelial cells." Environ Mol Mutagen 48(6): 451-461.
- Jordan, A., R. Scholz, K. Maier-Hauff, F. K. van Landeghem, N. Waldoefner, U. Teichgraeber, J. Pinkernelle, H. Bruhn, F. Neumann, B. Thiesen, A. von Deimling and R. Felix (2006). "The effect of thermotherapy using magnetic nanoparticles on rat malignant glioma." J Neurooncol 78(1): 7-14.
- Kadota, S., I. G. Fantus, G. Deragon, H. J. Guyda, B. Hersh and B. I. Posner (1987a). "Peroxide(s) of vanadium: a novel and potent insulin-mimetic agent which activates the insulin receptor kinase." Biochem Biophys Res Commun 147(1): 259-266.
- Kadota, S., I. G. Fantus, G. Deragon, H. J. Guyda and B. I. Posner (1987b). "Stimulation of insulin-like growth factor II receptor binding and insulin receptor kinase activity in rat adipocytes. Effects of vanadate and H₂O₂." J Biol Chem 262(17): 8252-8256.
- Karlsson, H. L., P. Cronholm, J. Gustafsson and L. Moller (2008). "Copper oxide nanoparticles are highly toxic: a comparison between metal oxide nanoparticles and carbon nanotubes." Chem Res Toxicol 21(9): 1726-1732.
- Kirsch-Volders, M., A. Vanhauwaert, U. Eichenlaub-Ritter and I. Decordier (2003). "Indirect mechanisms of genotoxicity." Toxicol Lett 140-141: 63-74.

- Kisin, E. R., A. R. Murray, M. J. Keane, X. C. Shi, D. Schwegler-Berry, O. Gorelik, S. Arepalli, V. Castranova, W. E. Wallace, V. E. Kagan and A. A. Shvedova (2007). "Single-walled carbon nanotubes: geno- and cytotoxic effects in lung fibroblast V79 cells." J Toxicol Environ Health A 70(24): 2071-2079.
- Kiss, B., T. Biro, G. Czifra, B. I. Toth, Z. Kertesz, Z. Szikszai, A. Z. Kiss, I. Juhasz, C. C. Zouboulis and J. Hunyadi (2008). "Investigation of micronized titanium dioxide penetration in human skin xenografts and its effect on cellular functions of human skin-derived cells." Exp Dermatol 17(8): 659-67.
- Klotz, L. O., N. J. Holbrook and H. Sies (2001). "UVA and singlet oxygen as inducers of cutaneous signaling events." Curr Probl Dermatol 29: 95-113.
- Knaapen, A. M., T. Shi, P. J. Borm and R. P. Schins (2002). "Soluble metals as well as the insoluble particle fraction are involved in cellular DNA damage induced by particulate matter." Mol Cell Biochem 234-235(1-2): 317-326.
- Kreyling, W. G., M. Semmler and W. Moller (2004). "Dosimetry and toxicology of ultrafine particles." J Aerosol Med 17(2): 140-152.
- Kreyling, W. G., M. Semmler-Behnke and W. Moller (2006). "Ultrafine particle-lung interactions: does size matter?" J Aerosol Med 19(1): 74-83.
- Krokan, H. E., R. Standal and G. Slupphaug (1997). "DNA glycosylases in the base excision repair of DNA." Biochem J 325 (Pt 1): 1-16.
- Kurath, M. and S. Maasen (2006). "Toxicology as a nanoscience?-disciplinary identities reconsidered." Part Fibre Toxicol 3: 6.
- Lan, W., X. Zhang, S. L. Kline-Smith, S. E. Rosasco, G. A. Barrett-Wilt, J. Shabanowitz, D. F. Hunt, C. E. Walczak and P. T. Stukenberg (2004). "Aurora B phosphorylates centromeric MCAK and regulates its localization and microtubule depolymerization activity." Curr Biol 14(4): 273-286.
- Landsiedel, R., M. D. Kapp, M. Schulz, K. Wiench and F. Oesch (2009). "Genotoxicity investigations on nanomaterials: methods, preparation and characterization of test material, potential artifacts and limitations - many questions, some answers." Mutat Res 681(2-3): 241-58.
- Le Hegarat, L., L. Puech, V. Fessard, J. M. Poul and S. Dragacci (2003). "Aneugenic potential of okadaic acid revealed by the micronucleus assay combined with the FISH technique in CHO-K1 cells." Mutagenesis 18(3): 293-298.
- Lecane, P. S., M. W. Karaman, M. Sirisawad, L. Naumovski, R. A. Miller, J. G. Hacia and D. Magda (2005). "Motexafin gadolinium and zinc induce oxidative stress responses and apoptosis in B-cell lymphoma lines." Cancer Res 65(24): 11676-88.
- Leonard, A. and G. B. Gerber (1994). "Mutagenicity, carcinogenicity and teratogenicity of vanadium compounds." Mutat Res 317(1): 81-88.
- Leopardi, P., P. Villani, E. Cordelli, E. Siniscalchi, E. Veschetti and R. Crebelli (2005). "Assessment of the in vivo genotoxicity of vanadate: analysis of micronuclei

- and DNA damage induced in mice by oral exposure." Toxicol Lett 158(1): 39-49.
- Li, N., C. Sioutas, A. Cho, D. Schmitz, C. Misra, J. Sempf, M. Wang, T. Oberley, J. Froines and A. Nel (2003). "Ultrafine particulate pollutants induce oxidative stress and mitochondrial damage." Environ Health Perspect 111(4): 455-460.
- Lieber, M., B. Smith, A. Szakal, W. Nelson-Rees and G. Todaro (1976). "A continuous tumor-cell line from a human lung carcinoma with properties of type II alveolar epithelial cells." Int J Cancer 17(1): 62-70.
- Limbach, L. K., Y. Li, R. N. Grass, T. J. Brunner, M. A. Hintermann, M. Muller, D. Gunther and W. J. Stark (2005). "Oxide nanoparticle uptake in human lung fibroblasts: effects of particle size, agglomeration, and diffusion at low concentrations." Environ Sci Technol 39(23): 9370-9376.
- Limbach, L. K., P. Wick, P. Manser, R. N. Grass, A. Bruinink and W. J. Stark (2007). "Exposure of engineered nanoparticles to human lung epithelial cells: influence of chemical composition and catalytic activity on oxidative stress." Environ Sci Technol 41(11): 4158-4163.
- Lloyd, D. R., D. H. Phillips and P. L. Carmichael (1997). "Generation of putative intrastrand cross-links and strand breaks in DNA by transition metal ion-mediated oxygen radical attack." Chem Res Toxicol 10(4): 393-400.
- Lloyd, D. R., P. L. Carmichael and D. H. Phillips (1998). "Comparison of the formation of 8-hydroxy-2'-deoxyguanosine and single- and double-strand breaks in DNA mediated by fenton reactions." Chem Res Toxicol 11(5): 420-427.
- Lobert, S., N. Isern, B. S. Hennington and J. J. Correia (1994). "Interaction of tubulin and microtubule proteins with vanadate oligomers." Biochemistry 33(20): 6244-6252.
- Loschen, G., L. Flohe and B. Chance (1971). "Respiratory chain linked H₂O₂ production in pigeon heart mitochondria." FEBS Lett 18(2): 261-264.
- Mann, J. J. and P. J. Fraker (2005). "Zinc pyrithione induces apoptosis and increases expression of Bim." Apoptosis 10(2): 369-79.
- Marcato-Romain, C. E., E. Pinelli, B. Pourrut, J. Silvestre and M. Guisresse (2009). "Assessment of the genotoxicity of Cu and Zn in raw and anaerobically digested slurry with the *Vicia faba* micronucleus test." Mutat Res 672(2): 113-8.
- Marquez, A., S. Villa-Trevino and F. Gueraud (2007). "The LEC rat: a useful model for studying liver carcinogenesis related to oxidative stress and inflammation." Redox Rep 12(1): 35-9.
- Mates, J. M., J. A. Segura, F. J. Alonso and J. Marquez (2008). "Intracellular redox status and oxidative stress: implications for cell proliferation, apoptosis, and carcinogenesis." Arch Toxicol 82(5): 273-99.

- Mateuca, R., N. Lombaert, P. V. Aka, I. Decordier and M. Kirsch-Volders (2006). "Chromosomal changes: induction, detection methods and applicability in human biomonitoring." Biochimie 88(11): 1515-31.
- Michiels, C., M. Raes, O. Toussaint and J. Remacle (1994). "Importance of S-glutathione peroxidase, catalase, and Cu/Zn-SOD for cell survival against oxidative stress." Free Radic Biol Med 17(3): 235-48.
- Migliore, L., R. Bocciardi, C. Macri and J. F. Lo (1993). "Cytogenetic damage induced in human lymphocytes by four vanadium compounds and micronucleus analysis by fluorescence in situ hybridization with a centromeric probe." Mutat Res 319(3): 205-213.
- Migliore, L., R. Scarpato and P. Falco (1995). "The use of fluorescence in situ hybridization with a beta-satellite DNA probe for the detection of acrocentric chromosomes in vanadium-induced micronuclei." Cytogenet Cell Genet 69(3-4): 215-219.
- Monteiller, C., L. Tran, W. MacNee, S. Faux, A. Jones, B. Miller and K. Donaldson (2007). "The pro-inflammatory effects of low-toxicity low-solubility particles, nanoparticles and fine particles, on epithelial cells in vitro: the role of surface area." Occup Environ Med 64(9): 609-615.
- Monteiro-Riviere, N. A., A. O. Inman and L. W. Zhang (2009). "Limitations and relative utility of screening assays to assess engineered nanoparticle toxicity in a human cell line." Toxicol Appl Pharmacol 234(2): 222-35.
- Morinville, A., D. Maysinger and A. Shaver (1998). "From Vanadis to Atropos: vanadium compounds as pharmacological tools in cell death signalling." Trends Pharmacol Sci 19(11): 452-460.
- Mroz, R. M., R. P. Schins, H. Li, E. M. Drost, W. MacNee and K. Donaldson (2007). "Nanoparticle carbon black driven DNA damage induces growth arrest and AP-1 and NFkappaB DNA binding in lung epithelial A549 cell line." J Physiol Pharmacol 58 Suppl 5(Pt 2): 461-470.
- Mroz, R. M., R. P. Schins, H. Li, L. A. Jimenez, E. M. Drost, A. Holownia, W. MacNee and K. Donaldson (2008). "Nanoparticle-driven DNA damage mimics irradiation-related carcinogenesis pathways." Eur Respir J 31(2): 241-251.
- Muller, J., I. Decordier, P. H. Hoet, N. Lombaert, L. Thomassen, F. Huaux, D. Lison and M. Kirsch-Volders (2008). "Clastogenic and aneugenic effects of multi-wall carbon nanotubes in epithelial cells." Carcinogenesis 29(2): 427-433.
- Mundt, K. E., R. M. Golsteyn, H. A. Lane and E. A. Nigg (1997). "On the regulation and function of human polo-like kinase 1 (PLK1): effects of overexpression on cell cycle progression." Biochem Biophys Res Commun 239(2): 377-385.
- Nakagawa, Y., S. Wakuri, K. Sakamoto and N. Tanaka (1997). "The photogenotoxicity of titanium dioxide particles." Mutat Res 394(1-3): 125-132.

- Nalepa, G. and J. W. Harper (2004). "Visualization of a highly organized intranuclear network of filaments in living mammalian cells." Cell Motil Cytoskeleton 59(2): 94-108.
- Nanocare, Reports (2008) <https://iai-piaserv1.iai.fzk.de/bscw/bscw.cgi/23749>
- Nanokommission der deutschen Bundesregierung (2008). "Verantwortlicher Umgang mit Nanotechnologien – Bericht und Empfehlungen der Nanokommission der deutschen Bundesregierung 2008." http://www.bmu.de/gesundheit_und_umwelt/nanotechnologie/nanodialog/doc/42655.php 1-70.
- Nechay, B. R., L. B. Nanninga and P. S. Nechay (1986). "Vanadyl (IV) and vanadate (V) binding to selected endogenous phosphate, carboxyl, and amino ligands; calculations of cellular vanadium species distribution." Arch Biochem Biophys 251(1): 128-138.
- Neeley, W. L. and J. M. Essigmann (2006). "Mechanisms of formation, genotoxicity, and mutation of guanine oxidation products." Chem Res Toxicol 19(4): 491-505.
- Nel, A., T. Xia, L. Madler and N. Li (2006). "Toxic potential of materials at the nanolevel." Science 311(5761): 622-627.
- Nemmar, A., P. H. Hoet, B. Vanquickenborne, D. Dinsdale, M. Thomeer, M. F. Hoylaerts, H. Vanbilloen, L. Mortelmans and B. Nemery (2002). "Passage of inhaled particles into the blood circulation in humans." Circulation 105(4): 411-414.
- Nikula, K. J., M. B. Snipes, E. B. Barr, W. C. Griffith, R. F. Henderson and J. L. Mauderly (1995). "Comparative pulmonary toxicities and carcinogenicities of chronically inhaled diesel exhaust and carbon black in F344 rats." Fundam Appl Toxicol 25(1): 80-94.
- Nociari, M. M., A. Shalev, P. Benias and C. Russo (1998). "A novel one-step, highly sensitive fluorometric assay to evaluate cell-mediated cytotoxicity." J Immunol Methods 213(2): 157-67.
- Nriagu, J. O. (1998). "History, occurrence and uses of vanadium". Vanadium in the environment. New York, Wiley: 1-24.
- Oberdorster, E. (2004). "Manufactured nanomaterials (fullerenes, C60) induce oxidative stress in the brain of juvenile largemouth bass." Environ Health Perspect 112(10): 1058-1062.
- Oberdorster, G., J. Ferin, R. Gelein, S. C. Soderholm and J. Finkelstein (1992). "Role of the alveolar macrophage in lung injury: studies with ultrafine particles." Environ Health Perspect 97: 193-199.

- Oberdorster, G. (1996). "Significance of particle parameters in the evaluation of exposure-dose-response relationships of inhaled particles." Inhal Toxicol 8 Suppl: 73-89.
- Oberdorster, G., J. N. Finkelstein, C. Johnston, R. Gelein, C. Cox, R. Baggs and A. C. Elder (2000). "Acute pulmonary effects of ultrafine particles in rats and mice." Res Rep Health Eff Inst(96): 5-74.
- Oberdorster, G., Z. Sharp, V. Atudorei, A. Elder, R. Gelein, A. Lunts, W. Kreyling and C. Cox (2002). "Extrapulmonary translocation of ultrafine carbon particles following whole-body inhalation exposure of rats." J Toxicol Environ Health A 65(20): 1531-1543.
- Oberdorster, G., E. Oberdorster and J. Oberdorster (2005). "Nanotoxicology: an emerging discipline evolving from studies of ultrafine particles." Environ Health Perspect 113(7): 823-839.
- Ohi, R., T. Sapra, J. Howard and T. J. Mitchison (2004). "Differentiation of cytoplasmic and meiotic spindle assembly MCAK functions by Aurora B-dependent phosphorylation." Mol Biol Cell 15(6): 2895-2906.
- Owusu-Yaw, J., M. D. Cohen, S. Y. Fernando and C. I. Wei (1990). "An assessment of the genotoxicity of vanadium." Toxicol Lett 50(2-3): 327-336.
- Papageorgiou, I., C. Brown, R. Schins, S. Singh, R. Newson, S. Davis, J. Fisher, E. Ingham and C. P. Case (2007). "The effect of nano- and micron-sized particles of cobalt-chromium alloy on human fibroblasts in vitro." Biomaterials 28(19): 2946-2958.
- Pastwa, E. and J. Blasiak (2003). "Non-homologous DNA end joining." Acta Biochim Pol 50(4): 891-908.
- Peters, A., A. Doring, H. E. Wichmann and W. Koenig (1997a). "Increased plasma viscosity during an air pollution episode: a link to mortality?" Lancet 349(9065): 1582-1587.
- Peters, A., H. E. Wichmann, T. Tuch, J. Heinrich and J. Heyder (1997b). "Respiratory effects are associated with the number of ultrafine particles." Am J Respir Crit Care Med 155(4): 1376-1383.
- Peters, A., E. Liu, R. L. Verrier, J. Schwartz, D. R. Gold, M. Mittleman, J. Baliff, J. A. Oh, G. Allen, K. Monahan and D. W. Dockery (2000). "Air pollution and incidence of cardiac arrhythmia." Epidemiology 11(1): 11-17.
- Peters, A., D. W. Dockery, J. E. Muller and M. A. Mittleman (2001a). "Increased particulate air pollution and the triggering of myocardial infarction." Circulation 103(23): 2810-2815.
- Peters, A., M. Frohlich, A. Doring, T. Immervoll, H. E. Wichmann, W. L. Hutchinson, M. B. Pepys and W. Koenig (2001b). "Particulate air pollution is associated with an acute phase response in men; results from the MONICA-Augsburg Study." Eur Heart J 22(14): 1198-1204.

- Pickrell, J. A., M. Dhakal, S. D. Castro, G. Gahkar, K. J. Klabunde, L. E. Erickson and F. W. Oehme (2006). Comparative Solubility of Nanoparticles and Bulk Oxides of Magnesium in Water and Lung Simulant Fluids, AIChE, San Francisco, CA.
- Poma, A., T. Limongi, C. Pisani, V. Granato and P. Picozzi (2006). "Genotoxicity induced by fine urban air particulate matter in the macrophages cell line RAW 264.7." Toxicol In Vitro 20(6): 1023-1029.
- Pope, C. A., 3rd, R. T. Burnett, M. J. Thun, E. E. Calle, D. Krewski, K. Ito and G. D. Thurston (2002). "Lung cancer, cardiopulmonary mortality, and long-term exposure to fine particulate air pollution." Jama 287(9): 1132-41.
- Prescott, G. J., R. J. Lee, G. R. Cohen, R. A. Elton, A. J. Lee, F. G. Fowkes and R. M. Agius (2000). "Investigation of factors which might indicate susceptibility to particulate air pollution." Occup Environ Med 57(1): 53-57.
- Provinciali, M., G. Di Stefano and N. Fabris (1995). "Dose-dependent opposite effect of zinc on apoptosis in mouse thymocytes." Int J Immunopharmacol 17(9): 735-44.
- Pryor, W. A. (1988). "Why is the hydroxyl radical the only radical that commonly adds to DNA? Hypothesis: it has a rare combination of high electrophilicity, high thermochemical reactivity, and a mode of production that can occur near DNA." Free Radic Biol Med 4(4): 219-223.
- Ramirez, P., D. A. Eastmond, J. P. Laclette and P. Ostrosky-Wegman (1997). "Disruption of microtubule assembly and spindle formation as a mechanism for the induction of aneuploid cells by sodium arsenite and vanadium pentoxide." Mutat Res 386(3): 291-298.
- Reddy, K. M., K. Feris, J. Bell, D. G. Wingett, C. Hanley and A. Punnoose (2007). "Selective toxicity of zinc oxide nanoparticles to prokaryotic and eukaryotic systems." Appl Phys Lett 90(213902): 2139021-2139023.
- Rehder, D., P. J. Costa, C. F. Galdes, M. C. Castro, T. Kabanos, T. Kiss, B. Meier, G. Micera, L. Pettersson, M. Rangel, A. Salifoglou, I. Turel and D. Wang (2002). "In vitro study of the insulin-mimetic behaviour of vanadium(IV, V) coordination compounds." J Biol Inorg Chem 7(4-5): 384-396.
- Rejman, J., V. Oberle, I. S. Zuhorn and D. Hoekstra (2004). "Size-dependent internalization of particles via the pathways of clathrin- and caveolae-mediated endocytosis." Biochem J 377(Pt 1): 159-169.
- Ress, N. B., B. J. Chou, R. A. Renne, J. A. Dill, R. A. Miller, J. H. Roycroft, J. R. Hailey, J. K. Haseman and J. R. Bucher (2003). "Carcinogenicity of inhaled vanadium pentoxide in F344/N rats and B6C3F1 mice." Toxicol Sci 74(2): 287-296.
- Riemschneider, S., H. P. Podhaisky, T. Klapperstuck and W. Wohlrab (2002). "Relevance of reactive oxygen species in the induction of 8-oxo-2'-deoxyguanosine in HaCaT keratinocytes." Acta Derm Venereol 82(5): 325-328.

- Rodriguez-Mercado, J. J., E. Roldan-Reyes and M. Altamirano-Lozano (2003). "Genotoxic effects of vanadium(IV) in human peripheral blood cells." Toxicol Lett 144(3): 359-369.
- Rojas, E., M. Valverde, L. A. Herrera, M. Altamirano-Lozano and P. Ostrosky-Wegman (1996). "Genotoxicity of vanadium pentoxide evaluate by the single cell gel electrophoresis assay in human lymphocytes." Mutat Res 359(2): 77-84.
- Roubicek, D. A., M. E. Gutierrez-Castillo, M. Sordo, M. E. Cebrian-Garcia and P. Ostrosky-Wegman (2007). "Micronuclei induced by airborne particulate matter from Mexico City." Mutat Res 631(1): 9-15.
- Royall, J. A. and H. Ischiropoulos (1993). "Evaluation of 2',7'-dichlorofluorescein and dihydrorhodamine 123 as fluorescent probes for intracellular H₂O₂ in cultured endothelial cells." Arch Biochem Biophys 302(2): 348-355.
- Sabbioni, E., G. Pozzi, S. Devos, A. Pintar, L. Casella and M. Fischbach (1993). "The intensity of vanadium(V)-induced cytotoxicity and morphological transformation in BALB/3T3 cells is dependent on glutathione-mediated bio-reduction to vanadium(IV)." Carcinogenesis 14(12): 2565-2568.
- Samet, J. M., L. M. Graves, J. Quay, L. A. Dailey, R. B. Devlin, A. J. Ghio, W. Wu, P. A. Bromberg and W. Reed (1998). "Activation of MAPKs in human bronchial epithelial cells exposed to metals." Am J Physiol 275(3 Pt 1): L551-L558.
- Santra, M., S. K. Das, G. Talukder and A. Sharma (2002). "Induction of micronuclei by zinc in human leukocytes: a study using cytokinesis-block micronucleus assay." Biol Trace Elem Res 88(2): 139-44.
- Savic, R., L. Luo, A. Eisenberg and D. Maysinger (2003). "Micellar nanocontainers distribute to defined cytoplasmic organelles." Science 300(5619): 615-618.
- Sayes, C. M. and D. B. Warheit (2008). "An in vitro investigation of the differential cytotoxic responses of human and rat lung epithelial cell lines using TiO₂ nanoparticles " International Journal of Nanotechnology 5(1): 15-29.
- Schaumann, F., P. J. Borm, A. Herbrich, J. Knoch, M. Pitz, R. P. Schins, B. Luettig, J. M. Hohlfeld, J. Heinrich and N. Krug (2004). "Metal-rich ambient particles (particulate matter 2.5) cause airway inflammation in healthy subjects." Am J Respir Crit Care Med 170(8): 898-903.
- Schins, R. P. (2002). "Mechanisms of genotoxicity of particles and fibers." Inhal Toxicol 14(1): 57-78.
- Schins, R. P. and A. M. Knaapen (2007). "Genotoxicity of poorly soluble particles." Inhal Toxicol 19 Suppl 1: 189-198.

- Schulze, C., A. Kroll, C.-M. Lehr, U. F. Schaefer, K. Becker, J. Schnekenburger, C. Schulze Isfort, R. Landsiedel and W. Wohlleben (2008). "Not ready to use: overcoming pitfalls when dispersing nanoparticles in physiological media." Nanotoxicology 2(2): 51-61.
- Sedgwick, B. (2004). "Repairing DNA-methylation damage." Nat Rev Mol Cell Biol 5(2): 148-57.
- Shacter, E., E. J. Beecham, J. M. Covey, K. W. Kohn and M. Potter (1988). "Activated neutrophils induce prolonged DNA damage in neighboring cells." Carcinogenesis 9(12): 2297-2304.
- Sharma, V., R. K. Shukla, N. Saxena, D. Parmar, M. Das and A. Dhawan (2009). "DNA damaging potential of zinc oxide nanoparticles in human epidermal cells." Toxicol Lett 185(3): 211-8.
- Shaver, A., J. B. Ng, D. A. Hall and B. I. Posner (1995). "The chemistry of peroxovanadium compounds relevant to insulin mimesis." Mol Cell Biochem 153(1-2): 5-15.
- Shi, X. and N. S. Dalal (1992). "Hydroxyl radical generation in the NADH/microsomal reduction of vanadate." Free Radic Res Commun 17(6): 369-376.
- Shi, X., H. Jiang, Y. Mao, J. Ye and U. Saffiotti (1996). "Vanadium(IV)-mediated free radical generation and related 2'-deoxyguanosine hydroxylation and DNA damage." Toxicology 106(1-3): 27-38.
- Shi, X. L., X. Y. Sun and N. S. Dalal (1990). "Reaction of vanadium(V) with thiols generates vanadium (IV) and thiyl radicals." FEBS Lett 271(1-2): 185-188.
- Shi, X. L. and N. S. Dalal (1991). "Flavoenzymes reduce vanadium(V) and molecular oxygen and generate hydroxyl radical." Arch Biochem Biophys 289(2): 355-361.
- Shibutani, S., M. Takeshita and A. P. Grollman (1991). "Insertion of specific bases during DNA synthesis past the oxidation-damaged base 8-oxodG." Nature 349(6308): 431-434.
- Sies, H. (1991). "Oxidative stress: from basic research to clinical application." Am J Med 91(3C): 31S-38S.
- Sies, H. (1993). "Strategies of antioxidant defense." Eur J Biochem 215(2): 213-9.
- Singh, N. P., M. T. McCoy, R. R. Tice and E. L. Schneider (1988). "A simple technique for quantitation of low levels of DNA damage in individual cells." Exp Cell Res 175(1): 184-191.
- Singh, S., T. Shi, R. Duffin, C. Albrecht, D. van Berlo, D. Hohr, B. Fubini, G. Martra, I. Fenoglio, P. J. Borm and R. P. Schins (2007). "Endocytosis, oxidative stress and IL-8 expression in human lung epithelial cells upon treatment with fine and ultrafine TiO₂: role of the specific surface area and of surface methylation of the particles." Toxicol Appl Pharmacol 222(2): 141-51.

- Sit, K. H., R. Paramanatham, B. H. Bay, K. P. Wong, P. Thong and F. Watt (1996). "Induction of vanadium accumulation and nuclear sequestration causing cell suicide in human Chang liver cells." Experientia 52(8): 778-785.
- Sliwinski, T., A. Czechowska, M. Kolodziejczak, J. Jajte, M. Wisniewska-Jarosinska and J. Blasiak (2009). "Zinc salts differentially modulate DNA damage in normal and cancer cells." Cell Biol Int 33(4): 542-7.
- Smith, P. K., R. I. Krohn, G. T. Hermanson, A. K. Mallia, F. H. Gartner, M. D. Provenzano, E. K. Fujimoto, N. M. Goeke, B. J. Olson and D. C. Klenk (1985). "Measurement of protein using bicinchoninic acid." Anal Biochem 150(1): 76-85.
- Speit, G. and A. Hartmann (1999). "The comet assay (single-cell gel test). A sensitive genotoxicity test for the detection of DNA damage and repair." Methods Mol Biol 113: 203-12.
- Sugden, P. H. and A. Clerk (2006). "Oxidative stress and growth-regulating intracellular signaling pathways in cardiac myocytes." Antioxid Redox Signal 8(11-12): 2111-24.
- Sung, P. and H. Klein (2006). "Mechanism of homologous recombination: mediators and helicases take on regulatory functions." Nat Rev Mol Cell Biol 7(10): 739-50.
- Suzuki, H., T. Toyooka and Y. Ibuki (2007). "Simple and easy method to evaluate uptake potential of nanoparticles in mammalian cells using a flow cytometric light scatter analysis." Environ Sci Technol 41(8): 3018-3024.
- Takenaka, S., E. Karg, C. Roth, H. Schulz, A. Ziesenis, U. Heinzmann, P. Schramel and J. Heyder (2001). "Pulmonary and systemic distribution of inhaled ultrafine silver particles in rats." Environ Health Perspect 109 Suppl 4: 547-551.
- Tamura, S., T. A. Brown, J. H. Whipple, Y. Fujita-Yamaguchi, R. E. Dubler, K. Cheng and J. Lerner (1984). "A novel mechanism for the insulin-like effect of vanadate on glycogen synthase in rat adipocytes." J Biol Chem 259(10): 6650-6658.
- Tasiopoulos, A. J., A. N. Troganis, Y. Deligiannakis, A. Evangelou, T. A. Kabanos, J. D. Woollins and A. Slawin (2000). "Synthetic analogs for oxovanadium(IV/V)-glutathione interaction: an NMR, EPR, synthetic and structural study of oxovanadium(IV/V) compounds with sulfhydryl-containing pseudopeptides and dipeptides." J Inorg Biochem 79(1-4): 159-166.
- Theogaraj, E., S. Riley, L. Hughes, M. Maier and D. Kirkland (2007). "An investigation of the photo-clastogenic potential of ultrafine titanium dioxide particles." Mutat Res 634(1-2): 205-219.
- Toya, T., K. Fukuda, M. Takaya and H. Arito (2001). "Lung lesions induced by intratracheal instillation of vanadium pentoxide powder in rats." Ind Health 39(1): 8-15.

- Toyokuni, S. (2008). "Molecular mechanisms of oxidative stress-induced carcinogenesis: from epidemiology to oxygenomics." IUBMB Life 60(7): 441-7.
- Trinkle-Mulcahy, L. and A. I. Lamond (2006). "Mitotic phosphatases: no longer silent partners." Curr Opin Cell Biol 18(6): 623-631.
- Tuo, J., S. P. Wolff, S. Loft and H. E. Poulsen (1998). "Formation of nitrated and hydroxylated aromatic compounds from benzene and peroxyxynitrite, a possible mechanism of benzene genotoxicity." Free Radic Res 28(4): 369-375.
- Tuo, J., L. Liu, H. E. Poulsen, A. Weimann, O. Svendsen and S. Loft (2000). "Importance of guanine nitration and hydroxylation in DNA in vitro and in vivo." Free Radic Biol Med 29(2): 147-155.
- Uhal, B. D., I. Joshi, A. L. True, S. Mundle, A. Raza, A. Pardo and M. Selman (1995). "Fibroblasts isolated after fibrotic lung injury induce apoptosis of alveolar epithelial cells in vitro." Am J Physiol 269(6 Pt 1): L819-28.
- Unfried, K., C. Schurkes and J. Abel (2002). "Distinct spectrum of mutations induced by crocidolite asbestos: clue for 8-hydroxydeoxyguanosine-dependent mutagenesis in vivo." Cancer Res 62(1): 99-104.
- Valko, M., M. Izakovic, M. Mazur, C. J. Rhodes and J. Telser (2004). "Role of oxygen radicals in DNA damage and cancer incidence." Mol Cell Biochem 266(1-2): 37-56.
- Valko, M., C. J. Rhodes, J. Moncol, M. Izakovic and M. Mazur (2006). "Free radicals, metals and antioxidants in oxidative stress-induced cancer." Chem Biol Interact 160(1): 1-40.
- Veranth, J. M., E. G. Kaser, M. M. Veranth, M. Koch and G. S. Yost (2007). "Cytokine responses of human lung cells (BEAS-2B) treated with micron-sized and nanoparticles of metal oxides compared to soil dusts." Part Fibre Toxicol 4: 2.
- Vevers, W. F. and A. N. Jha (2008). "Genotoxic and cytotoxic potential of titanium dioxide (TiO₂) nanoparticles on fish cells in vitro." Ecotoxicology 17(5): 410-20.
- Villani, P., E. Cordelli, P. Leopardi, E. Siniscalchi, E. Veschetti, A. M. Fresegna and R. Crebelli (2007). "Evaluation of genotoxicity of oral exposure to tetravalent vanadium in vivo." Toxicol Lett 170(1): 11-8.
- Wan, C. P., E. Myung and B. H. Lau (1993). "An automated micro-fluorometric assay for monitoring oxidative burst activity of phagocytes." J Immunol Methods 159(1-2): 131-8.
- Wang, J. J., B. J. Sanderson and H. Wang (2007a). "Cyto- and genotoxicity of ultrafine TiO₂ particles in cultured human lymphoblastoid cells." Mutat Res 628(2): 99-106.
- Wang, J. J., B. J. Sanderson and H. Wang (2007b). "Cytotoxicity and genotoxicity of ultrafine crystalline SiO₂ particulate in cultured human lymphoblastoid cells." Environ Mol Mutagen 48(2): 151-157.

- Wang, Y. Z. and J. C. Bonner (2000). "Mechanism of extracellular signal-regulated kinase (ERK)-1 and ERK-2 activation by vanadium pentoxide in rat pulmonary myofibroblasts." Am J Respir Cell Mol Biol 22(5): 590-596.
- Warheit, D. B., R. A. Hoke, C. Finlay, E. M. Donner, K. L. Reed and C. M. Sayes (2007). "Development of a base set of toxicity tests using ultrafine TiO₂ particles as a component of nanoparticle risk management." Toxicol Lett 171(3): 99-110.
- Wayner, D. D., G. W. Burton and K. U. Ingold (1986). "The antioxidant efficiency of vitamin C is concentration-dependent." Biochim Biophys Acta 884(1): 119-23.
- Webb, D. R., S. E. Wilson and D. E. Carter (1986). "Comparative pulmonary toxicity of gallium arsenide, gallium(III) oxide, or arsenic(III) oxide intratracheally instilled into rats." Toxicol Appl Pharmacol 82(3): 405-416.
- Wei, C. I., M. A. Al Bayati, M. R. Culbertson, L. S. Rosenblatt and L. D. Hansen (1982). "Acute toxicity of ammonium metavanadate in mice." J Toxicol Environ Health 10(4-5): 673-687.
- Weisburger, J. H. and G. M. Williams (2000). "The distinction between genotoxic and epigenetic carcinogens and implication for cancer risk." Toxicol Sci 57(1): 4-5.
- Whiteman, M., A. Jenner and B. Halliwell (1997). "Hypochlorous acid-induced base modifications in isolated calf thymus DNA." Chem Res Toxicol 10(11): 1240-1246.
- Whiteman, M., J. P. Spencer, A. Jenner and B. Halliwell (1999). "Hypochlorous acid-induced DNA base modification: potentiation by nitrite: biomarkers of DNA damage by reactive oxygen species." Biochem Biophys Res Commun 257(2): 572-576.
- WHO Regional Office for Europe Copenhagen, Denmark. (2000). Vanadium. Air Quality Guidelines - Second Edition.
- Wichmann, H. E., C. Spix, T. Tuch, G. Wolke, A. Peters, J. Heinrich, W. G. Kreyling and J. Heyder (2000). "Daily mortality and fine and ultrafine particles in Erfurt, Germany part I: role of particle number and particle mass." Res Rep Health Eff Inst (98): 5-86; discussion 87-94.
- Willems, M., E. Wagner, R. Laing and S. Penman (1968). "Base composition of ribosomal RNA precursors in the HeLa cell nucleolus: further evidence of non-conservative processing." J Mol Biol 32(2): 211-220.
- Wiseman, H. and B. Halliwell (1996). "Damage to DNA by reactive oxygen and nitrogen species: role in inflammatory disease and progression to cancer." Biochem J 313 (Pt 1): 17-29.
- Wolff, R. K., R. F. Henderson, A. F. Eidson, J. A. Pickrell, S. J. Rothenberg and F. F. Hahn (1988). "Toxicity of gallium oxide particles following a 4-week inhalation exposure." J Appl Toxicol 8(3): 191-199.

- Worle-Knirsch, J. M., K. Pulskamp and H. F. Krug (2006). "Oops they did it again! Carbon nanotubes hoax scientists in viability assays." Nano Lett 6(6): 1261-1268.
- Worle-Knirsch, J. M., K. Kern, C. Schleh, C. Adelhelm, C. Feldmann and H. F. Krug (2007). "Nanoparticulate vanadium oxide potentiated vanadium toxicity in human lung cells." Environ Sci Technol 41(1): 331-336.
- Wottrich, R., S. Diabate and H. F. Krug (2004). "Biological effects of ultrafine model particles in human macrophages and epithelial cells in mono- and co-culture." Int J Hyg Environ Health 207(4): 353-61.
- Wyatt, M. D. and D. L. Pittman (2006). "Methylating agents and DNA repair responses: Methylated bases and sources of strand breaks." Chem Res Toxicol 19(12): 1580-94.
- Xu, A., L. J. Wu, R. M. Santella and T. K. Hei (1999). "Role of oxyradicals in mutagenicity and DNA damage induced by crocidolite asbestos in mammalian cells." Cancer Res 59(23): 5922-6.
- Yang, H., C. Liu, D. Yang, H. Zhang and Z. Xi (2009). "Comparative study of cytotoxicity, oxidative stress and genotoxicity induced by four typical nanomaterials: the role of particle size, shape and composition." J Appl Toxicol 29(1): 69-78.
- Yang, X., K. Wang, J. Lu and D. C. Crans (2003). "Membrane transport of vanadium compounds and the interaction with the erythrocyte membrane." Coord Chem Rev 237(1-2): 103-111.
- Yang, X. G., X. D. Yang, L. Yuan, K. Wang and D. C. Crans (2004). "The permeability and cytotoxicity of insulin-mimetic vanadium compounds." Pharm Res 21(6): 1026-1033.
- Zenzen, V., E. Fauth, H. Zankl, C. Janzowski and G. Eisenbrand (2001). "Mutagenic and cytotoxic effectiveness of zinc dimethyl and zinc diisononyldithiocarbamate in human lymphocyte cultures." Mutat Res 497(1-2): 89-99.
- Zhang, Z., C. Huang, J. Li, S. S. Leonard, R. Lanciotti, L. Butterworth and X. Shi (2001). "Vanadate-induced cell growth regulation and the role of reactive oxygen species." Arch Biochem Biophys 392(2): 311-320.
- Zhang, Z., S. S. Leonard, C. Huang, V. Vallyathan, V. Castranova and X. Shi (2003). "Role of reactive oxygen species and MAPKs in vanadate-induced G(2)/M phase arrest." Free Radic Biol Med 34(10): 1333-1342.
- Zhao, L., J. Chang and W. Zhai (2005). "Effect of crystallographic phases of TiO₂ on hepatocyte attachment, proliferation and morphology." J Biomater Appl 19(3): 237-52.
- Zhao, Z., Z. Tan, C. D. Diltz, M. You and E. H. Fischer (1996). "Activation of mitogen-activated protein (MAP) kinase pathway by pervanadate, a potent inhibitor of tyrosine phosphatases." J Biol Chem 271(36): 22251-22255.

- Zhong, B. Z., Z. W. Gu, W. E. Wallace, W. Z. Whong and T. Ong (1994). "Genotoxicity of vanadium pentoxide in Chinese hamster V79 cells." Mutat Res 321(1-2): 35-42.
- Zhong, B. Z., W. Z. Whong and T. M. Ong (1997). "Detection of mineral-dust-induced DNA damage in two mammalian cell lines using the alkaline single cell gel/comet assay." Mutat Res 393(3): 181-187.
- Zhou, B. B. and S. J. Elledge (2000). "The DNA damage response: putting checkpoints in perspective." Nature 408(6811): 433-9.
- Zychlinski, L., J. Z. Byczkowski and A. P. Kulkarni (1991). "Toxic effects of long-term intratracheal administration of vanadium pentoxide in rats." Arch Environ Contam Toxicol 20(3): 295-298.

Publications

Parts of this work have already been published:

Posters

Niemeier, Nicole; Fischer, Kathrin B.; Krug, Harald F.

„Uptake and Transport of Nanoparticles in Cells: Mechanisms and Toxicological Aspects“

Signal Transductions Meeting, Weimar, Germany, November 2006

Nau, Katja; Geiger, Dominik W.; Niemeier Nicole; Fischer, Kathrin B.; Krug, Harald F.

„Uptake mechanisms and toxicological aspects of synthetic nanoparticles in human cells“

EuroNanoForum 2007, Düsseldorf, Germany, June 2007

Fischer, Kathrin B.; Krug, Harald F.

„Biological effects of synthetic vanadium oxide nanoparticles in human lung cells“

CFN SummerSchool Nanobiology 2007, Bad Herrenalb, Germany, August 2007

EEMS 2007, Basel, Switzerland, September 2007

Signal Transductions Meeting, Weimar, Germany, November 2007

Fischer, Kathrin B.; Krug, Harald F.

„Genotoxic potential of synthetic metal oxide nanoparticles“

INIS 2008, Hannover, Germany, June 2008

Fischer, Kathrin B.; Krug, Harald F.

„Genotoxic potential of synthetic metal oxide nanoparticles“

Nanotox 2008, Zürich, Switzerland, September 2008

Curriculum Vitae

Personal Data

Name Kathrin Barbara Fischer
 Address Solitüdenstrasse 15
 CH-9012 St.Gallen, Switzerland
 Date of birth August, 11th, 1980
 Place of birth Würzburg, Germany
 Marital status single

Education

Since 06/2006 Ph.D. thesis "*Genotoxicity of synthetic nanomaterials*"
 Supervisor: Prof. Harald F. Krug
 Research Center Karlsruhe, Institute of Toxicology and
 Genetics, Germany (06/2006 – 02/2009)
 Swiss Federal Laboratories for Material Testing and
 Research (EMPA) St. Gallen, Laboratory of Materials-
 Biology Interactions, Switzerland (since 03/2009)

09/2005 – 07/2006 Master thesis "*Role of mismatch repair and cytosine-
 methylation in the sensitivity of cells for genotoxic agents*"
 Supervisor: Prof. Helga Stopper
 University of Würzburg, Institute of Toxicology, Germany
 Degree: Master of Science

08/2004 – 07/2005 Biomedical Research School, Umeå, Sweden

03/2004 – 07/2004 Bachelor thesis "*Simultaneous Quantitation of the
 Metabolites 6 β -Hydroxytestosterone / Estradiol and 4,4-
 Dimethyl-5 α -cholestra-8,14,24trienol (FF-MAS) after
 Inhibition of CYP 19 and CYP 51 by Environmental
 Poisons by LC-APPI-MS-MS*"
 Supervisor: Dr. Wolfgang Völkel
 University of Würzburg, Institute of Toxicology, Germany
 Degree: Bachelor of Science

10/2001 – 07/2004 Study of biomedicine
 University of Würzburg, Germany

10/2000 – 09/2001 Study of biology
 University of Würzburg, Germany

09/1991 – 06/2000 Röntgen Gymnasium Würzburg, Germany
 Graduation *Abitur*

Qualifications

02/2009	DGPT course „Molecular celltoxicology“, Helmholtz Center, Munich, Germany
10/2008	DGPT course „Clinical toxicology“, BBGes, Berlin, Germany
10/2008	DGPT course „Ecotoxicology“, University of Frankfurt, Germany
03/2008	EEMS workshop “Automated analysis of micronucleus scoring”, Brussels, Belgium
02/2007 – 08/2007	Organization of CFN-Summer School “Nanobiology”, Bad Herrenalb, Germany

Scholarships and Awards

04/2002 – 07/2006	Foundation of German Business (Stiftung der Deutschen Wirtschaft), Klaus Murmann Fellowship Program
05/2005	Best oral presentation at the SNIB 2005 (Student’s Network in Bioscience), Uppsala, Sweden

Memberships

Since 2009	Deutsche Gesellschaft für Pharmakologie und Toxikologie (DGPT)
Since 2007	Gesellschaft für Umwelt-Mutationsforschung (GUM) (German section of the European Environmental Mutagenesis Society EEMS)

Publications

Trösken, Eva-Regina; Fischer, Kathrin et al.
„Inhibition of human CYP19 by azoles used as antifungal agents and aromatase inhibitors, using a new LC-MS/MS method for the analysis of estradiol product formation“, Toxicology. 2006 Feb 15;219(1-3):33-40.

Acknowledgements / Danksagungen

Ein herzliches Dankeschön an

Prof. Harald F. Krug, dafür, dass er mir dieses spannende Thema überlassen hat, und mich trotz der Entfernung betreut und unterstützt hat. Vielen Dank auch, dass ich auf vielen Tagungen, Workshops und Kursen mein toxikologisches Wissen vertiefen durfte. Herzlichen Dank weiterhin für die Möglichkeit, meine Arbeit an der EMPA fortzusetzen, sowie für die vielfältige Hilfe beim Umzug in die Schweiz.

Prof. Manfred Metzler, der sich so kurzfristig bereiterklärt hat, die Aufgabe des Zweitprüfers zu übernehmen.

Prof. Claus Feldmann für die Herstellung und Überlassung der Vanadiumoxid-nanomaterialien.

Dr. Christel Adelhelm und Tobias Weingärtner am IMF, mit deren Hilfe ich die Löslichkeits- und Aufnahmebestimmungen durchführen durfte.

Hans-Jürgen Schindler von der EMPA Dübendorf für die Durchführung der BET-Messungen.

Petra Klug, unserer Nanocare-Sekretärin, für die sprachlichen Korrekturen dieser Arbeit (und natürlich auch für die vielfältige Hilfe mit allem möglichen Papierkram).

Prof. Doris Marko und ihrer ganzen Arbeitsgruppe, die mir mit Rat und Tat bei den unterschiedlichsten Fragen und Problemen zur Seite standen.

Prof. Helga Stopper, bei der ich während meiner Masterarbeit viele Dinge lernen durfte, die ich in meiner Doktorarbeit gebrauchen konnte. Außerdem hatte sie auch weiterhin für ihre ehemalige Studentin immer ein offenes Ohr für Fragen und mir in einige Problemen den entscheidenden Hinweis zur Lösung gegeben.

Meinen Nanocare-Kollegen, insbesondere Katja, die neben Unterstützung in arbeitstechnischen Fragen und auch immer wieder freundliche „Nachbarschaftshilfe“ geleistet hat. Außerdem erinnere ich mich gerne an die vergnüglichen Plauderstunden mit ihr. Danke ebenfalls an Nicole für die nette Atmosphäre im Büro und im Labor, und für die gute Zusammenarbeit bei Postern oder Berichten.

Meinen Kollegen am ITG, für praktische und theoretische Hilfe im Labor und außerhalb. Ganz besonderen Dank an Sylvie Özdemir, die mir auch über die gemeinsame Zeit im FZK eine gute Freundin geblieben ist.

Meinen Kollegen an der EMPA, die mich so freundlich aufgenommen haben. Besonderen Dank an Cordula und Tina fürs Korrekturlesen dieser Arbeit.

Meinen Eltern, die mich unterstützten, wohin meine Wege mich auch führten, und so großes Verständnis für mein unstetes Leben zeigen.

Meinen Geschwistern für all die vergnüglichen Stunden, wenn wir uns mal sehen, was leider auf Grund der Entfernungen nicht oft möglich ist.

Meinen Freunden, allen voran Julia, Dagmar, Nicole, Christopher und Wilfried, die sich in den vergangenen Jahren um mein Wohlergehen gesorgt haben, mit mir die Freuden und Leiden des (Forscher)lebens teilten und immer für mich da waren. Sowie Noemi, der besten Nachbarin und Freundin, die man sich wünschen kann.